

**PMFSEL REPORT NO. 86-4  
MAY 1986**

**SEISMIC STRENGTHENING OF A  
REINFORCED CONCRETE FRAME  
USING REINFORCED CONCRETE PIERS**

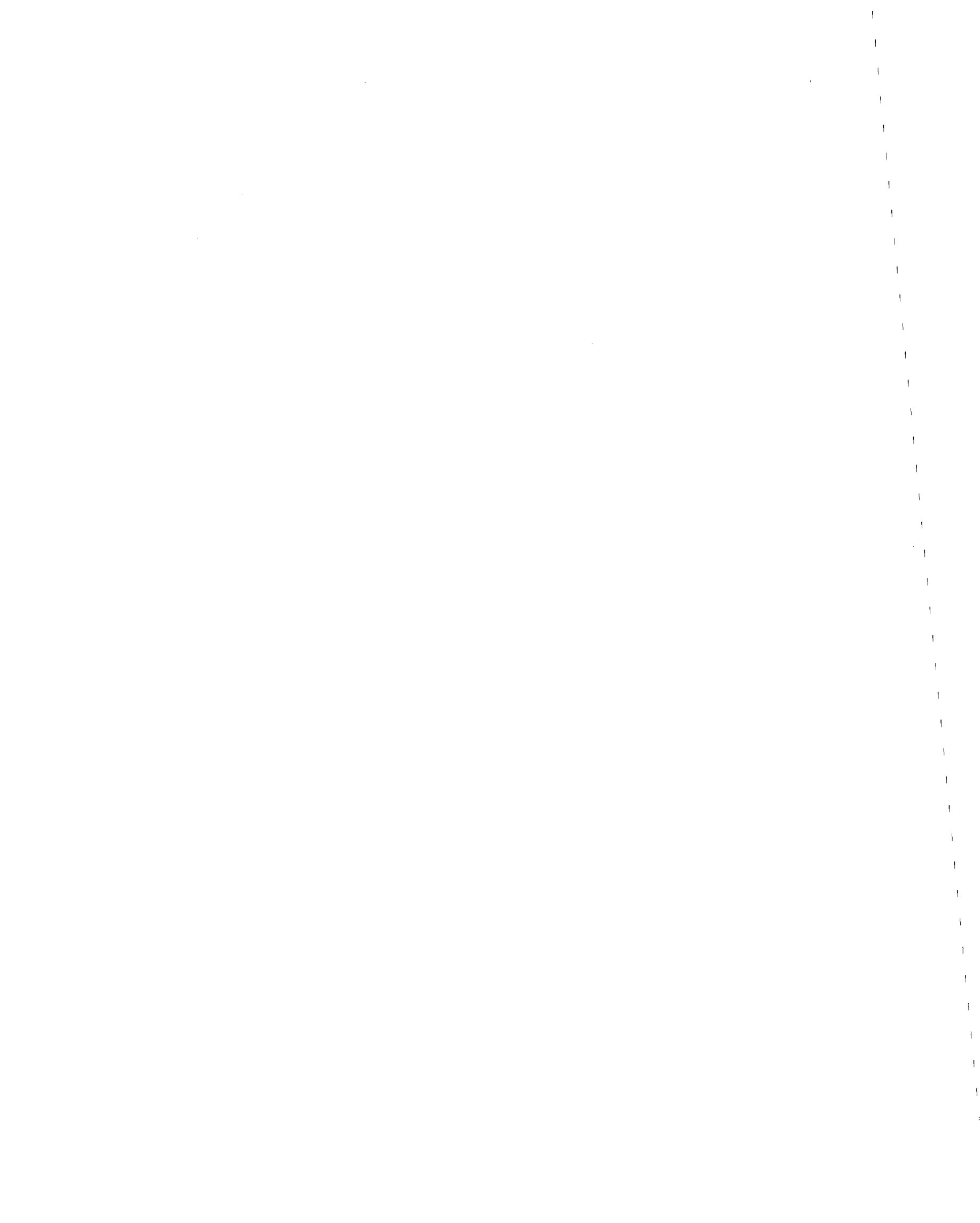
**By**

**Carol E. Roach**

**James O. Jirsa**

**Report on a Research Project  
Sponsored by  
National Science Foundation  
Grant No. CEE-8201205**

**PHIL M. FERGUSON STRUCTURAL ENGINEERING LABORATORY  
Department of Civil Engineering / Bureau of Engineering Research  
The University of Texas at Austin**



<b>REPORT DOCUMENTATION PAGE</b>	<b>1. REPORT NO.</b> NSF/ENG-86022	<b>2.</b>	<b>3. Recipient's Accession No.</b> PB87 148151AS
<b>4. Title and Subtitle</b> Seismic Strengthening of a Reinforced Concrete Frame Using Reinforced Concrete Piers		<b>5. Report Date</b> May 1986	
<b>7. Author(s)</b> C.E. Roach; J.O. Jirsa		<b>6.</b>	
<b>9. Performing Organization Name and Address</b> University of Texas Phil M. Ferguson Structural Engineering Laboratory 10100 Burnet Road Austin, TX 78758		<b>8. Performing Organization Rept. No.</b> PMFSEL 86-4	
<b>12. Sponsoring Organization Name and Address</b> Directorate for Engineering (ENG) National Science Foundation 1800 G Street, N.W. Washington, DC 20550		<b>10. Project/Task/Work Unit No.</b>	
<b>15. Supplementary Notes</b>		<b>11. Contract(C) or Grant(G) No.</b> (C) (G) CEE8201205	
<b>16. Abstract (Limit: 200 words)</b> A two-third scale model of two bays and two stories of an exterior moment resisting frame of a reinforced concrete building was constructed. The prototype exterior frame had deep spandrel beams which resulted in short clear spans in the slender columns. The existing frame was deficient in seismic resistance in terms of ductility and strength. The column shear capacity was relatively low. The frame was retrofitted with reinforced concrete piers around each of the columns to increase the column capacities and shift the mode of failure of the frame from shear in the columns to flexural hinging in the beams. The strengthened frame was subjected to reversed, cyclic loads, with a maximum interstory drift of 0.5%, until flexural hinging of the beams occurred. Behavior of the strengthened frame is discussed with special emphasis on its ductility, lateral strength, and lateral stiffness. Pier behavior and interaction with the original frame are considered. A discussion of nominal capacities calculated using ACI 318-83 is included.		<b>13. Type of Report &amp; Period Covered</b>	
<b>17. Document Analysis a. Descriptors</b> Structural engineering Buildings Cyclic loads Shear properties <b>b. Identifiers/Open-Ended Terms</b> Earthquake engineering  <b>c. COSATI Field/Group</b>		<b>14.</b>	
<b>18. Availability Statement</b>  NTIS	<b>19. Security Class (This Report)</b>	<b>21. No. of Pages</b>	
	<b>20. Security Class (This Page)</b>	<b>22. Price</b>	



**PMFSEL REPORT NO. 86-4  
MAY 1986**

**SEISMIC STRENGTHENING OF A  
REINFORCED CONCRETE FRAME  
USING REINFORCED CONCRETE PIERS**

**By**

**Carol E. Roach  
James O. Jirsa**

**Report on a Research Project  
Sponsored by  
National Science Foundation  
Grant No. CEE-8201205**



SEISMIC STRENGTHENING OF A REINFORCED CONCRETE FRAME  
USING REINFORCED CONCRETE PIERS

by

Carol E. Roach

and

James O. Jirsa

Report on a Research Project

Sponsored by

National Science Foundation

Grant No. CEE-8201205

Phil M. Ferguson Structural Engineering Laboratory  
Department of Civil Engineering  
BUREAU OF ENGINEERING RESEARCH  
THE UNIVERSITY OF TEXAS AT AUSTIN

May 1986

The contents of this report reflect the views of the authors who are responsible for the facts and accuracy of the data presented herein. The contents do not necessarily reflect the view or policies of the National Science Foundation. This report does not constitute a standard, specification, or regulation.

## A C K N O W L E D G E M E N T S

The research was conducted as part of the Master of Science program of Carol E. Roach under the direction of Dr. James O. Jirsa. Dr. Ramon Carrasquillo provided invaluable direction and advice in all matters. Appreciation is expressed to Loring Wyllie, Jr., Chris Poland, and Maryann Wagner of H. J. Degenkolb Associates, Inc., San Francisco, California, with whom this research was jointly conducted. The authors gratefully acknowledge support from the National Science Foundation under Grant No. CEE-8201205.

The authors would like to thank the staff at Ferguson Structural Engineering Laboratory; George Modine, Gorham Hinckley, Blake Stassney, Dick Marshal, Pat Ball, Bill Gehrman, Laurie Golding, and Maxine DeButts. Special thanks to Jean Gehrke for her expert drafting and to Carol Booth for her patience in typing the drafts of the thesis and the report.

The authors would also like to express appreciation to the many graduate research assistants who helped with the project. Special thanks go to co-workers Tommy Bush, Elizabeth Jones, and Marc Badoux who worked with Carol Roach throughout the program and without whom the project could not have been accomplished.

## TABLE OF CONTENTS

Chapter		Page
1	RESEARCH PROGRAM AND BACKGROUND.....	1
	1.1 Research Program.....	1
	1.1.1 Introduction.....	1
	1.1.2 Objective and Scope.....	2
	1.2 Background.....	7
	1.2.1 Changes in Building Codes.....	7
	1.2.2 Methods and Philosophies of Seismic Strengthening.....	8
	1.2.3 Related Experimentation.....	9
2	DESIGN, CONSTRUCTION AND TESTING.....	15
	2.1 Prototype.....	15
	2.1.1 Prototype Building Design.....	15
	2.1.2 Strengthening of the Prototype Building....	18
	2.2 Existing Frame Model.....	26
	2.2.1 Design of the Existing Frame Model.....	26
	2.2.2 Construction of Existing Frame Model.....	34
	2.3 Strengthened Frame Model.....	39
	2.3.1 Strengthening Design for the Existing Frame Model.....	39
	2.3.2 Construction of Piers.....	39
	2.4 Constructibility and Aesthetics.....	49
	2.5 Test Setup.....	53
	2.5.1 Loading and Reaction .....	53
	2.5.2 Beam Reactions.....	59
	2.5.3 Out-of-Plane Bracing.....	64
	2.5.4 Data Acquisition.....	64
	2.5.5 Test Procedure.....	67
3	RESULTS OF STRENGTHENING.....	77
	3.1 Test of Existing Frame Model.....	77
	3.2 Test of Strengthened Frame Model.....	77
	3.2.1 General.....	77
	3.2.2 0.05% Drift Cycles.....	80
	3.2.3 0.125% Drift Cycles.....	82
	3.2.4 0.25% Drift Cycles.....	82
	3.2.5 0.5% Drift Cycles.....	86
	3.3 Summary.....	98

TABLE OF CONTENTS (continued)

Chapter		Page
4	ANALYSIS OF PIER BEHAVIOR.....	101
	4.1 General.....	101
	4.2 Analysis of Data.....	102
	4.2.1 Interstory Drift.....	102
	4.2.2 Crack Patterns.....	102
	4.2.3 Stresses in Longitudinal Pier Reinforcement .....	106
	4.2.4 Slip at New/Existing Concrete Interface...	112
	4.2.5 Stresses in the Dowels.....	119
	4.2.6 Stresses in the Stirrups.....	125
	4.3 Summary.....	129
5	CALCULATED CAPACITIES.....	131
	5.1 General.....	131
	5.2 Ultimate Load of Strengthened Frame Model.....	131
	5.3 Nominal Shear Capacities of Model Pier.....	136
	5.4 Summary.....	139
6	SUMMARY AND CONCLUSIONS.....	141
	6.1 Test Program.....	141
	6.2 Results of Pier Strengthening.....	142
	6.2.1 Constructibility and Aesthetics.....	142
	6.2.2 Performance of Strengthened Frame.....	142
	6.3 Behavior of the Piers.....	142
	6.3.1 Flexural Behavior.....	143
	6.3.2 Shear Behavior.....	143
	6.3.3 Interaction.....	144
	6.4 Conclusions.....	144
	REFERENCES.....	147

LIST OF TABLES

Table		Page
2.1	Concrete Mix Proportions.....	37
3.1	Loads and Drifts for Cycles to 0.25% Drift.....	87
3.2	Loads and Drifts for Cycles to 0.5% Drift.....	91
4.1	Slip Behavior.....	113

## LIST OF FIGURES

Figure	Page
1.1 Example building with deep beam - short column exterior frame.....	4
1.2 Typical short column shear failure. Olive View Hospital, San Fernando 1971.....	5
1.3 Severe damage due to short column shear failure. Hokodate College, Tokachi-oki 1968. [10].....	5
1.4 Test specimen during three phases of testing.....	6
1.5 Methods of seismic strengthening.....	10
1.6 Results from cast-in-place wing walls. Higashi and Kokusho. [14].....	12
1.7 Results from precast panel wing walls. Higashi and Kokusho. [14].....	13
1.8 Truss analogy for precast wing walls. Higashi, et al. [6].....	14
2.1 Prototype building, plan and elevation.....	16
2.2 Details of exterior moment resisting frame.....	17
2.3 Design loads for prototype building based on UBC earthquake regulations.....	19
2.4 Evaluation of exterior frame failure mode.....	20
2.5 Details of reinforced concrete pier.....	22
2.6 Reinforcement in pier.....	23
2.7 Load transfer actions in pier strengthening.....	25
2.8 Evaluation of failure mode of strengthened frame.....	27
2.9 Test Specimen (existing structure)- twobays between 3rd and 5th stories of exterior moment resisting frame.....	29

LIST OF FIGURES (continued)

Figure	Page
2.10 Details of 2/3 scale model of existing frame.....	30
2.11 Boundary constraints modeled on test specimen.....	31
2.12 Final design of test specimen.....	32
2.13 Section through slab and drop panel.....	33
2.14 Frame location on floor wall reaction system.....	35
2.15 Casting stages for construction of existing frame model and concrete compressive strengths for each casting stage.....	36
2.16 Casting stage 3. Concrete placed to top of second level slab.....	38
2.17 Casting stage 2. Forms in place for first level beam and column.....	38
2.18 Placing concrete in upper portion of beam form.....	40
2.19 Forms were stripped after casting stage 2.....	40
2.20 The completed existing frame model.....	41
2.21 Model retrofitted with R/C piers.....	42
2.22 Details of 2/3 scale model of R/C pier.....	43
2.23 Frame prepared by sandblasting surface and chipping groove in column face.....	44
2.24 Drilling holes for dowels.....	44
2.25 Mixing epoxy ingredients.....	46
2.26 Placing epoxy in dowel hole with caulking gun.....	46
2.27 Casting stages for construction of R/C pier strengthening and concrete compressive strengths for each casting stage.....	47

LIST OF FIGURES (continued)

Figure		Page
2.28	Frame with dowels in place before constructing reinforcing cage.....	48
2.29	Boundary elements in place with three of four longitudinal bars.....	48
2.30	Transverse and longitudinal steel in place.....	50
2.31	Hooked #3 longitudinal bars in window area.....	50
2.32	Concrete was placed from the interior of the frame using a chute which emptied into the formwork.....	51
2.33	Inside formwork in place after casting lower 4 ft of pier.....	51
2.34	Exterior formwork for casting stage 1.....	52
2.35	The completed R/C pier strengthening scheme.....	52
2.36	Loading frame and connection to reaction wall.....	55
2.37	Connection of loading frame to buttresses of reaction wall.....	56
2.38	Loading frame at third level.....	57
2.39	Loading frame connection to reaction wall buttresses.....	57
2.40	Loading frame, hydraulic rams and box/plate assemblage at loading point.....	58
2.41	Structural steel assembly embedded in drop panel - column area, shown in formwork before placing concrete.....	60
2.42	Reaction assemblage under first level slab.....	61
2.43	Reaction assemblage.....	62
2.44	Reaction assemblage and drop panel on first level....	63
2.45	Test frame with boundary restraints.....	63

LIST OF FIGURE (continued)

Figure	Page
2.46 Steel struts to provide vertical deflection restraints at ends of beams.....	65
2.47 Out-of-plane brace at first level.....	66
2.48 Out-of-plane braces at third level.....	66
2.49 Strain gage locations in the original frame.....	68
2.50 Strain gage locations on the longitudinal reinforcement in the pier.....	69
2.51 Strain gage locations on dowels and transverse reinforcement in the pier.....	70
2.52 Locations of load cells in the boundary restraints...	71
2.53 Orientation and Location of LVDTs.....	72
2.54 LVDT (channel 182) and dial gage measuring vertical deflection of the first level beam.....	73
2.55 LVDT (channel 180) measuring horizontal deflection of the first level beam.....	73
2.56 LVDT (channel 188) used to measure slip between the original column and the pier.....	74
2.57 Data acquisition equipment by northeast corner of frame.....	74
3.1 Load vs. drift for test of existing frame model.....	78
3.2 Deformation history of the strengthened frame model..	79
3.3 Load vs. drift for the strengthened frame and existing frame models for cycles to 0.05% drift.....	81
3.4 Load vs. drift for three cycles to low (0.125%) drift.....	83
3.5 Crack pattern after three cycles to 0.125% drift.....	84

LIST OF FIGURES (continued)

Figure	Page
3.6 Locations of yielded bars in beams indicated by strain gages after three cycles to 0.125% drift.....	85
3.7 Load vs. drift for three cycles to medium (0.25%) drift.....	88
3.8 Crack pattern after three cycles to 0.25% drift.....	89
3.9 Locations of yielded bars in beams indicated by strain gages after three cycles to 0.25% drift.....	90
3.10 Load vs. drift for three cycles to high (0.5%) drift.....	93
3.11 Crack pattern after three cycles to 0.5% drift.....	94
3.12 Large flexural crack with some concrete spalling at 0.5% drift. Interior of first level beam, north of south pier.....	95
3.13 Crack pattern on exterior face of north end, first level beam, 0.5% drift.....	95
3.14 Marked shear cracks on interior of north pier, second level, 0.5% drift.....	96
3.15 Marked shear cracks on interior of north pier, first level, 0.5% drift.....	96
3.16 Locations of yielded bars in beams indicated by strain gages after three cycles to 0.5% drift.....	97
3.17 Envelope of load vs. drift plots for all cycles strengthened frame test.....	100
4.1 Interstory drift for last three cycles of loading....	103
4.2 Crack patterns of piers after three cycles to 0.5% drift.....	104
4.3 Crack pattern, interior window segment, north pier, second level, three cycles to 0.5% drift.....	105

xiii

LIST OF FIGURES (continued)

Figure	Page
4.4 Assumed behavior pattern of window segment under north loading conditions.....	107
4.5 Stress gradients across top and bottom cross sections of north pier, first level.....	108
4.6 Stress gradients across top and bottom cross sections of north pier, second level.....	109
4.7 Stress gradients across top and bottom cross sections of south column, first level.....	111
4.8 Stress gradients across top and bottom cross sections of south column, second level.....	111
4.9 Locations of LVDTs and compression struts, window segment, north pier, second level.....	113
4.10 Load vs. slip for LVDT 190.....	115
4.11 Load vs. slip for LVDT 187.....	115
4.12 Load vs. slip for LVDT 192.....	116
4.13 Load vs. slip for LVDT 195.....	116
4.14 Load vs. slip for LVDT 193.....	117
4.15 Load vs. slip for LVDT 194.....	117
4.16 Load vs. slip for LVDT 188.....	118
4.17 Load vs. slip for LVDT 189.....	118
4.18 Load vs. stress for dowel 166 and load vs. slip for LVDT 192.....	120
4.19 Load vs. stress for dowel 167 and load vs. slip for LVDT 194.....	121
4.20 Load vs. stress for dowel 161.....	123
4.21 Load vs. stress for dowel 163.....	123

LIST OF FIGURES (continued)

Figure	Page
4.22 Load vs. stress for dowel 157.....	124
4.23 Load vs. stress for dowel 158.....	124
4.24 Suggested design for dowels.....	126
4.25 Load vs. stress for stirrup gage 147.....	127
4.26 Load vs. stress for stirrup gage 150.....	127
4.27 Load vs. stress for stirrup gage 156.....	128
5.1 Idealized failure mechanism for all beams hinged and infinitely stiff columns.....	132
5.2 Relationship between angles of rotation $\phi$ and $\theta$ .....	134
5.3 Comparison of model with the calculated failure load of the existing frame model, the predicted failure load of the strengthened frame and the maximum loads on the frame.....	137
5.4 Comparison of maximum shear applied to the piers and the calculated nominal strengths of the piers....	140



## CHAPTER 1

### RESEARCH PROGRAM AND BACKGROUND

#### 1.1 Research Program

1.1.1 Introduction. In areas of high seismic risk it is of extreme importance that reinforced concrete buildings be adequate in terms of strength and ductility. There are a number of existing reinforced concrete buildings which, although designed in compliance with earlier building codes, are found to be deficient when evaluated by more modern, current codes. Seismic strengthening of deficient reinforced concrete buildings is undertaken for two reasons: (1) local building codes or regulations, especially in areas of high seismic risk, often require strengthening to meet current seismic regulations when a change is made in a building's occupancy or potential hazard; (2) concern for the safety of building occupants and protection of financial investment has encouraged many building owners to voluntarily strengthen selected buildings. Seismic strengthening has become particularly important with the rapidly rising cost of construction making renovation of existing structures increasingly attractive economically.

Seismic strengthening of existing buildings involves retrofitting the structure to increase strength against lateral loads, increase ductility or increase both strength and ductility. Seismic strengthening schemes must be based on a thorough analysis of the strengths and weaknesses of the existing lateral force resisting system and of the possible consequences of strengthening. The strengthening scheme must provide strength without transferring the potential of severe damage to the next weakest link of the building. Because these schemes may involve materials different from those in the original building, interaction of these different materials must be understood. Other important considerations in seismic strengthening design are: the effect of the strengthening on the function and aesthetics of the building; constructibility of the scheme and interference with normal operation of the building; and economic feasibility of the design.

Retrofitting existing structures for seismic strengthening is a challenging engineering problem for which there is little available guidance. Building codes are written

to address new construction using modern materials and techniques. They do not include provisions for evaluating available strength of old and archaic materials and designs. The state-of-the-art of seismic strengthening uses methods which have been developed largely through experience and engineering judgement. The methods used for reinforced concrete buildings include additional shear walls, concrete or masonry infill walls, precast or cast-in-place reinforced concrete wing walls, structural steel diagonal bracing and jacketing columns with steel or concrete.

As the frequency of seismic strengthening increases, there is an increasing need for experimentation leading to a thorough understanding of the interaction of these strengthening techniques with the original structure. Connections between the strengthening and original structure are of particular interest because they sharply influence the interaction. Previous research conducted on strengthening of members and frame assemblages have been performed on small scale specimens, typically a maximum of one-half scale for columns and one-third scale for frame tests [1,2,3,4,5,6,7,8]. There is a need for research involving large scale specimens which better model the connections and details of strengthening techniques. In addition, there is a need that this research be performed with the cooperation and assistance of design engineers. Dialogue between researchers and designers is important because seismic strengthening techniques have been empirically developed by designers and they will be responsible for incorporating any research results into practice.

1.1.2 Objective and Scope. The objective of this research was to investigate strengthening techniques for a selected reinforced concrete frame system. The investigation was a cooperative effort between a design engineering group from H. J. Degenkolb Associates (HJDA) and a research team at The University of Texas at Austin. The focus of the investigation was an experimental study of a two-third scale model of a portion of a reinforced concrete moment resisting frame. The research plan had two features which distinguished it from previous research on seismic strengthening in the United States. First, the project combined the resources of a university research laboratory and a structural engineering design firm. The research team at The University of Texas was able to take advantage of the professional experience of the HJDA design engineers working in an area in which little guidance is set forth in codes and design requirements. Second, the experimental

work involved a large scale specimen and thereby decreased or eliminated the effects of scale in the connections and details.

The structural system investigated was a reinforced concrete exterior frame system with deep, stiff spandrel beams framing into flexible columns having low shear strength. This form of construction for exterior frames of reinforced concrete buildings was a popular design in California in the 1950s and 1960s [9] because there was no need for exterior architectural walls. The deep spandrel beams formed the exterior wall with clear space at the correct height for windows. The deep beams also shortened the clear span of the flexible columns. An example building with a deep beam - short column exterior frame is pictured in Fig. 1.1. Studies of earthquake failures have indicated that the weak link in these framing systems is usually the column shear capacity. Column shear failures are potentially very hazardous non-ductile failures. Fig. 1.2 is a picture of a typical short column shear failure due to earthquake loading. A shear failure can drastically reduce the load carrying capacity of the column endangering the gravity system and stability of the building. An example of an earthquake failure in a building of this type in which the building suffered severe damage is pictured in Fig. 1.3.

The experimental program in this study involved strengthening and testing a two-third scale model of two bays and two stories of this type of exterior moment resisting frame of a prototype reinforced concrete building. Two strengthening schemes were investigated. One strengthening scheme involved casting reinforced concrete piers around the existing columns of the frame. The other scheme was a structural steel X-bracing system mounted on the exterior of the frame. Figure 1.4 is a drawing of the test specimen unstrengthened, strengthened with reinforced concrete piers and strengthened with a steel X-bracing system. The design of the prototype frame and strengthening schemes was carried out by the engineering team at H. J. Degenkolb Associates. The construction and testing of the model was accomplished at the Ferguson Structural Engineering Laboratory.

The project was carried out in three phases. The first phase was to construct and test the unstrengthened or existing frame. The second phase was to cast the reinforced concrete piers around the columns and test the strengthened frame. The third phase involved removing the reinforced concrete piers and returning the frame to its original dimensions. After removal of the piers, the frame was retrofitted with a steel bracing system



Fig. 1.1 Example building with deep beam-short column exterior frame

Reproduced from  
best available copy.

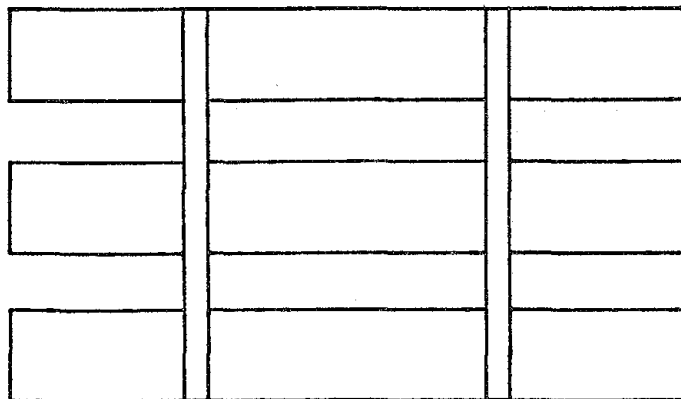




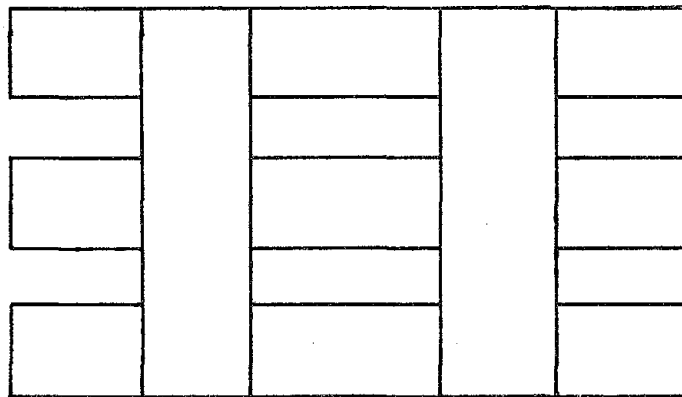
Fig. 1.2 Typical short column shear failure  
Olive View Hospital, San Fernando  
1971



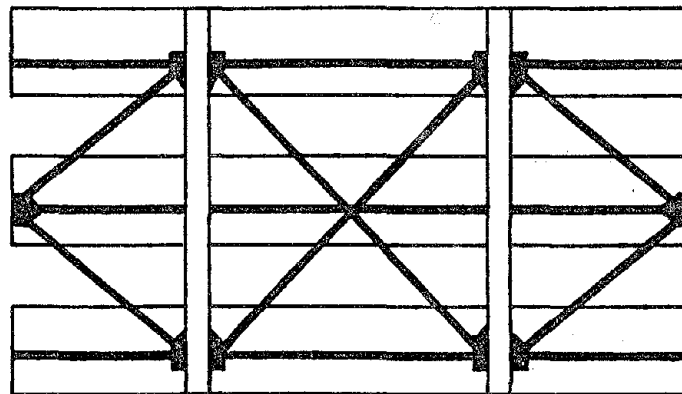
Fig. 1.3 Severe damage due to short column  
shear failure. Hokodate Coleege,  
Tokachi-oki 1968 [10]



a. Existing or unstrengthened frame.



b. R/C pier strengthened frame.



c. Steel bracing strengthened frame.

Fig. 1.4 Test specimen during three phases of testing

and tested again [18]. This report will address only the first two phases of the project with the main emphasis being on the construction and testing of the reinforced concrete strengthening scheme. The third phase of the frame is relevant to the discussion in that the need to reuse the frame affected decisions made while testing the first strengthening scheme.

Testing of the model frame involved subjecting the frame to reversed cyclic lateral deformations. These deformations were accomplished by laterally loading the frame at the top level and restraining it at the bottom level. The degree of damage to the frame was measured in levels of percent drift. In reference to buildings, percent drift is the percentage that the relative horizontal movement between two levels or stories is of the vertical distance between them. Drift was considered a good indication of severity of loading and was a reference readily understood by structural engineers. Testing the existing frame involved two cycles of reversed loading to a very low drift level. The purpose of testing the unstrengthened frame was to determine its stiffness and behavior under lateral loads, but not to damage the frame in any way. The pier strengthened frame was tested under reversed cyclic loading to four different drift levels, three cycles at each drift level. The strengthened frame was tested to determine its uncracked stiffness, cracked stiffness, and strength under lateral loading; as well as to gain information on the interaction between the original frame and strengthening elements.

## 1.2 Background

1.2.1 Changes in Building Codes. An increasing knowledge about earthquakes and structural behavior during earthquakes has provided an impetus for review and upgrading of codes in regard to construction in areas of high seismicity. The current building codes and requirements have much stricter and more complicated earthquake regulations for strength and ductility than those of the 1950s and 1960s [11]. The changes in earthquake regulations are illustrated in a comparison of the 1955 edition of the Uniform Building Code (UBC) to the 1982 edition. In the 1955 edition of the UBC the Provisions for Lateral Bracing (Earthquake Regulations) were located in the Appendix and were suggested for inclusion by cities located within an area subject to earthquake shocks. [12] In contrast, the 1982 UBC has the earthquake regulations in the main text and it is stated that

"Every building or structure and every portion thereof shall be designed and constructed to resist stresses produced by lateral forces as provided in this section." [13]

The stricter and more complicated strength requirements are illustrated by a comparison of the lateral force formula in the earthquake regulations of the 1955 UBC and the 1982 UBC. The lateral force requirements of the UBC are taken from the "Recommended Lateral Force Requirements" of the Structural Engineers Association of California (SEAOC). Earlier recommendations of the SEAOC were based on available data and dynamic principles. The Horizontal Force Formula used in the 1955 UBC yields a horizontal force which was a product of the tributary weight and a numerical constant based on the structural element designed, the number of contributing stories and the zone of seismic disturbance [12].

After the 1971 San Fernando, California earthquake; new criteria were established based on past experience and correlation of seismic performance and design data of the affected buildings [11]. These criteria were incorporated in the 1982 edition of the UBC. The Minimum Lateral Force Formula yields a lateral force which is a product of tributary weight and several numerical constants. The values of the numerical constants were based on factors such as: the zone of seismic disturbance, the occupancy of the building, the ductility of the structural system, the natural period of the structure and the site-structure resonance [13]. The resulting minimum lateral seismic force is, in general, higher than the horizontal force of the 1955 UBC. In addition to changes in strength requirements, current codes are much stricter in reference to the ductility requirements of members and lateral force resisting systems.

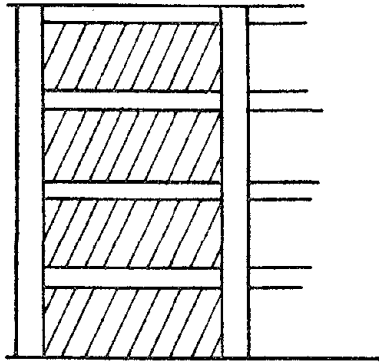
1.2.2 Methods and Philosophies of Seismic Strengthening. The method of seismic strengthening applied to a structure should be selected with careful consideration of the goals established. In general, new elements are added to an existing structure for increased strength and existing elements are reinforced to increase frame ductility. In the addition of new elements to increase strength, the effect of the strengthening scheme is of extreme importance. The strengthening scheme must provide continuity to prevent transferring potential failure to another area of the structure. The preservation of adequate ductility of the structure is essential for satisfactory performance in expected ranges of inelastic deformation. Methods of increasing the lateral strength of reinforced concrete frames

include the addition of shear walls, infilled walls, wing walls and structural steel bracing.

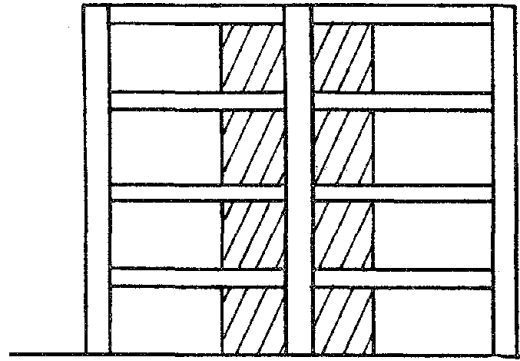
The addition of cast-in-place reinforced concrete shear walls is a frequently used strengthening scheme. In addition to casting the shear wall, provisions must be made for footings to support the additional weight and floor systems must be checked for adequacy in diaphragm strength. Cast-in-place or precast panel infill walls (Fig. 1.5a) are also used to increase strength. They should be well bonded to the frame. Dowels epoxy-grouted into the original frame can provide adequate anchorage. Mechanical wedge anchors are sometimes used. Infill walls are particularly suited to maintaining the aesthetic value of the building. A wing wall strengthening (Fig. 1.5b) technique is generally applied to buildings with strong beams and weak columns. The lateral strength of these buildings is significantly improved by strengthening the column with wing walls. These walls are either cast-in-place or precast panels connected to the existing concrete by the same methods as infill walls. Structural steel bracing systems (Fig. 1.5c) are also used in providing additional strength. They have the major advantage of adding little weight, important in seismic load consideration and foundation design. The steel bracing system is usually in the form of a braced frame along a portion or all of the building perimeter [9].

When the goal of strengthening is increased ductility, the method used usually involves strengthening certain elements of the frame. Many reinforced concrete frames lack ductility due to inadequate shear capacity of the column. In these cases, the columns can be strengthened with a steel or concrete jacket (Fig. 1.5d). In many cases where the flexural capacity of the columns is adequate, a gap is left at the top and bottom of the jacketing to prevent increasing the flexural capacity of the columns [9]. For frames in which masonry walls reduce the column length and create short, weak and brittle columns, slits can be introduced between the column and the wall to restore the flexibility of the column [1].

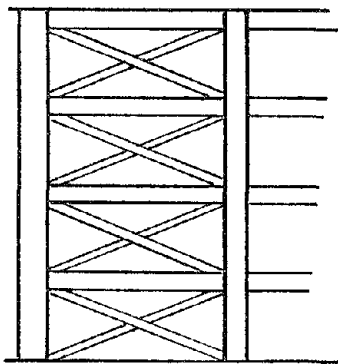
1.2.3 Related Experimentation. There has been little experimentation in the United States on strengthening techniques. In Japan, seismic strengthening has been the subject of much more research and discussion. The Japanese Ministry of Construction has prepared a guideline on "Seismic Retrofitting Design of Existing Reinforced Concrete Buildings" aimed primarily at Japanese structural systems. This guideline was based on research data accumulated in Japanese studies on strengthening.



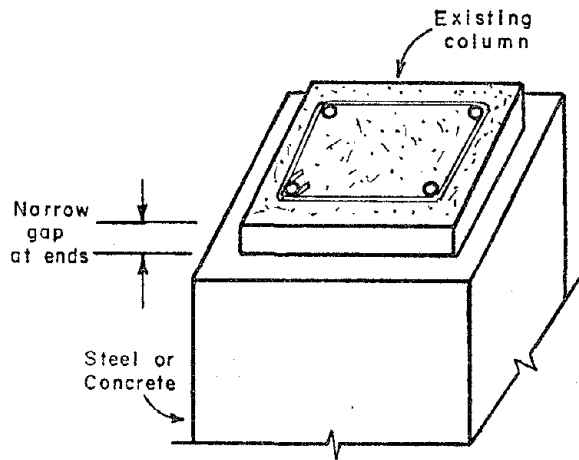
a. Infill walls.



b. Wing walls.



c. Steel bracing.



d. Column jacket.

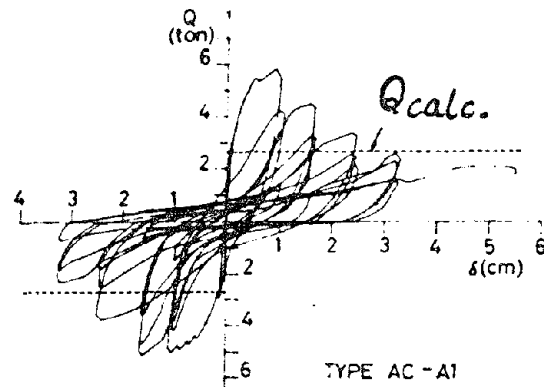
Fig. 1.5 Methods of seismic strengthening

For the most part the Japanese experimentation has concentrated on strengthening columns to improve ductility [ 3,14] , increasing stiffness and strength with infill walls [ 3,6,7,14] and adding a structural steel bracing system to frames [ 3,4] .

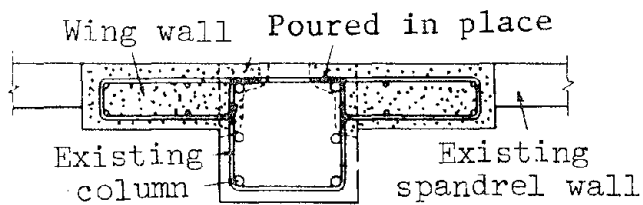
None of the Japanese experimentation has direct application to the reinforced concrete strengthening scheme which is the subject of this report. The most directly related experimentation is that of the strengthening by reinforced concrete wing walls. The wing wall design accomplishes the same purpose as the use of pier strengthening, increasing the shear strength in the area between beams and increasing the lateral stiffness of the frame.

Some of the earliest data on wing wall strengthening was reported by Higashi and Kokusho [14] . Their research involved one-story one-bay frames with wing walls. The cast-in-place wing walls were connected by welding the transverse reinforcement in the wing walls to the hoops of the original column. Wing walls constructed from precast panels were mechanically connected to the columns and beams of the frame. Higashi and Kokusho concluded that rigidities and strengths of the cast-in-place wing walls were almost the same as those of monolithic wing walls and columns. Some of the results published by Higashi and Kokusho are shown in Figs. 1.6 and 1.7.

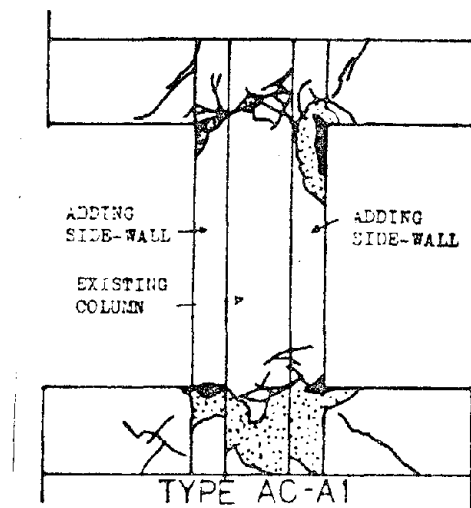
Further experimental work on wing wall strengthening was done by Higashi et al. [3,7] on three-story one-bay frames and three-story two-bay frames with only one bay strengthened. The wing walls in these tests were constructed using precast panels connected to the beams of the frame with mechanical anchors and mortar grout. Higashi et al. concluded that precast panels have the advantage of providing sufficient ductility in a frame and that precast panels can be idealized as a truss element for strength calculations. The truss analogy is illustrated in Fig. 1.8. In this figure, the  $Q_c$  term is the shear carried by the column and the precast wing wall panels act as compression struts carrying shear,  $Q_t$ .



a. Lateral load ( $Q$ ) vs. lateral deflection ( $\delta$ ).  
 $Q_{calc}$  is the shear strength of the un-strengthened column.

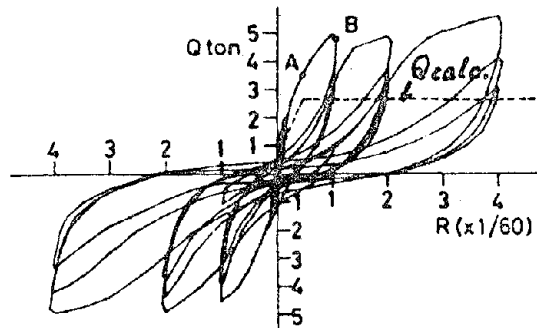


b. Wing wall design.

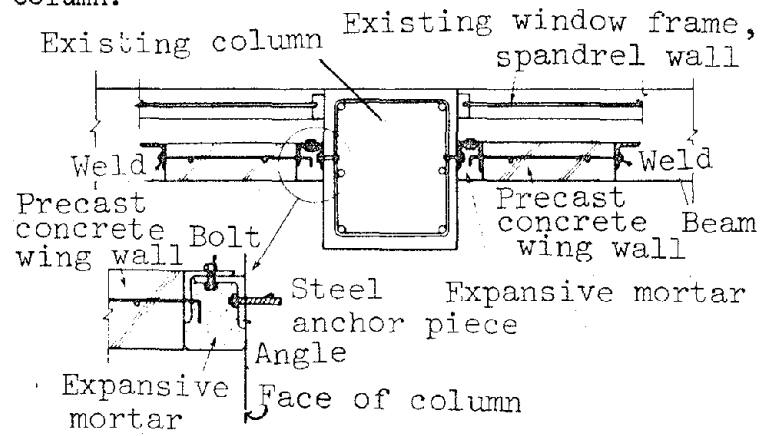


c. Typical crack pattern.

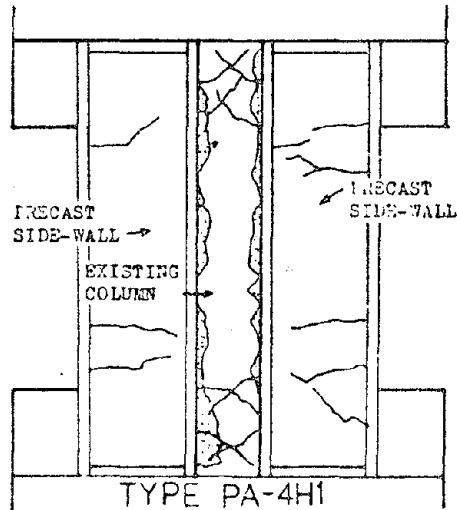
Fig. 1.6 Results from cast-in-place wing walls.  
 Higashi and Kokusho [14]



a. Lateral load (Q) vs. lateral deflection ( $\delta$ ).  
 $Q_{cal}$  is the shear strength of the un-strengthened column.



b. Wing wall design.



c. Typical crack pattern.

Fig. 1.7 Results from precast panel wing walls.  
 Higashi and Kokusho [14]



## CHAPTER 2

### DESIGN, CONSTRUCTION, AND TESTING

#### 2.1 Prototype

2.1.1 Prototype Building Design. The experimental specimen modeled a portion of a prototype building designed by the engineers at H. J. Degenkolb Associates of San Francisco. The building was chosen as typical of a building, approximately thirty years old, in need of strengthening to meet current earthquake regulations. The building was assumed to be in Earthquake Zone 4, the zone classification of highest seismic risk. It was a seven story, reinforced concrete building designed under the 1955 edition of the Uniform Building Code (UBC). Figure 2.1 is a plan and elevation of the prototype building. Its dimensions were 228 ft (eleven bays) by 56 ft (four bays) with 10 ft story heights. The lateral load was resisted in the short, 56 ft direction, by four shear walls. The two exterior walls as well as two interior walls which spanned one-half the building width served as shear walls. In the long direction, the majority of the lateral load was carried by the exterior moment resisting frame of the building. The interior of the building was a flat plate system. The exterior frame had a 21 ft typical bay length with 18 in. square typical columns and 6 ft deep, 8 in. wide spandrel beams.

This was a moment resisting frame of the deep beam - short column type noted in Chapter 1 as usually inadequate in ductility for earthquake conditions.

The engineering team at H. J. Degenkolb Associates designed the exterior moment resisting frame of the prototype building using portal analysis. The member forces were estimated using design earthquake loads for the building calculated using the earthquake regulations located in the Appendix of the 1955 UBC. The working stress method of design was used for the reinforced concrete members as specified by the 1955 UBC. The specified compressive strength of the concrete was 3000 psi. The specified yield strengths of the standard reinforcing bars were 60 ksi for the longitudinal column bars and 40 ksi for all other reinforcement. These material strengths were typical of design in the 1950s and 1960s. The reinforcing for the columns and beams in the exterior frame are detailed in Fig. 2.2. The six

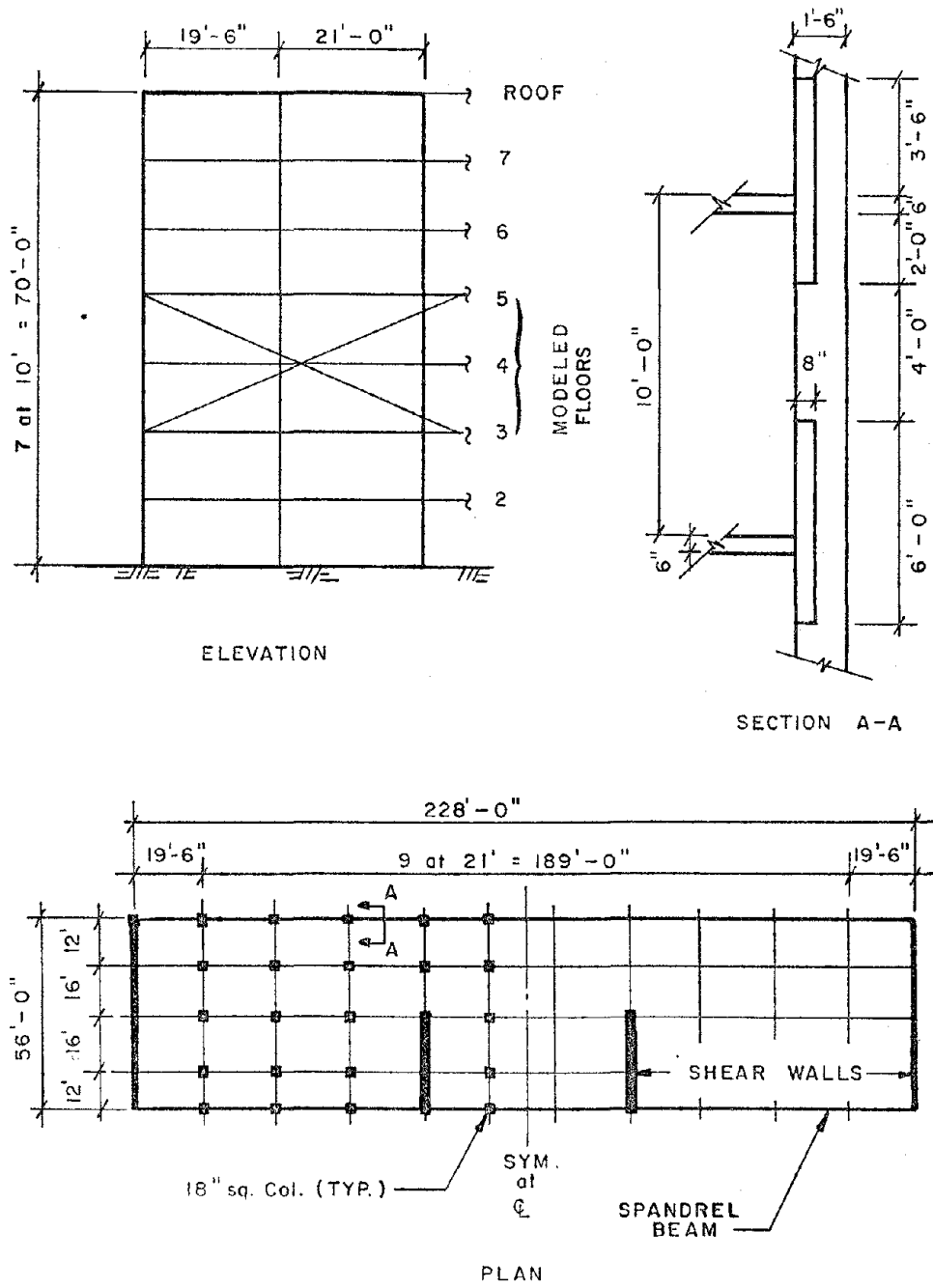
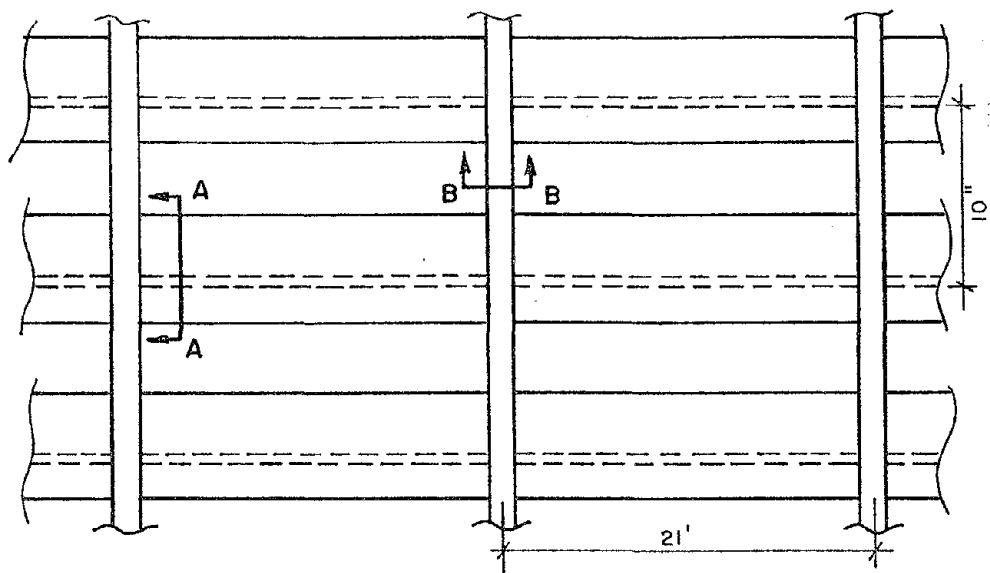
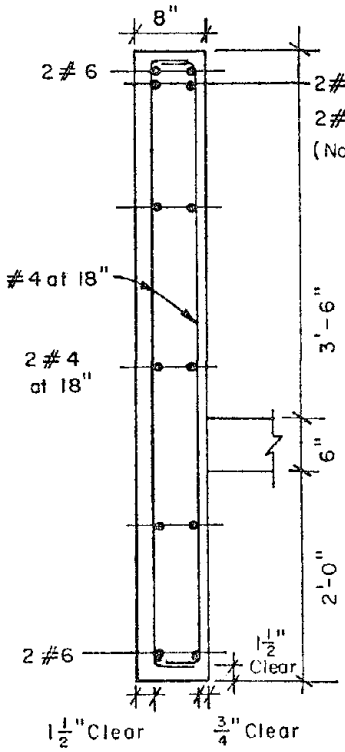


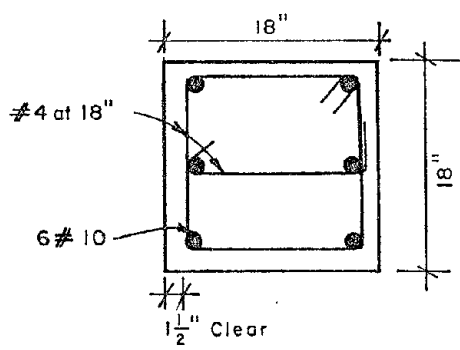
Fig. 2.1 Prototype building, plan and elevation



ELEVATION



SECTION A-A



SECTION B-B

Fig. 2.2 Details of exterior moment resisting frame

#10 column bars were spliced just above the slab level on each floor. The bottom layer of positive moment steel in the beam was spliced in the column area. All other longitudinal reinforcement in the beam was spliced in the midpoint of each bay. Two extra #6 or #8 bars were placed in the negative moment region of the spandrel beams for added negative moment capacity.

2.1.2 Strengthening of the Prototype Building. The prototype building was evaluated according to current earthquake regulations as specified in the 1982 edition of the Uniform Building Code (UBC) and the 1983 edition of the American Concrete Institute Building Code Regulations (ACI 318-83). The design earthquake loads for the prototype building from both the 1955 UBC and the 1982 UBC are seen in Fig. 2.3. The 1982 design loads are over twice those of the 1955 UBC. Figure 2.4 shows an evaluation of the member nominal capacities and failure mode of the exterior moment resisting frame. Member nominal capacities;  $M_{nb}^-$ ,  $M_{nb}^+$ ,  $V_{nb}$ ,  $M_{nc}$ ,  $V_{nc}$ ; were calculated using ACI 318-83 specifications. The calculations were made using design material strengths of 3000 psi concrete compressive strength and yield strengths of 60 ksi for longitudinal column bars and 40 ksi for all other steel. The evaluation of the prototype building revealed the moment resisting frame was deficient in strength and in its performance as a ductile frame.

The investigation of the failure mode of the moment resisting frame revealed that the weak link would be the short (4 ft) columns between beams. The nominal shear capacity of a typical short column calculated using ACI 318-83 Eqs. 11-3 and 11-17 was 51 k. Under lateral loads, the shear developed in the column due to end moments would exceed the nominal shear capacity of the column before 40% of the calculated nominal flexural capacity of the column developed and before 30% of the calculated nominal flexural capacity of the beams developed. A column shear failure is a non-ductile failure which endangers the building's gravity load carrying system.

In addition to the weak columns, the frame did not meet many of the requirements of Appendix A of ACI 318-83 [16]. Appendix A contains special provisions for design and construction in high seismic risk regions. The prototype building did not meet the special requirements for minimum transverse reinforcement spacing, minimum flexural strength of columns, width to depth ratio of beams and splice requirements.

The moment resisting frame was also inadequate in terms of strength. As seen in Fig. 2.3, the earthquake design loads

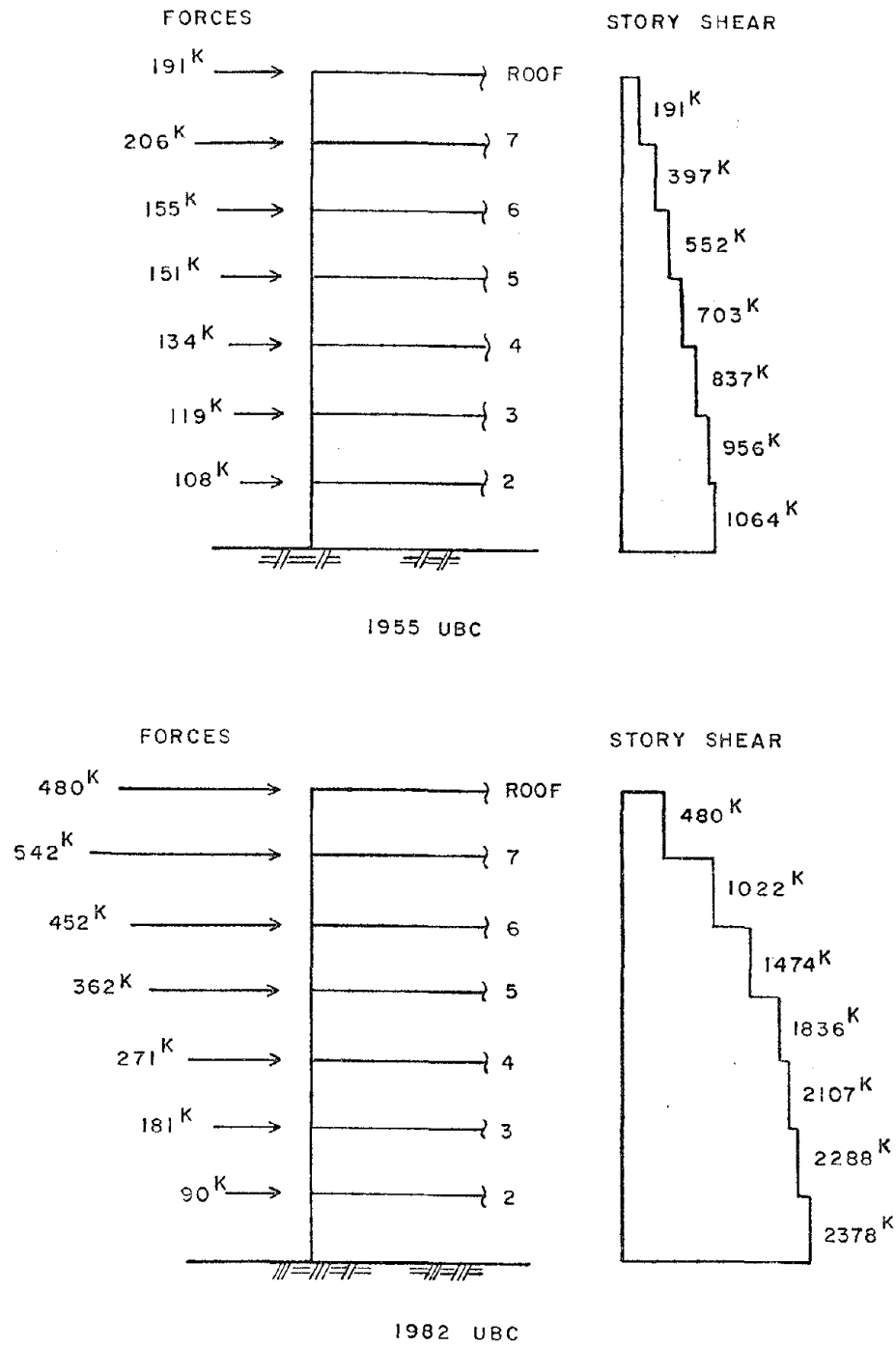


Fig. 2.3 Design loads for prototype building based on UBC earthquake regulations

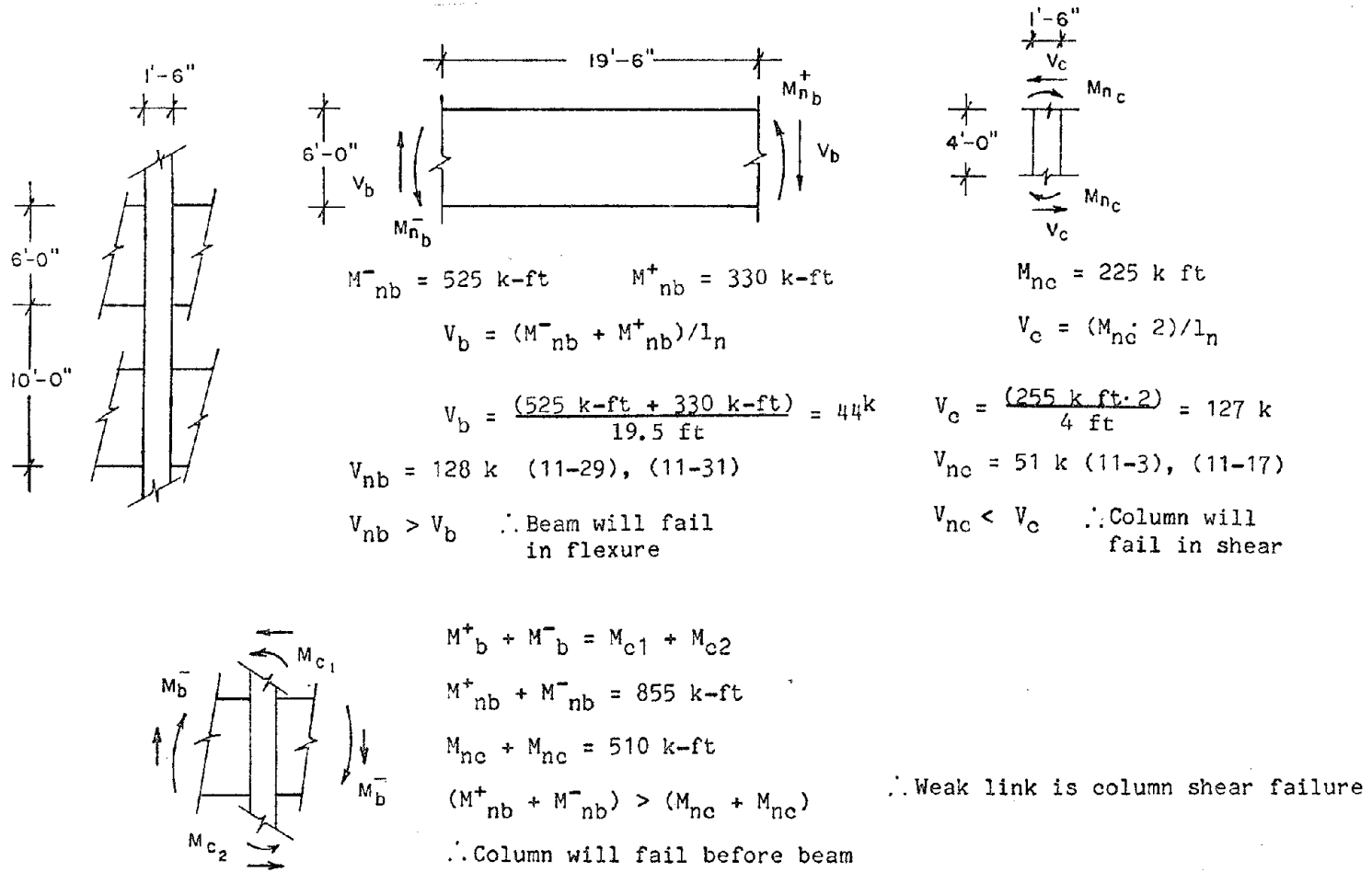


Fig. 2.4 Evaluation of exterior frame failure mode

for the prototype building calculated using the 1982 UBC were over twice the 1955 UBC design loads. It was assumed that the exterior columns, which were shorter and stiffer than the interior columns, carried the major portion of the lateral load. The first level story shear for the 1955 UBC earthquake loads was 1064 k which could distribute 48 k to each of the 22 exterior columns. The first level story shear for the 1982 UBC earthquake loads was 2378 k which could distribute 108 k to each of the 22 exterior columns. With a calculated shear capacity of 51 k the columns are severely inadequate for the 1982 design earthquake loads.

The purpose in strengthening the prototype building was to increase the ductility and the lateral strength of the exterior moment-resisting frame. The strengthening scheme used involved retrofitting the exterior frame with reinforced concrete piers cast around the exterior three sides of each of the columns along the entire height of the structure. The piers were designed to create very strong columns to resist lateral loads and fully develop the flexural capacity of the beams. Developing the flexural capacity of the beams would change the failure mode of the frame from the non-ductile column shear failure to a ductile flexural beam failure. In addition to strength and ductility requirements, constructibility and aesthetics were important considerations in the strengthening design.

The reinforced concrete pier design increased the column width to 7 ft 6 in. and the thickness to 1 ft 8 in. The pier was 12 in. thick along the spandrel beam face and 1 ft 8 in. thick in the 4 ft window opening between spandrel beams. The pier connected to the exterior frame through concrete adhesive bond and epoxy-grouted dowels. To increase bond of new concrete to old concrete, the design included sandblasting the surface area of the existing frame against which the pier would be cast. The dowel design required standard reinforcing bars, epoxy-grouted into the exterior frame and cast into the pier. The strengthening was designed using ultimate strength requirements in the 1982 UBC and ACI 318-83. The specified concrete compressive strength was 3000 psi. A yield strength of 60 ksi was specified for the deformed reinforcing bars.

The pier design is illustrated in Figs. 2.5 and 2.6. Figure 2.5 has a section of the new column at the spandrel beam face and in the window opening. Figure 2.6 is an elevation of the new column illustrating the sandblasted area and the dowel locations. Although the original frame could not be altered to satisfy the requirements of ACI 318-83 Appendix A ("Special

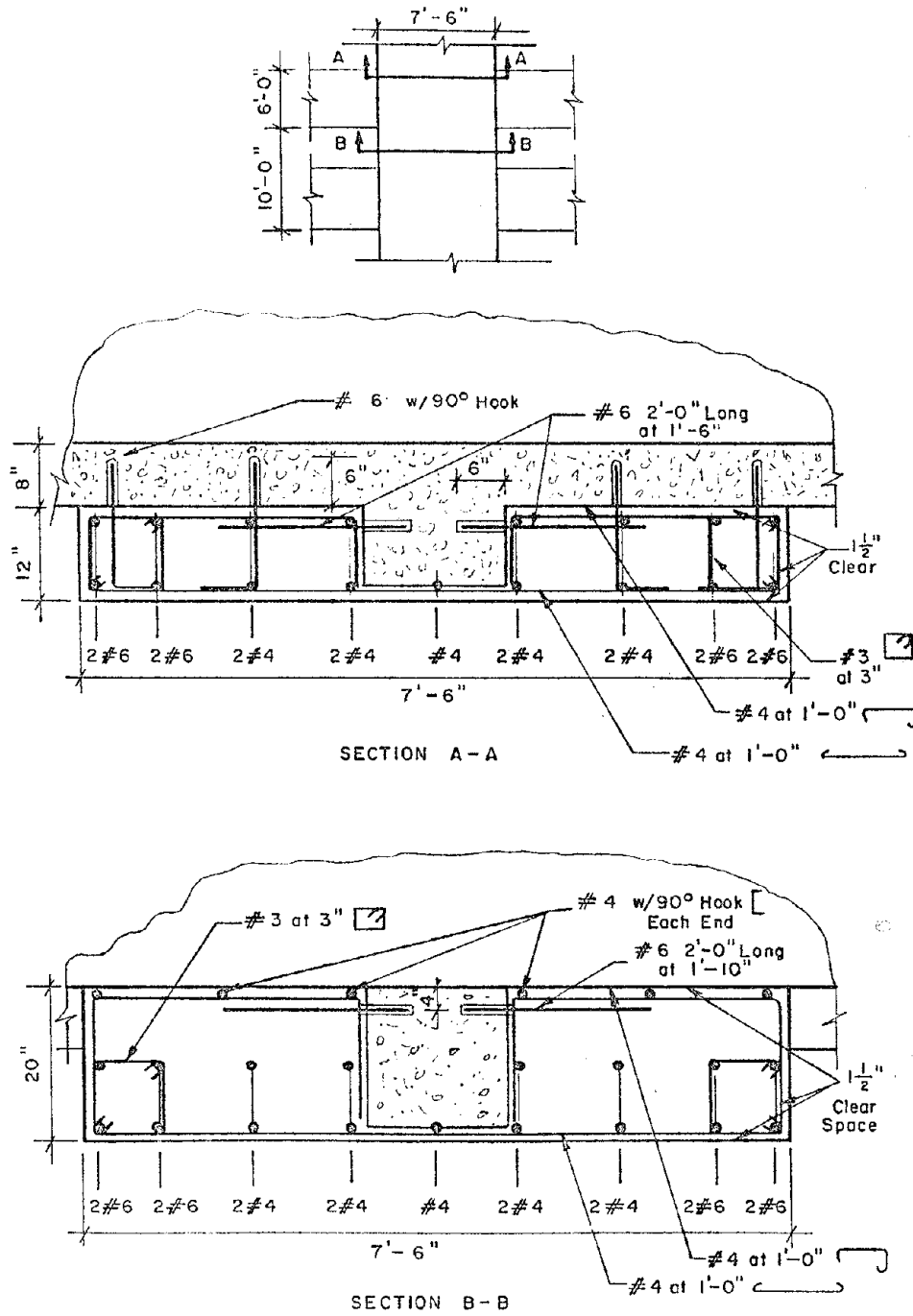


Fig. 2.5 Details of reinforced concrete pier

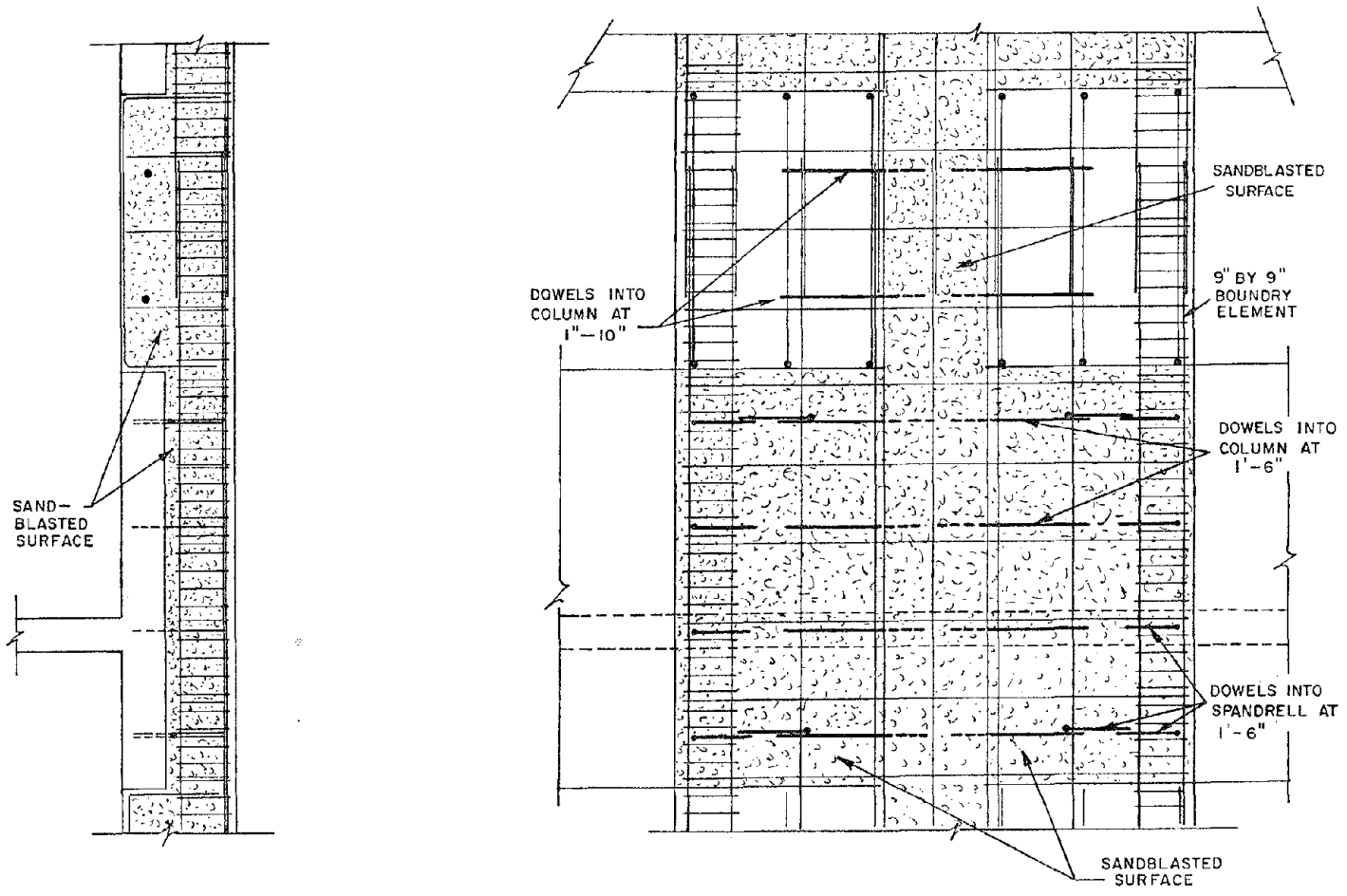


Fig. 2.6 Reinforcement in pier

Provisions for Seismic Design"), the strengthening was designed to meet the requirements for buildings in zones of high seismic risk. The pier was designed according to section A.5 of ACI 318-83 for structural walls, diaphragms and trusses. The design called for boundary elements at both ends of the new column. To be conservative, the steel in the boundary elements was designed to carry the entire overturning moment in the new column. Each of the 9 in. x 9 in. boundary elements had four #6 longitudinal bars and, to satisfy confinement requirements, #3 hoops at 3 in. spacing. In addition to the boundary elements there were nine #4 longitudinal bars continuous along the new column. No. 4 stirrups were placed across the entire width of the new column at a 1 ft spacing as indicated in Fig. 2.5.

To enhance monolithic behavior of the strengthened frame, provisions were made for load transfer between the original frame and the strengthening elements. At low loads shear transfer was anticipated to occur through bond between old and new concrete. After adhesive bond was overcome, load transfer through lug action, shear-friction, and dowels was expected.

The lug action was created by extending the piers into the window opening between the spandrel beams creating a concrete shear key. With this configuration the spandrel beam was expected to transfer forces into the wing wall through compression of old concrete against new concrete along the top and bottom faces of the spandrel beam.

Transfer of forces would also occur due to shear-friction between concrete surfaces. The majority of the shear-friction would occur on the spandrel beam face. Dowels, epoxy-grouted into the spandrel beam, were designed as shear-friction reinforcement across the new/existing concrete interface. These dowels are shown in Figs. 2.5 and 2.6. The strengthening design also called for epoxy-grouted dowels across the old-to-new concrete surface on either side of the column. All of the dowels were #6 reinforcing bars ( $F_y = 60$  ksi) epoxy-grouted with an embedment of 6 in. The dowel embedment was designed according to results of tests conducted by Luke at The University of Texas [17]. Besides serving as shear-friction reinforcement, the dowels provided connections between the original frame and the new column to encourage monolithic behavior. Figure 2.7 illustrates the transfer actions assumed to be involved in the reinforced concrete strengthening design.

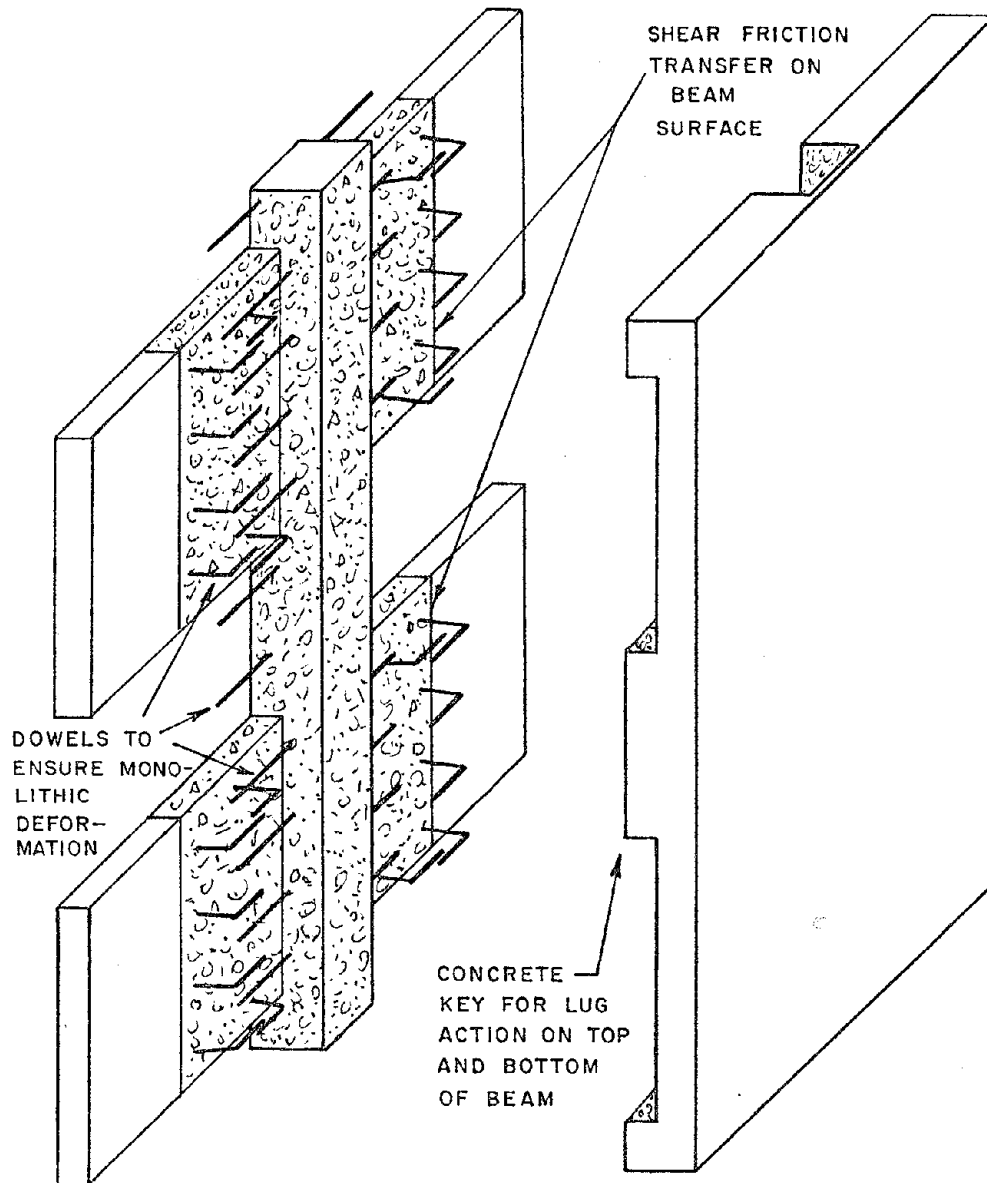


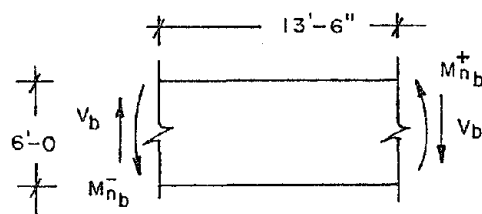
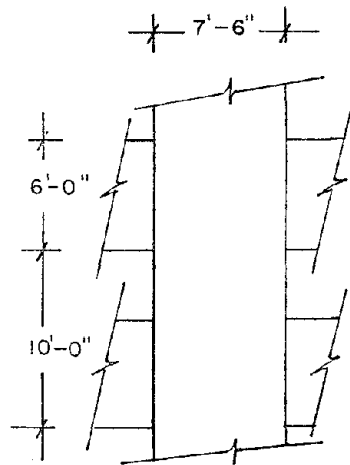
Fig. 2.7 Load transfer actions in pier strengthening

The strengthened frame was evaluated according to the 1983 ACI regulations using design material strengths, and the results are shown in Fig. 2.8. The original column had a calculated nominal flexural capacity of 255 k ft in comparison to 2545 k ft for the strengthened column. The calculated nominal shear capacity of the original column was increased from 51 k to 365 k for the strengthened column. The nominal shear capacities of the columns were calculated using Eqs. 11-3 and 11-17 of ACI 318-83. The nominal shear capacity of 365 k well exceeded the design earthquake first story shear of 119 k per column. Figure 2.8 also illustrates that the failure mode of the frame was changed with the strengthening scheme. The weak link in the strengthened frame under lateral loads would be flexural hinging of the beams at the joint. Flexural hinging of the beams is a ductile failure and does not directly endanger the gravity system of the building. The beam hinging should occur before 57% of the shear capacity and before 17% of the flexural capacity developed in the strengthened column. Although the flexural capacity was in excess of that needed to develop joint failure, it was necessary to provide adequate capacity against overturning at the ground level.

The evaluation of the strengthening scheme revealed that the main goals of increasing lateral strength and ductility of the exterior moment-resisting frame were accomplished. The lateral strength of the retrofitted frame was calculated to be four times that of the original frame. The strengthened frame should carry approximately two times the 1982 UBC design earthquake loads before beam hinging. The failure mode of the frame was altered to that of a ductile, flexural failure which would allow further deformation without endangering the gravity load carrying system. Evaluating the strengthening scheme with respect to aesthetics and constructibility is a subjective matter and would be more readily discussed after a presentation of the construction of the experimental model and new columns.

## 2.2 Existing Frame Model

2.2.1 Design of the Existing Frame Model. The test specimen was a 2/3 scale model of two bays between the third and fifth stories of the exterior moment resisting frame of the prototype building. The bottom of the model corresponded to the bottom of the third story spandrel beam of the frame and the top of the model corresponded to the top of the fifth story spandrel beam. These will henceforth be referred to as the first, second and third levels of the model frame. The model dimensions were



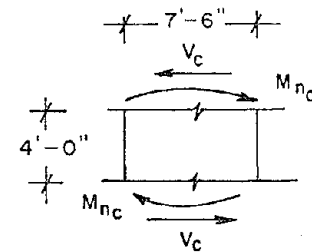
$$M_{nb}^- = 525 \text{ k-ft} \quad M_{nb}^+ = 330 \text{ k-ft}$$

$$V_b = (M_{nb}^- + M_{nb}^+) / l_n$$

$$V_b = \frac{(525 \text{ k-ft} + 330 \text{ k-ft})}{13.5 \text{ ft}} = 63 \text{ k}$$

$$V_{nb} = 123 \text{ k} \text{ (11-29), (11-31)}$$

$V_{nb} > V_b \therefore$  Beam will fail in flexure

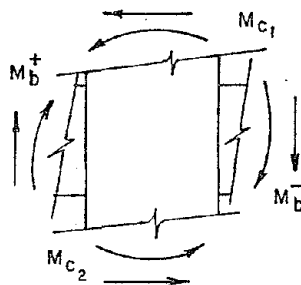


$$M_{nc} = 2545 \text{ k-ft}$$

$$V_c = (M_{nc} \cdot 2) / l_n$$

$$V_c = \frac{(2545 \text{ k-ft} \cdot 2)}{4 \text{ ft}} = 1273 \text{ k}$$

$$V_{nc} = 365 \text{ k} \text{ (11-3), (11-17)}$$



$$M_b^+ + M_b^- = M_{c1} + M_{c2}$$

$$M_{nb}^+ + M_{nb}^- = 855 \text{ k-ft}$$

$$M_{nc} + M_{nc} = 5090 \text{ k-ft}$$

$$(M_{nb}^+ + M_{nb}^-) \ll (M_{nc} + M_{nc})$$

$\therefore$  Maximum beam moment will develop first

Approximate Maximum  $V_c$ :

$$M_c = 1/2(855 \text{ k-ft}) = 427 \text{ k-ft}$$

$$V_c = (2 \cdot M_c) / l_n$$

$$V_c = (855 \text{ k-ft}) / 4 \text{ ft} = 214 \text{ k}$$

$$V_{nc} = 365 \text{ (11-3), (11-17)}$$

$V_{nc} > V_c$  Column will not fail in shear

$\therefore$  Weak link is flexural failure of beams

Fig. 2.8 Evaluation of failure mode of strengthened frame.

developed by scaling all dimensions of the prototype frame by a 2/3 scale factor. A 4 ft width of slab was added on the inside of the frame at each level to allow for some redistribution of loads into the slab and to better represent the restraints on the spandrel beams. Figure 2.9 is a drawing of the model of the existing frame.

The design yield strength of the reinforcing steel for the model was 60 ksi for the column longitudinal steel and 40 ksi for all other reinforcement. Some reinforcing bars could not be scaled exactly but total steel area at critical sections was scaled closely. The reinforcing bar with an area closest to the desired area was used; that is, #10, #8, #6 and #4 were scaled to #7, #5, #4 and #3, respectively. The details of the model frame are shown in Fig. 2.10. Indicated in Fig. 2.10 are the locations of the 18 in. column lap splice, the 12 in. beam lap splices and the extra negative reinforcement in the beam. Also indicated are the extra stirrups in the beam and column in the joint area.

To model the behavior of two interior bays of the prototype frame, boundary constraints were added to the test specimen as indicated in Fig. 2.11. The ends of beams (midspan) were restrained against vertical deformations. Loads were applied through the third level slab and reactions were provided through the first level slab. Column bases were supported on neoprene pads and uplift was controlled through the base reactions. Out-of-plane bracing was provided at the first and third levels. To accommodate these constraints, some changes were made in the original model frame.

Because of the high loads in the slab at the loading points on the third level and the reactions on the first level, a 2 in. deep drop panel was added to the 4 in. slab at these locations. The drop panels were 5 ft wide centered on the columns as shown in Fig. 2.12. The reinforcement for the 4 in. slab and the 6 in. drop panel area is detailed in Fig. 2.13. To create vertical reactions on the ends of the beam at each level, structural steel struts were added to the model at the ends of the cantilever beams. The beams were lengthened by 8 in. and the slab was shortened by 8 in. at the ends of the frame to create clearance for the steel struts. The first level beam also had a 16-1/2 in. by 9 in. blocked out section at the bottom to create clearance for the floor reactions of the struts. The final design of the test specimen, referred to as the unstrengthened or existing frame, is illustrated in Fig. 2.12.

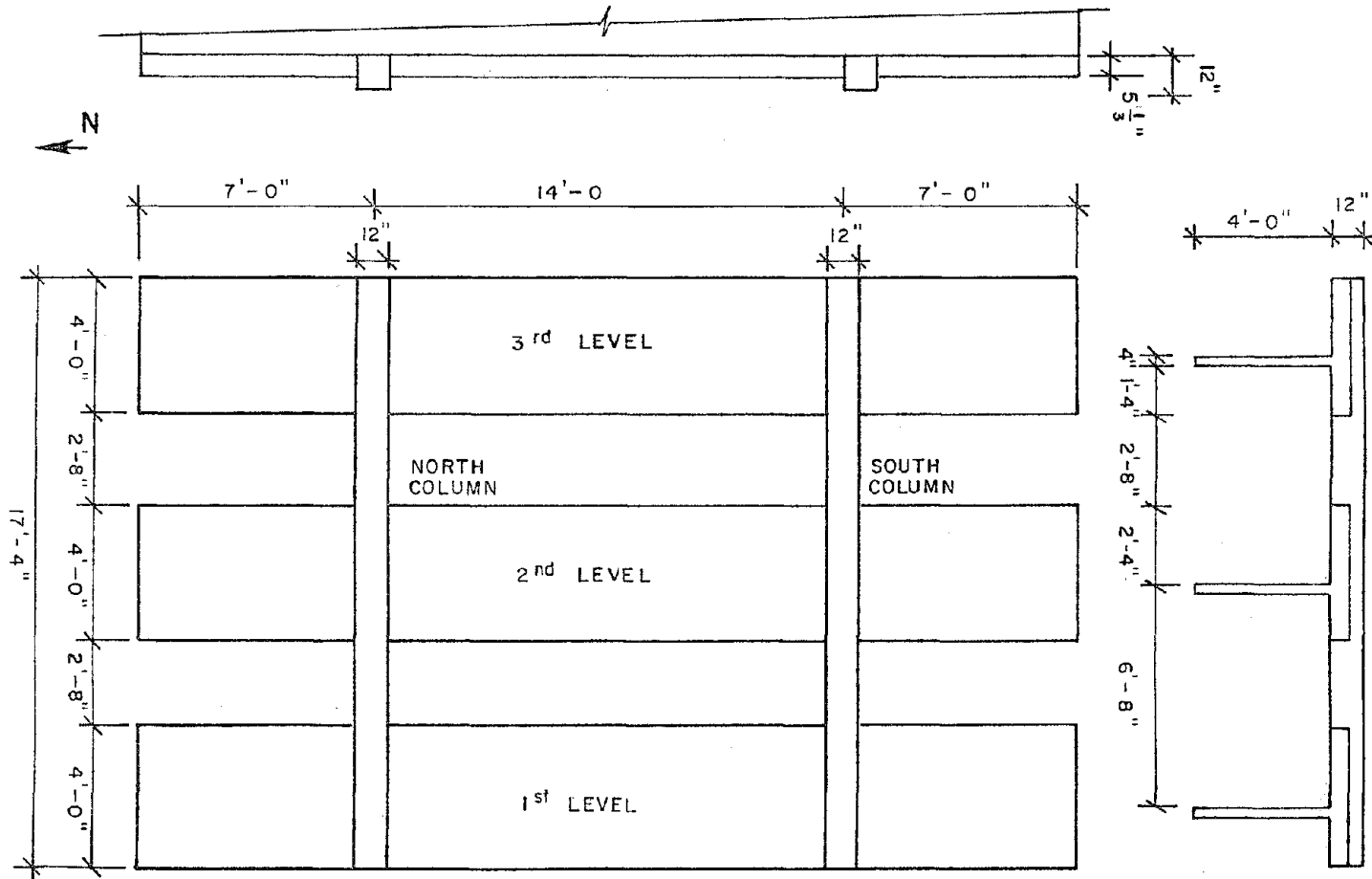
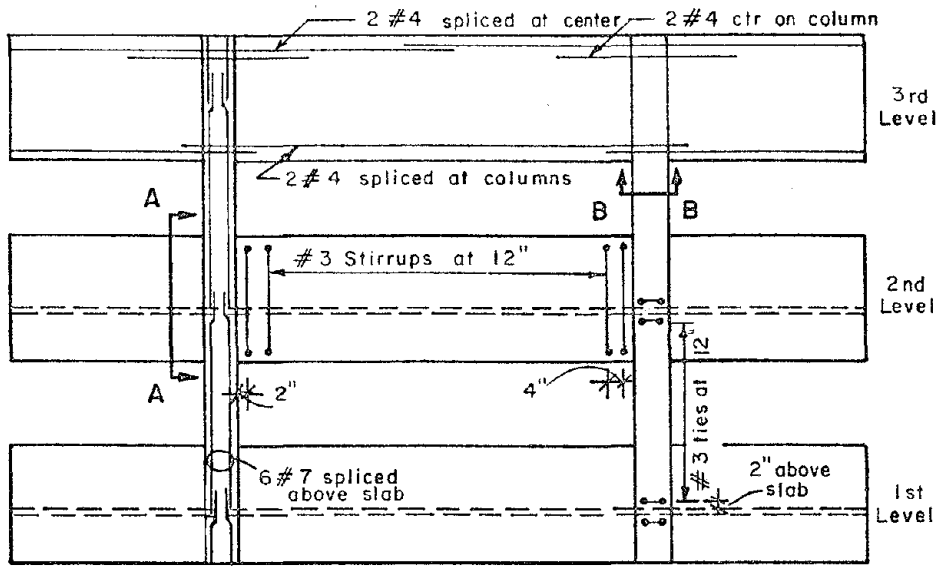


Fig. 2.9 Test Specimen (existing structure) - two bays between 3rd and 5th stories of exterior moment resisting frame



ELEVATION

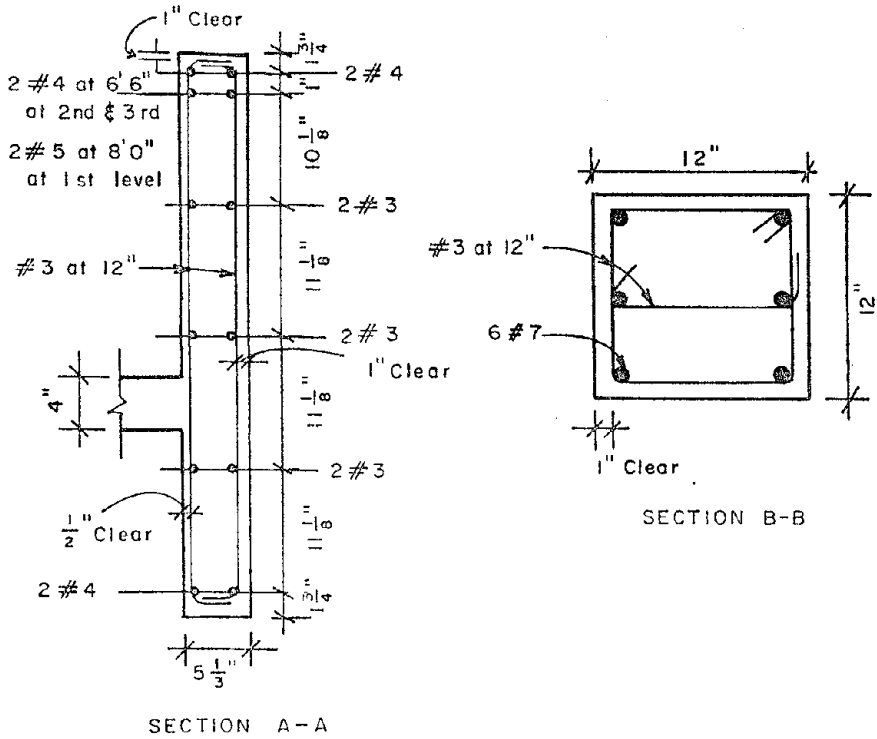


Fig. 2.10 Details of 2/3 scale model of existing frame.

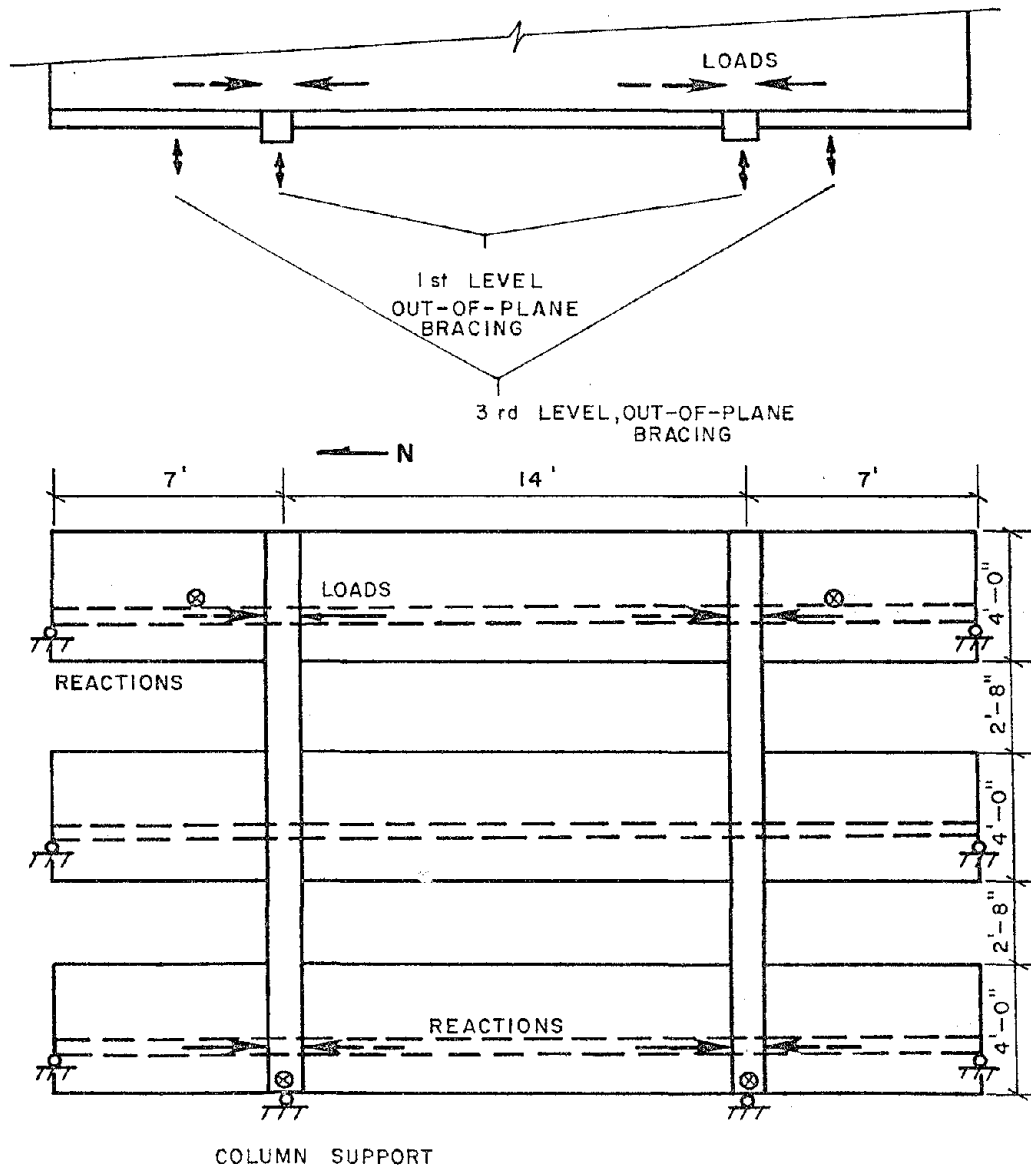


Fig. 2.11 Boundary constraints modeled on test specimen

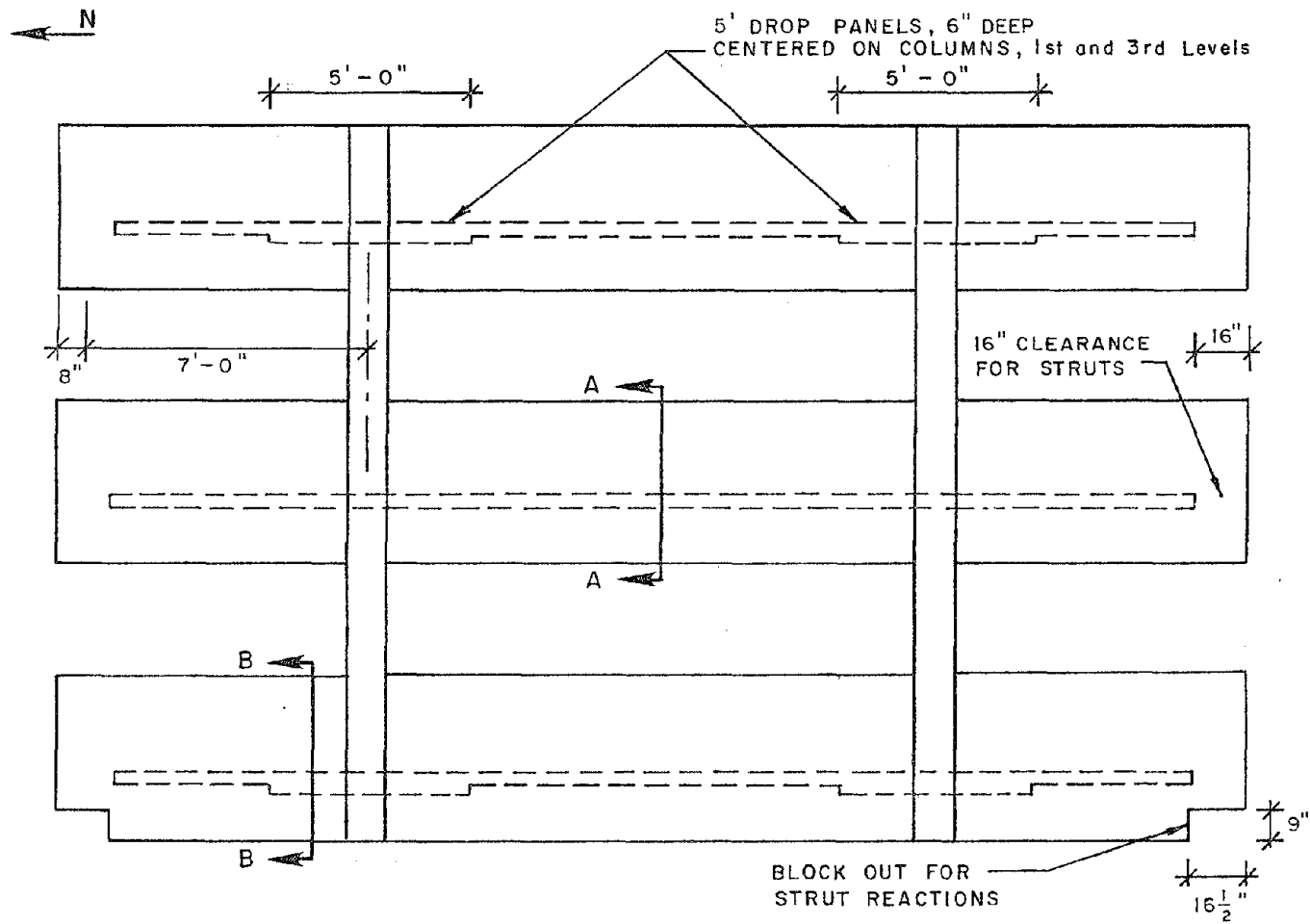


Fig. 2.12 Final design of test specimen.

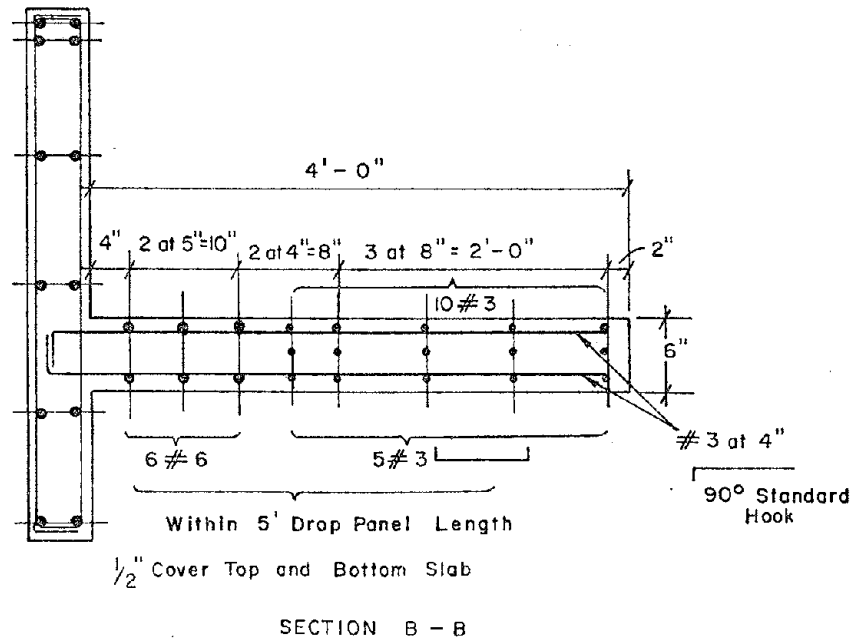
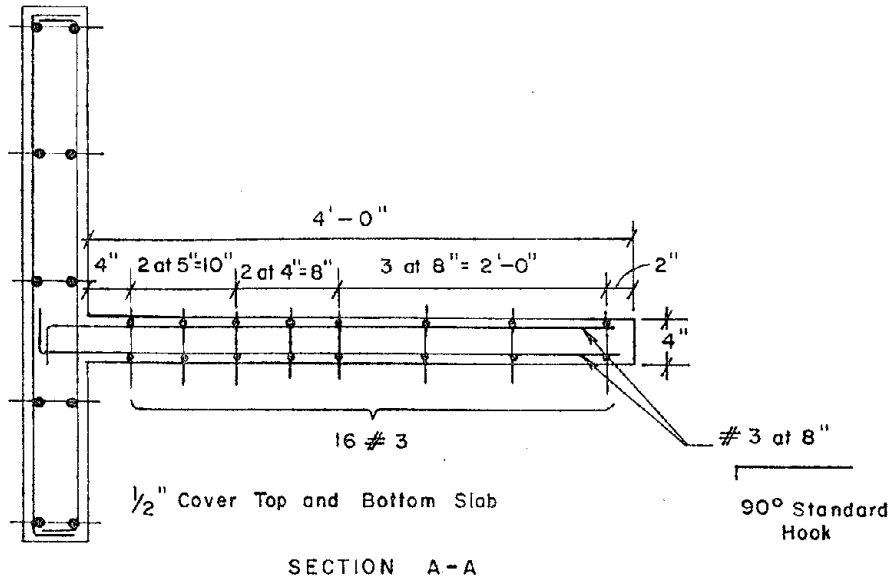


Fig. 2.13 Section through slab and drop panel

2.2.2 Construction of the Existing Frame Model. The existing frame was constructed in place in the Phil M. Ferguson Structural Engineering Laboratory. The frame was oriented in the north-south direction on the floor-wall reaction system in Ferguson Laboratory as seen in Fig. 2.14. The construction techniques were typical of those used for cast-in-place reinforced concrete buildings. The construction was completed in six casting stages; the sequence of the casting stages is indicated in Fig. 2.15. Figure 2.15 also indicates the concrete compressive strengths for each of the casting stages, determined from testing 6 in. x 12 in. control cylinders. The yield strengths of the reinforcement were tested to be between 55 ksi and 65 ksi with ultimate stresses 50% greater. Each floor level was cast in two stages. In the first stage, the bottom of the spandrel beam and the slab were cast. In the second stage, the upper portion of the spandrel beam and the column were cast. In the sixth stage no columns were needed. A commercial ready mix supplier delivered the designated concrete mix. The concrete mix, listed in Table 2.1, was the same for each cast.

The concrete was placed using a concrete bucket and transported by an overhead crane. Internal concrete vibrators were used for compaction. The mix was designed for a 4-1/2 in. slump. However, additional water was added to the truck at the laboratory to increase the slump to a value in the range of 6 to 8 in. to facilitate placing of the concrete around the narrow reinforcing cages. Nine control cylinders, 6 in. by 12 in., were cast from each casting stage. After each cast was completed, the concrete was covered with polyethylene sheets for moist curing.

For the first cast at each level of the frame (stages 1, 3 and 5), concrete was placed to the top of the slab as is typical in construction. At this stage the forms were in place for the slab, the bottom inside face of the spandrel beam and the outside faces of the beam and column. The beam cage was in place, as was the slab steel and the column cages. The slab forms were supported by shores and the beam forms were held in place with standard button-type snap ties. One lift was placed in the bottom of the spandrel beam, approximately 8 in. deep, and a second lift finished the beam and slab to the top of the slab level. Figure 2.16 shows placement of the slab at the second level. After placing the concrete, the slab was screeded and the beam concrete surface was roughened for better bond at the cold joint.

In the second cast for the first two levels of the frame (casting stages 2 and 4) the upper portion of the beam and

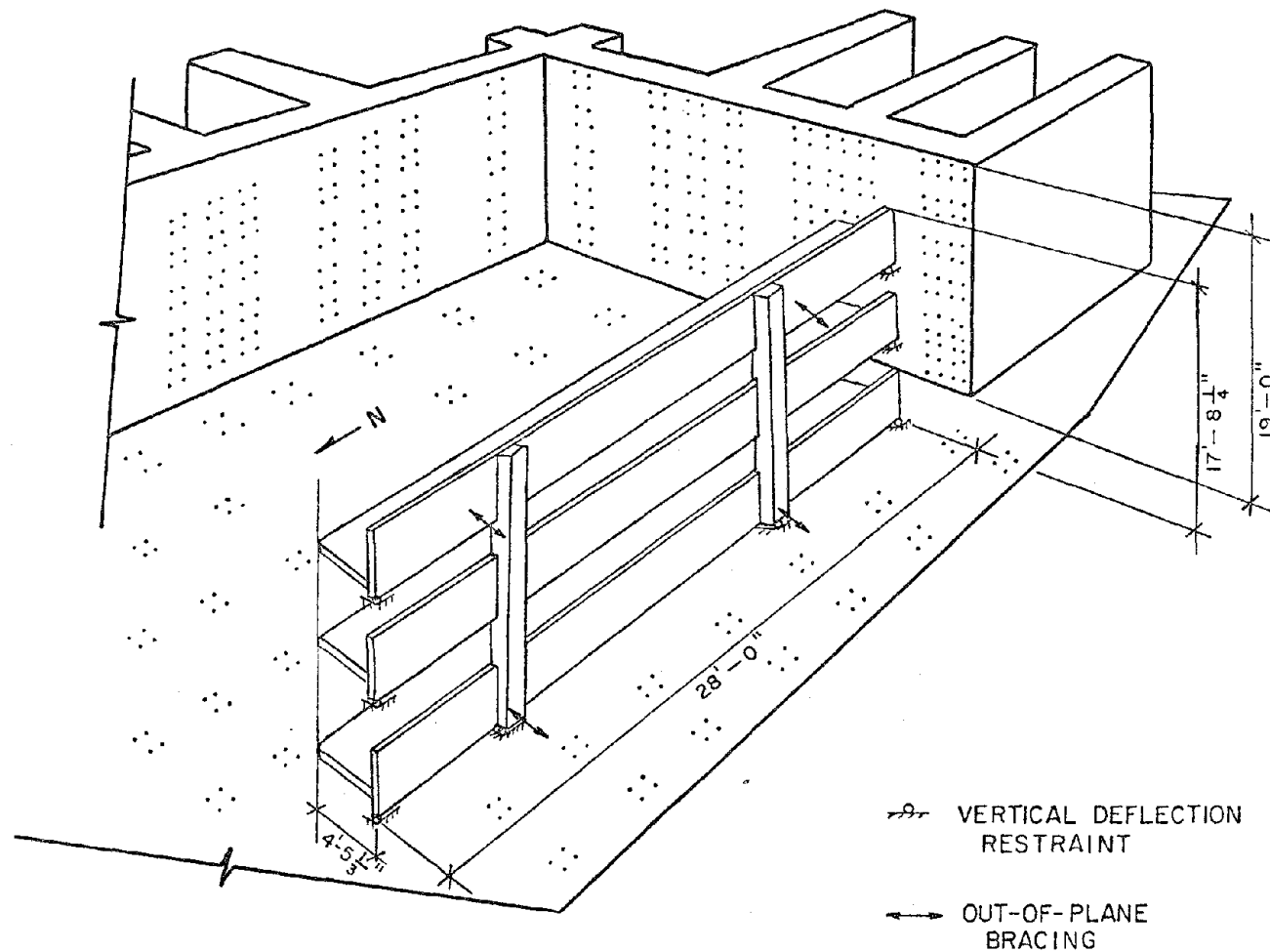
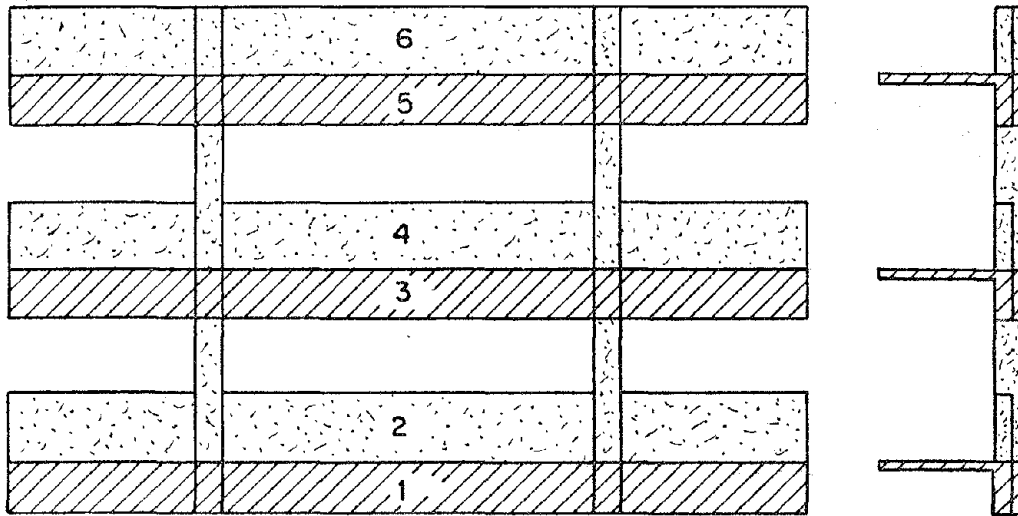


Fig. 2.14 Frame location on floor wall reaction system



6	[5950]	(5450)*
5	[2810]	(2580)
4	[4350]	(3730)
3	[4520]	(4350)
2	[4750]	(4560)
1	[3990]	( )**

[ ]  $f'_c$  OF CONCRETE AT TIME OF STRENGTHENED FRAME TEST

( )  $f'_c$  AT 28 DAYS ( )\*  $f'_c$  AT 47 DAYS

( )\*\* UNAVAILABLE

Fig. 2.15 Casting stages for construction of existing frame model and concrete compressive strengths for each casting stage

Table 2.1 Concrete Mix Proportions

---

Concrete Mix Design (3000 psi)	
Proportions per cu yd	
Water	250 lb
Cement (4-1/2 Sacks)	420 lb
Fine Aggregate	1360 lb
Coarse Aggregate	1735 lb
Spec 494 Water Reducer-Retarding Admixture	13 oz
Solair Air Entraining Admixture	3 oz

---

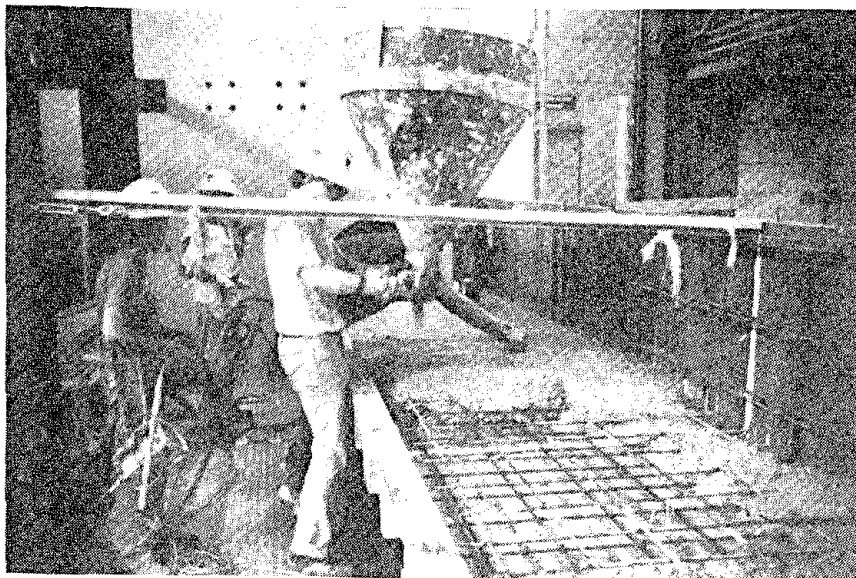


Fig. 2.16 Casting stage 3. Concrete placed to top of second level slab

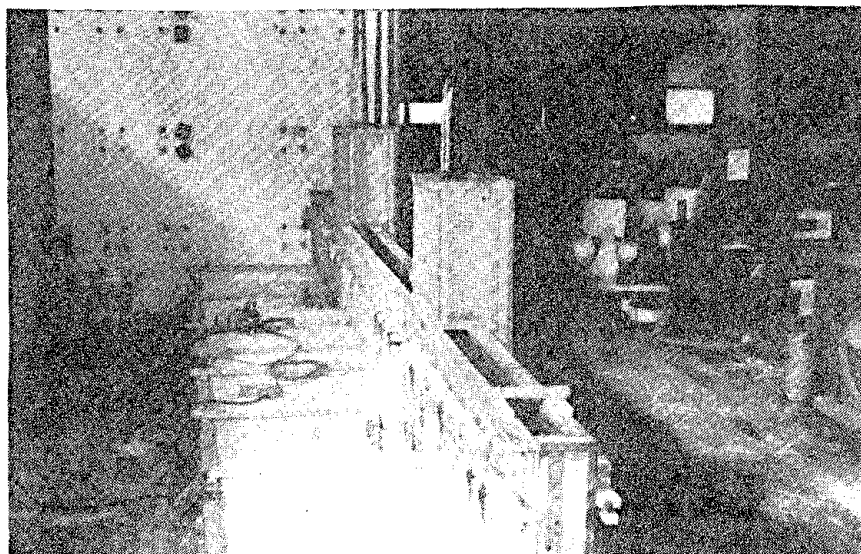


Fig. 2.17 Casting stage 2. Forms in place for first level beam and column

the short columns were cast. The column bars were spliced just above the slab to the bars embedded below. The forms for the top part of the inside of the beam were placed on the previously cast slab and held in place with snap ties. The column cages were completed for the columns and the forms were bolted into place. Figure 2.17 shows the forms just before casting stage 2. During these stages, concrete was placed in the beam forms in two lifts (Fig. 2.18). When the beam forms were filled plywood was nailed across the forms on either side of the column to prevent the concrete from slumping out of the beam forms. Next, the two columns were cast in two lifts each. Casting stage 6 followed this pattern but there were no columns.

The forms were stripped after completing the second cast at each level (stages 2, 4 and 6). At that time shores were left in place to support the new slab and the formwork was moved up to the next level. Figure 2.19 is a picture of the frame after stripping the forms after casting stage 2. The forms were stripped approximately fourteen days after casting. Figure 2.20 is a picture of the completed existing frame model.

### 2.3 Strengthened Frame Model

2.3.1 Strengthening Design for the Existing Frame Model. The piers for the existing frame model are shown in Fig. 2.21. The reinforcing for the model piers is detailed in Fig. 2.22. Grade 60 reinforcing bars were used throughout the new piers except for the hoops in the boundary elements where Grade 40 1/4 in. diameter plain bars were used. The 15 in. lap splices for the longitudinal bars were located at the midheight of the window opening.

2.3.2 Construction of Piers. First, the existing frame was prepared for fabrication of the piers. The surfaces against which concrete was to be cast were lightly sandblasted, roughening the surface to increase the bond of new concrete to old concrete. A vertical groove was chipped in the middle of the outside face of each of the columns (Fig. 2.23). This was necessary to provide proper cover of the reinforcement across the face of the existing columns.

The final step in preparing the frame was placement of the epoxy-grouted dowels. The holes were drilled in the frame (Fig. 2.24) with a rotary concrete hammer using a 3/4 in. bit (1/4 in. larger than the dowel bar diameter). The holes were then cleaned using the method recommended by Chon et al.[18]. The cleaning process involved removing the largest portion of the

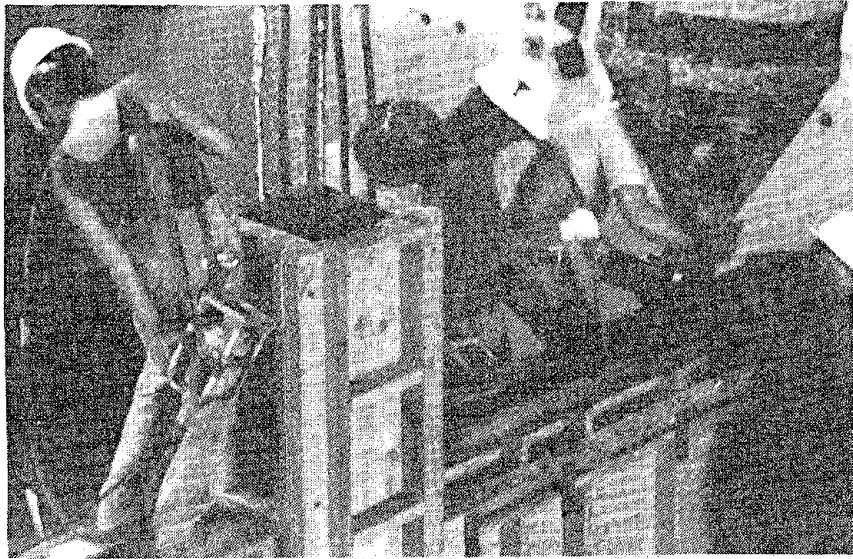


Fig. 2.18 Placing concrete in upper portion of beam form

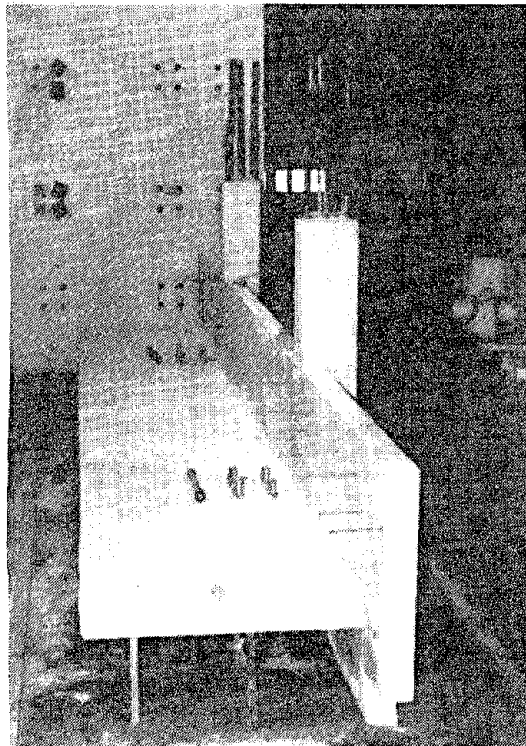


Fig. 2.19 Forms were stripped after casting stage 2

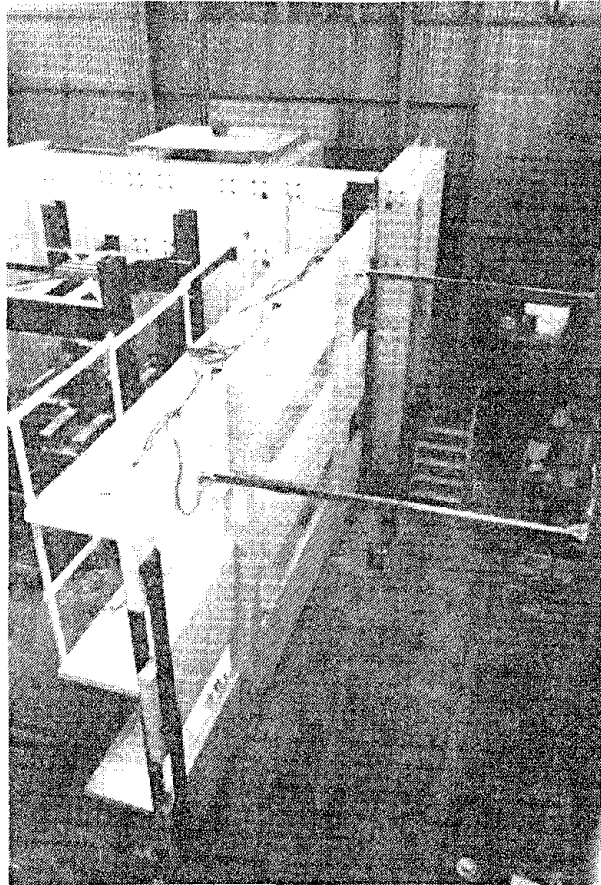


Fig. 2.20 The completed existing frame model

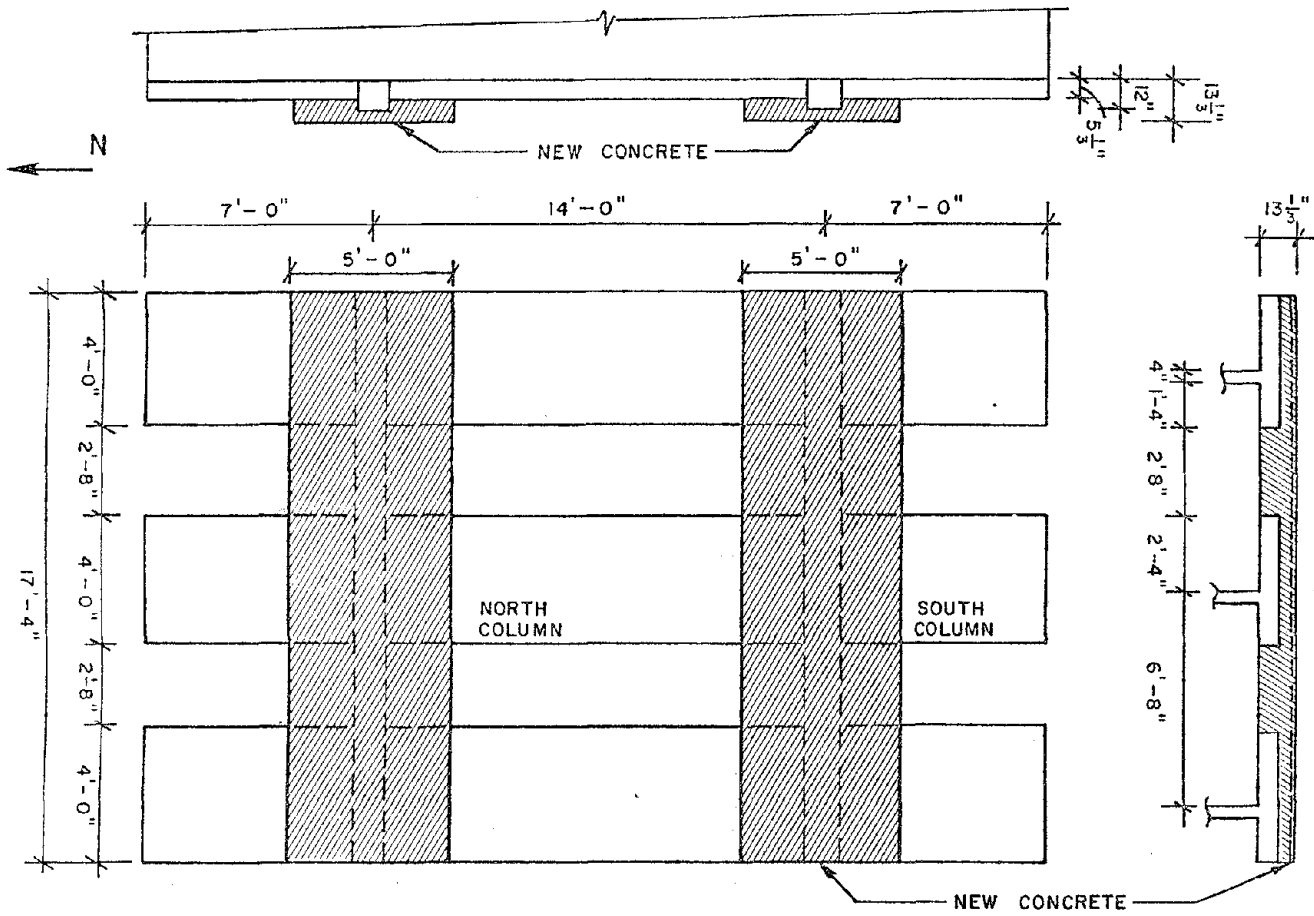


Fig. 2.21 Model retrofitted with R/C piers

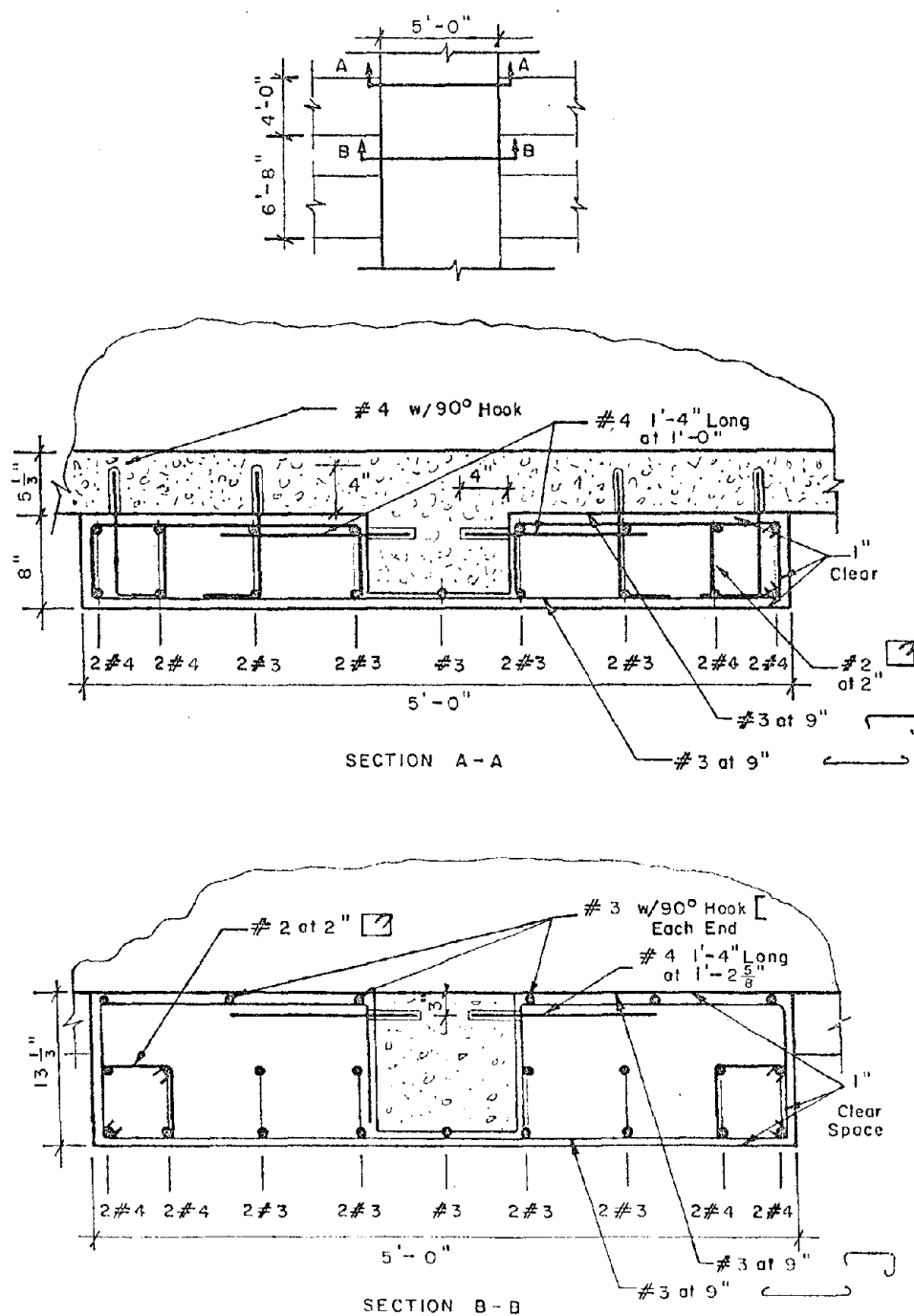


Fig. 2.22 Details of 2/3 scale model of R/C pier

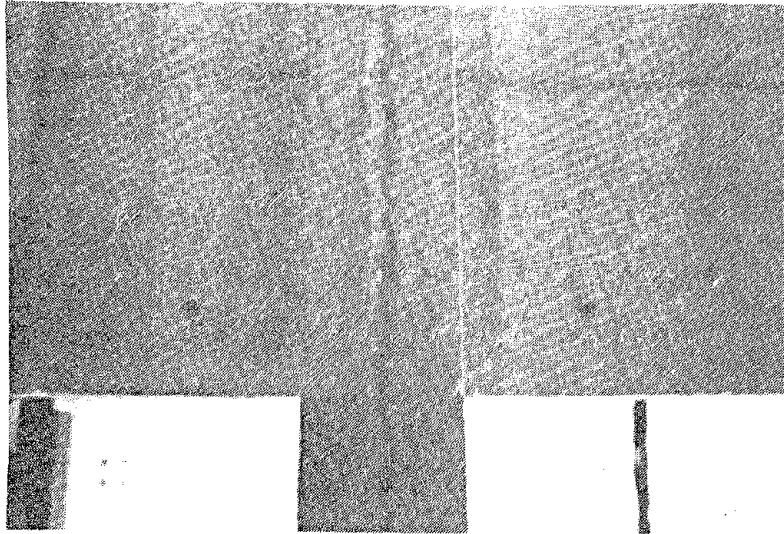


Fig. 2.23 Frame prepared by sandblasting surface and chipping groove in column face

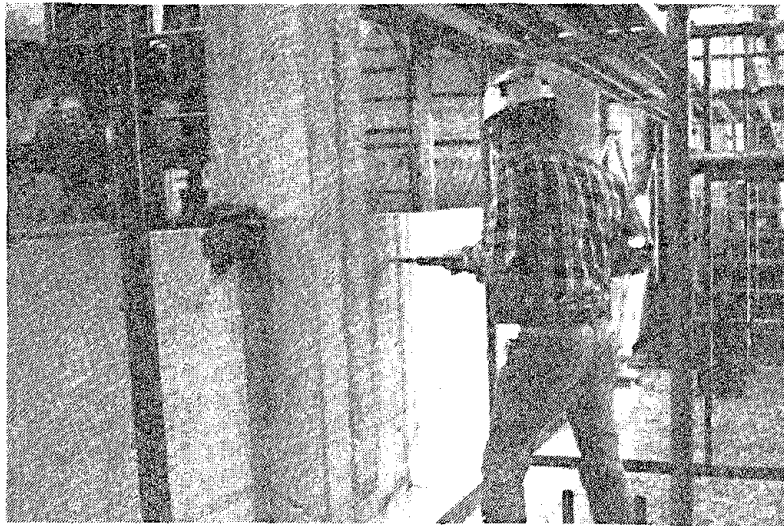


Fig. 2.24 Drilling holes for dowels

dust from the hole with a stiff bristle bottle brush, vacuuming the hole, using a toothbrush to loosen any remaining dust and vacuuming the hole again.

The dowels were epoxy-grouted into the frame using Adhesive Engineering Concrete 1411, a medium viscosity, non-sag epoxy. After thoroughly mixing the two ingredients of the epoxy (Fig 2.25), the epoxy was placed in the hole using a caulking gun. As the hole filled, the gun was slowly retracted (Fig. 2.26). The dowels were inserted while turning them 180 degrees. One hundred thirty-five dowels were epoxy-grouted into the frame using one gallon of the Concrete 1411. The potlife time of the epoxy, 2-1/2 hours, was not exceeded. The epoxy cured for two days before the reinforcing cage was placed.

The reinforced concrete strengthening was cast using the techniques discussed previously. The concrete mix design was the same as that used in the existing frame construction. The slump was again increased to 6 to 8 in. by adding water to the truck at the laboratory. A high slump was desirable because of the need for good compaction in highly congested areas. The two piers were constructed in three casting stages. The casting stages and concrete compressive strengths are shown in Fig. 2.27. The yield strengths of the reinforcement used were tested to be approximately 74 ksi with ultimate stresses 50% greater. The first two casting stages were each a full story height, 6 ft 8 in. In the third stage, the remaining 4 ft of the piers were cast. Nine 6 in. by 12 in. control cylinders were cast during each stage.

The reinforcing cages for the piers were constructed after the epoxy set around the dowels. The combination of the stiff boundary elements with ties at 2 in. spacing, the need for threading the cage between previously epoxy-grouted dowels and tying the cage against existing concrete complicated the construction of the pier reinforcement. Each of the pier cages was constructed in what was considered the optimum procedure. The first step was to tie the #2 hoops to two of the #4 longitudinal reinforcing bars of each boundary element. These boundary element cages were then placed against the frame with the two #4 bars on the face of the boundary element farthest from the column and the hoops threaded between the appropriate dowels. A third longitudinal bar of the boundary element was threaded down through the hoops in the inside corner of the element as seen in Fig. 2.29. The inside and outside #3 stirrups were then hooked around the two boundary elements and tied in place. In order to place the remaining #4 bars in the boundary element



Fig. 2.25 Mixing epoxy ingredients

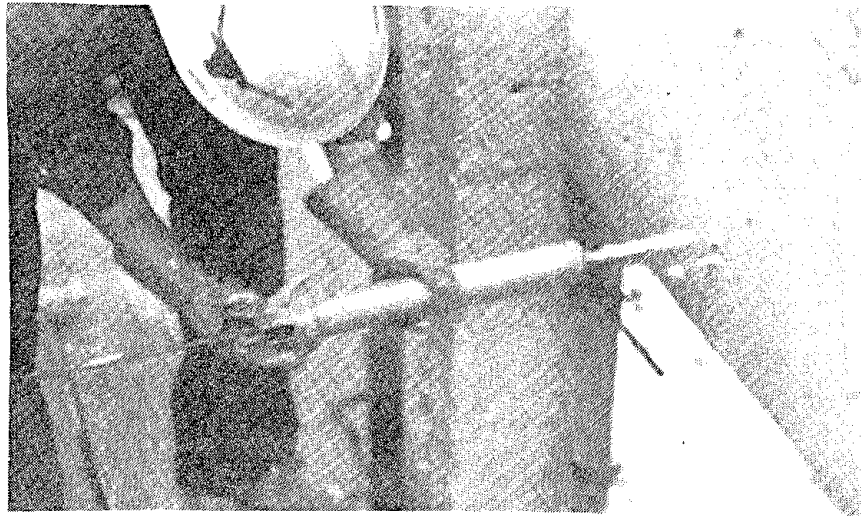
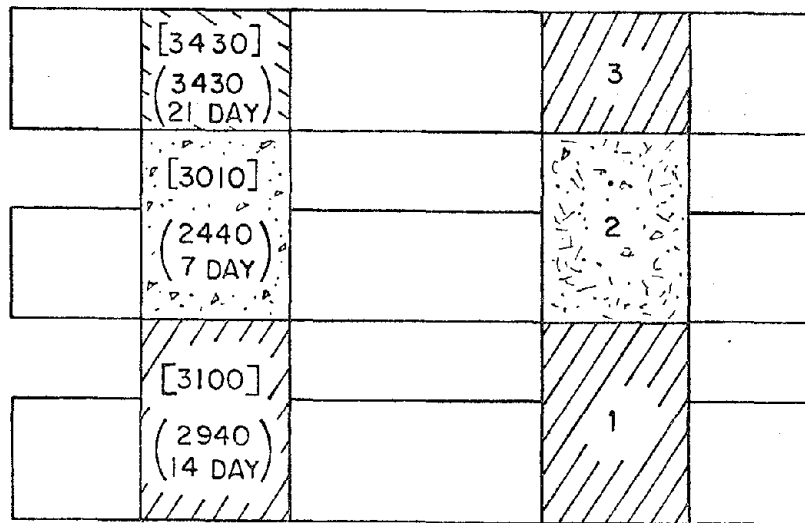
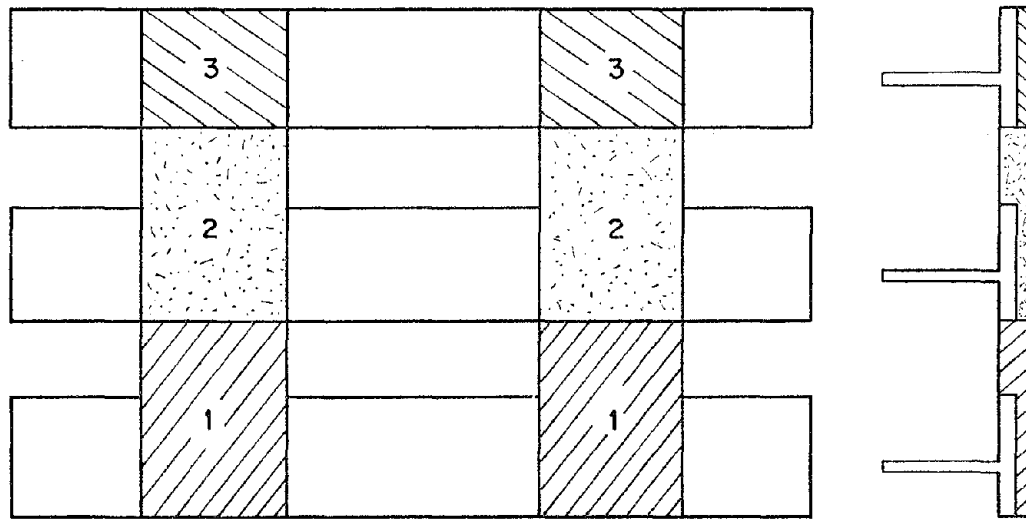


Fig. 2.26 Placing epoxy in dowel hole with caulking gun



[ ]  $f'_c$  OF CONCRETE AT TIME OF STRENGTHENED FRAME TEST

Fig. 2.27 Casting stages for construction of R/C pier strengthening and concrete compressive strengths for each casting stage.

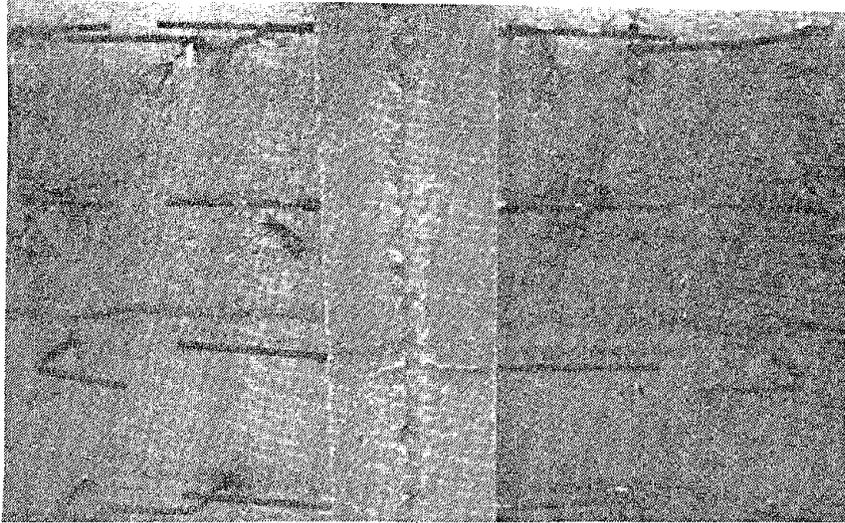


Fig. 2.28 Frame with dowels in place before constructing reinforcing cage

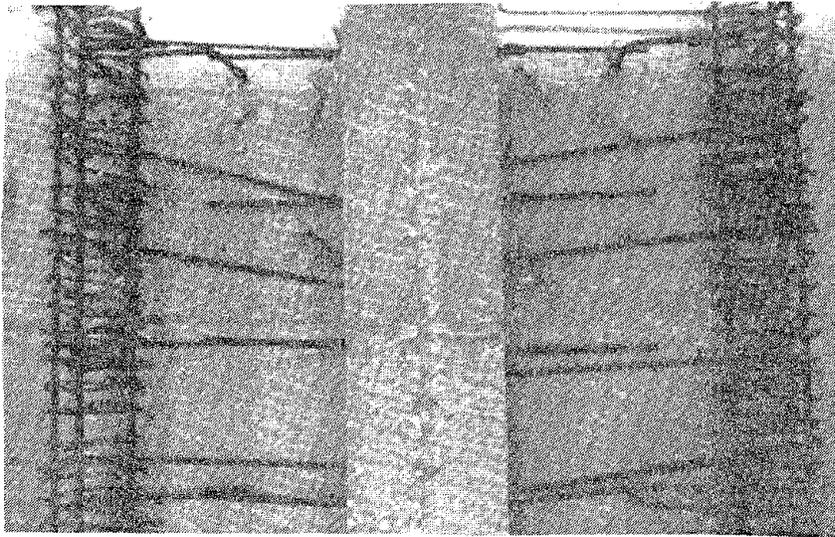


Fig. 2.29 Boundary elements in place with three or four longitudinal bars

hoops, the boundary element cage had to be rotated out of position. The rest of the longitudinal bars in the piers were then threaded down through the transverse steel and tied in place (Fig. 2.30). Finally, the inside #3 hooked bars (within the window segments) were tied as seen in Fig. 2.31. Because the bars were spliced at the window segment, it was necessary to tie two stages of reinforcement prior to placing concrete for the first stage.

Casting one story at each stage was convenient for alignment and logistic purposes. However, placing concrete seven feet through very narrow cages was likely to cause segregation of the aggregate and paste, as well as making compaction difficult. For this reason, the forms were built so that the concrete could be placed at two different heights. The forms were constructed so that the exterior three sides of the formwork were in place for the entire cast. The interior piece which would form the inside of the strengthened column in the space between beams was a separate piece. For the first part of the cast the exterior formwork was in place and the interior formwork was left off. The concrete was placed from the backside (interior) of the frame into a chute which emptied into the formwork over the top of the beam (Fig. 2.32). In this manner, the first 4 ft of casts 1 and 2 was placed and vibrated from the interior of the frame. After casting the first 4 ft, the inside formwork was bolted into place (Fig. 2.33). The remaining 2 ft 8 in. was placed from the top of the exterior formwork. In field construction, the formwork would have been broken and the entire pier cast from the exterior of the building. After each cast the concrete was covered with polyethylene for moist curing. The forms were stripped after two to three days and were used in the next casting stage. Figure 2.34 is a picture of the exterior of the construction sequence and Fig. 2.35 is a picture of the completed piers.

#### 2.4 Constructibility and Aesthetics

As previously mentioned, constructibility and aesthetics are important considerations in designing a strengthening scheme. The construction of the piers for the existing model frame in the laboratory demonstrated, to some degree, the constructibility of the scheme. The most important drawback to the scheme is the necessity of disrupting normal operations in the building during construction. During the field construction of the piers, the windows would have to be removed during construction and the rooms on the building exterior cleared. However, the pier could be constructed one story at a time. The windows could be removed and the rooms cleared just

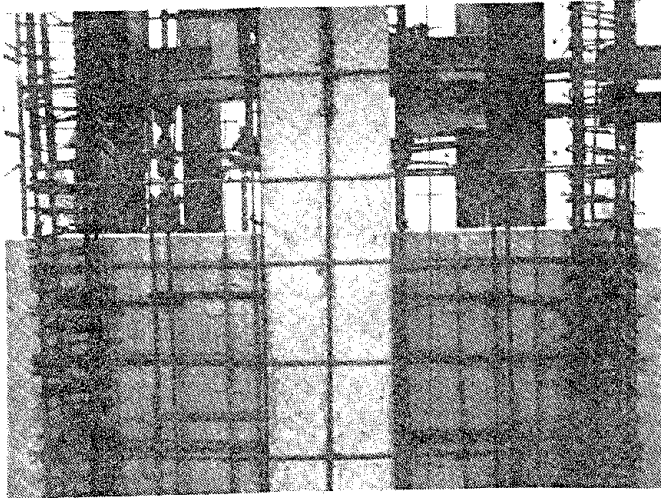


Fig. 2.30 Transverse and longitudinal steel in place

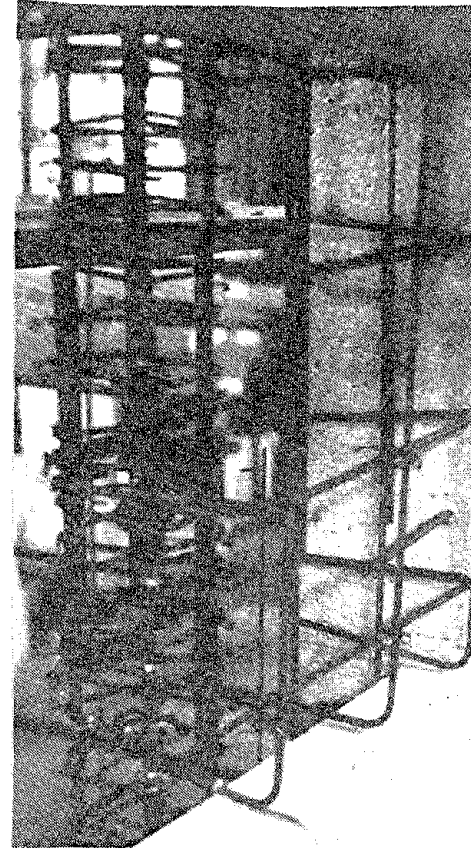


Fig. 2.31 Hooked #3 longitudinal bars in window area



Fig. 2.32 Concrete was placed from the interior of the frame using a chute which emptied into the formwork

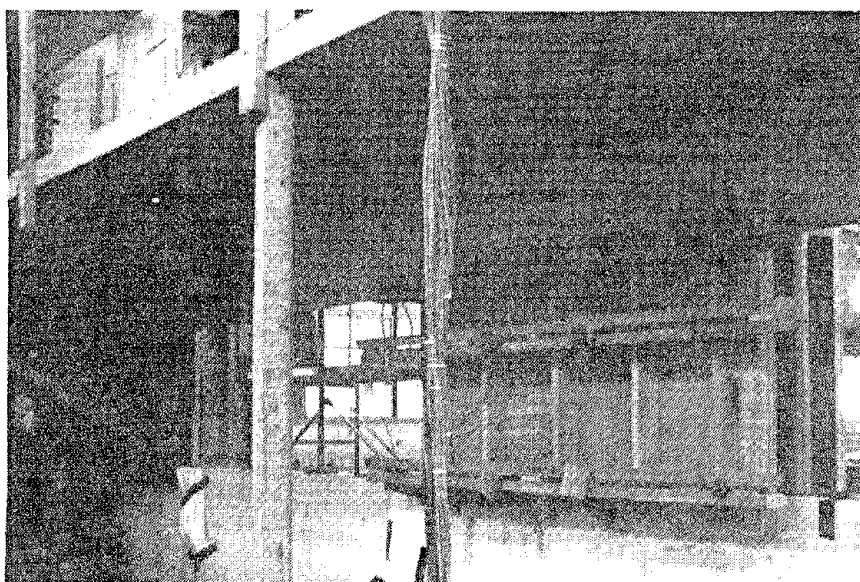


Fig. 2.33 Inside formwork in place after casting lower 4 ft of pier

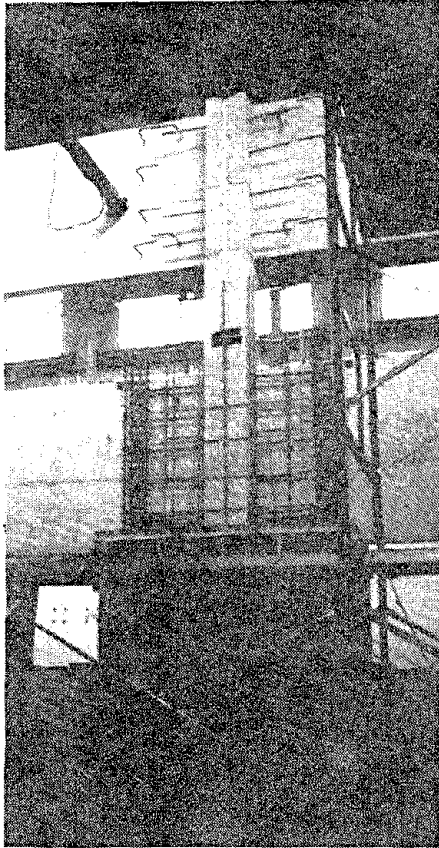


Fig. 2.34 Exterior formwork for casting stage 1

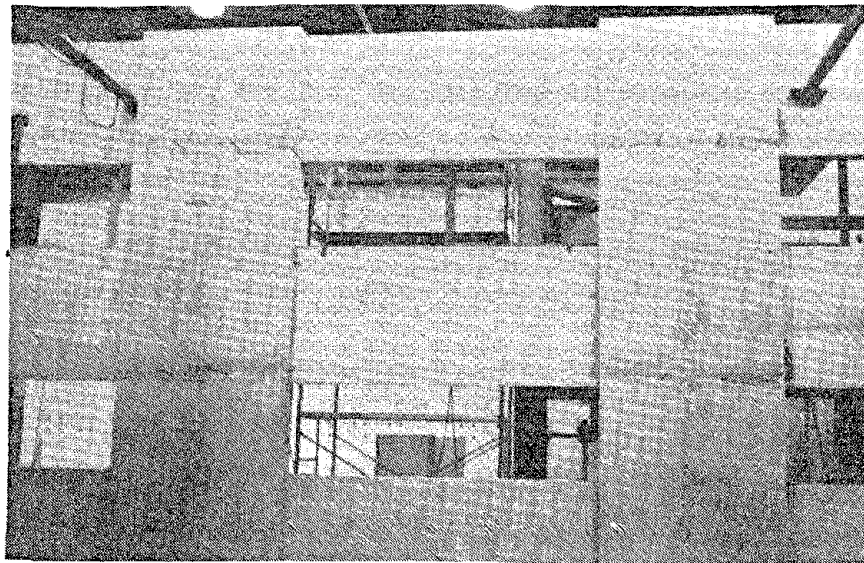


Fig. 2.35 The completed R/C pier strengthening scheme

before construction of each story of the pier. After which, the exterior could be finished and the rooms reoccupied for that story. The process of sandblasting, drilling dowel holes and epoxy-grouting dowels was not a complicated or lengthy operation. The greatest difficulty in this process was drilling the dowel holes so that they missed the reinforcement in the existing frame. Having a working knowledge of the reinforcement in the building to be strengthened while designing the dowel locations would diminish the difficulty in construction. As mentioned, tying the reinforcing cage was complicated by the stiffness of the boundary elements, threading the reinforcement around previously set dowels and tying the reinforcement against the existing concrete. However the procedure used in construction of the model pier worked well and repetition would probably speed up the process.

The pier strengthening was a constructible scheme with no major difficulties. It would interfere with normal operations of different portions of the building for short periods of time. The aesthetics of the reinforced concrete pier strengthening is a subjective matter. The piers would diminish the window space on the face of the exterior frame strengthened. The reinforced concrete piers gave the frame an appearance of balanced strength and stiffness that the existing model frame did not have.

## 2.5 Test Setup

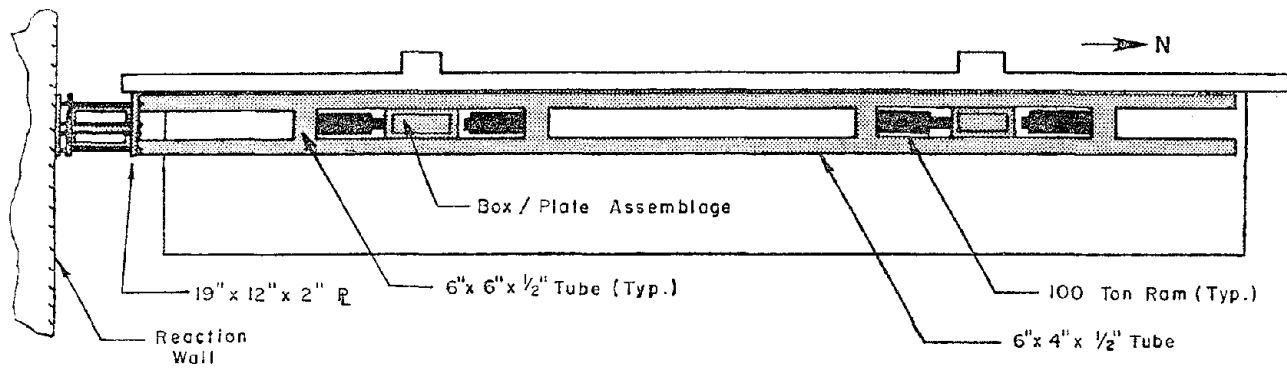
2.5.1 Loading and Reaction. The purpose of the experimental program was to subject the strengthened frame to simulated earthquake conditions. Simulating earthquake motions consisted of introducing reversed cyclic (static) lateral loads into the frame at the third or top level while reactions were provided on the first level through the reaction floor. In an actual building the interstory shear due to earthquake motions is distributed to lower floors through the columns. Introducing high magnitude lateral loads into the columns of the experimental frame would have required considerable change in the column design in the area of loading. To avoid changing the column design and decreasing the integrity of the frame as a model, the loads were introduced into the frame through the slab at the two column locations.

The loading system involved using the reaction wall, a loading frame, hydraulic rams, a hydraulic pump and a steel box/plate assemblage to introduce loads into the third level slab. Loading took place when a hydraulic ram acted against the

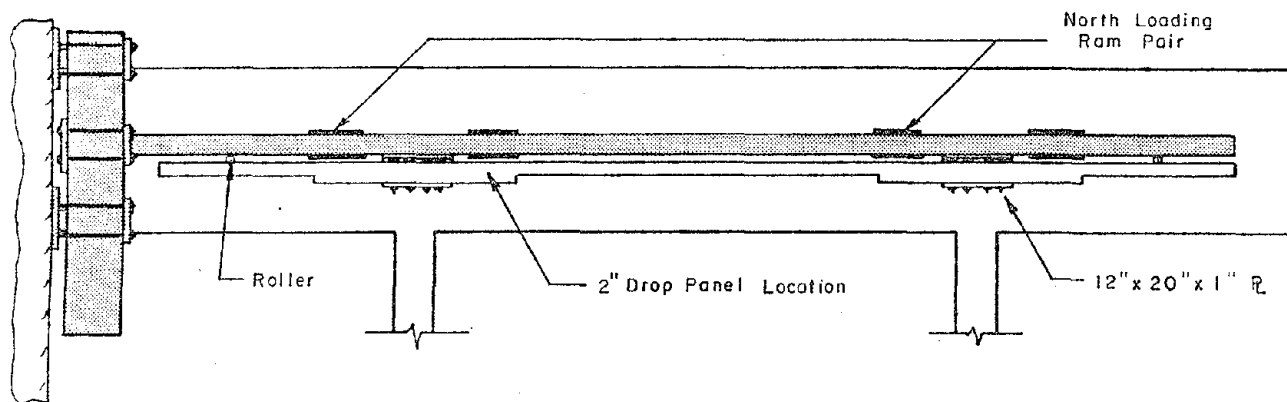
loading frame which, in turn, acted against the reaction wall. The loading frame rested on rollers on the third level slab. It was constructed from two lengths of 6x4x1/2 in. structural steel tube. These tubes were connected by four 6x6x1/2 in. structural steel tube cross pieces welded between them. On the south end of the loading frame the steel tubes were welded to a 19x12x2 in. A36 steel plate. This plate was connected to a builtup section of two 18 in. deep channels. This builtup section was connected to the reaction wall by a group of four 1-1/4 in. A193B7 threaded rods. Each set of four rods went through the reaction wall and connected to a plate on a built up section which spanned behind the buttresses of the reaction wall. This arrangement was necessary to meet loading requirements of the reaction wall. Figure 2.36 shows the plan and elevation of the loading frame. The figure illustrates the connection of the loading frame to the reaction wall. The connection of the 1-1/4 in. rods behind the buttresses is shown in Fig. 2.37. The loading frame and connection behind the reaction wall are pictured in Figs. 2.38 and 2.39.

The load was applied to the frame with four, 100 ton, hydraulic center hole rams. These rams were located in the clear space on either side of each column between the loading frame cross piece and the box/plate assemblage on the slab. The rams were connected hydraulically in pairs, each pair connected in parallel, as indicated in Fig. 2.36 so that identical load would be applied at each column. One pair of 100 ton, hydraulic rams was active at any one time and the loading frame was capable of delivering 400 kips to the frame in either direction. The rams on the south side of each column loaded the frame in the north direction, putting the loading frame in compression. The rams on the north side of each column loaded the frame in the south direction, putting the loading frame in tension. When not active, the rams were retracted and hung on 2 in. pins welded to the loading frame cross braces and the box/plate. A plan and elevation of a loading area is illustrated in Fig. 2.40.

The box section of the box/plate was constructed from 1 in. A572 GR50 steel plate and was welded to a 12x20x1-1/4 in. A36 steel plate. Under the slab was a 12x20x1 in. steel plate. Eight 1-1/4 in. A193B7 threaded rods were used to prestress the plates to the slab. The load was transferred from the box/plate into the slab through shear-friction. To strengthen the slab for the high loads at the loading points, 2 in. drop panels were designed for a 5 ft length of 4 in. slab centered on the column. In addition to increased reinforcing bar sizes, the drop panel area was reinforced with a 6x6x1/2 in. structural steel tube.



PLAN



ELEVATION

Fig. 2.36 Loading frame and connection to reaction wall

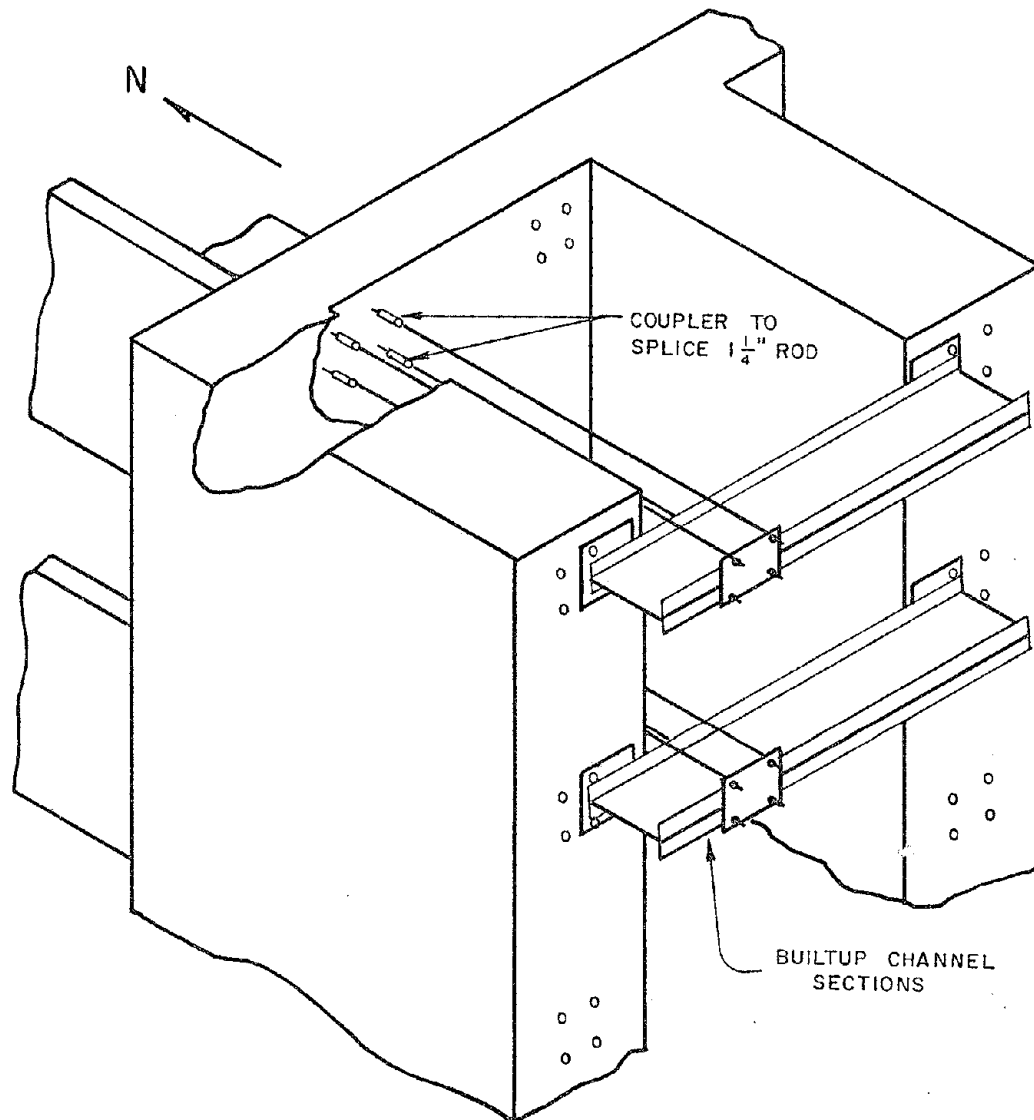


Fig. 2.37 Connection of loading frame to buttresses of reaction wall

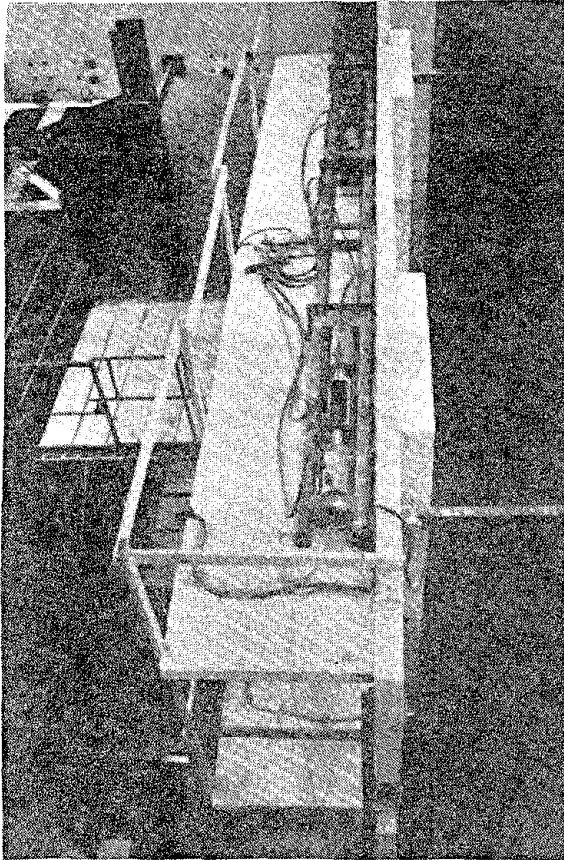


Fig. 2.38 Loading frame at third level

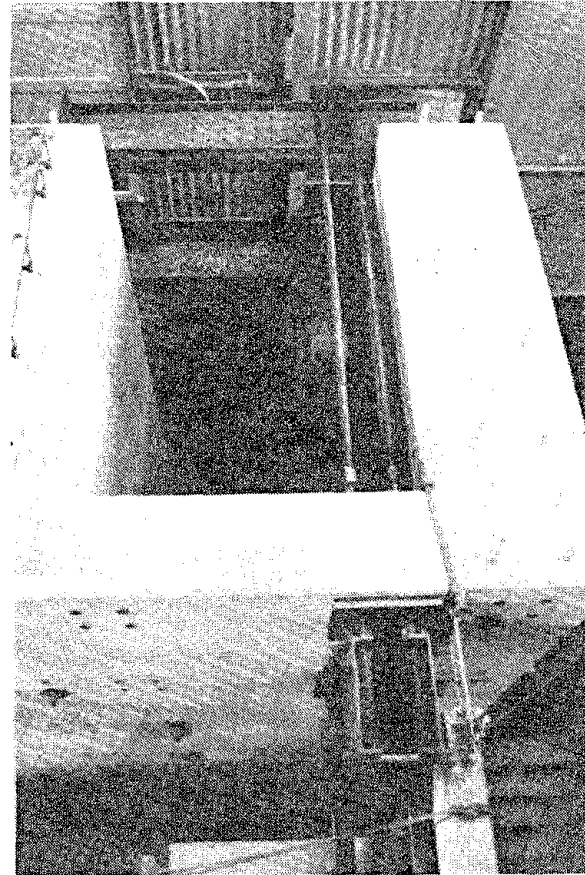


Fig. 2.39 Loading frame connection to reaction wall buttresses

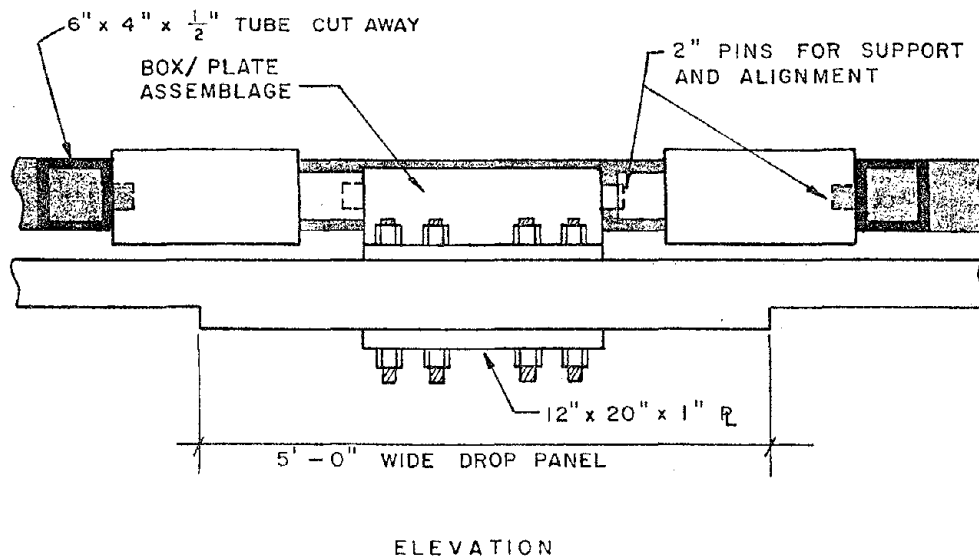
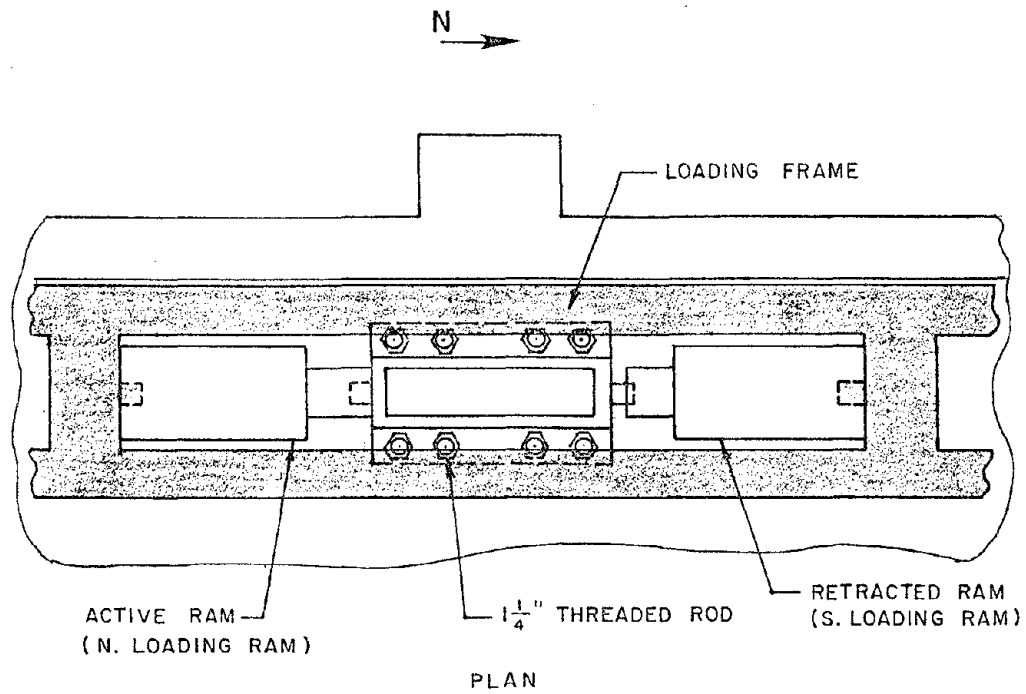


Fig. 2.40 Loading frame, hydraulic rams and box/plate assemblage at loading point

The tube was oriented perpendicular to the box/plate and was designed considering the torsion introduced into the slab during loading. The tube was welded to the midpoint of a 28 in. long channel (C8x18.75) at 90 degrees. The channel was embedded in the column and was added to the frame to increase the shear transfer between the slab and the column. In Fig. 2.41 the location of the structural steel assembly in the drop panel-column area is shown.

The reaction points on the first level of the frame were located directly under the loading points on the third level. The slab around the reaction locations had 2 in. drop panels 5 ft long with the same design, including the tube and channel, as the drop panels on the third level around the loading locations. The reactions were accomplished by attaching a plate prestressed to the slab to a reaction assemblage prestressed to the reaction floor. The plate on top of the slab was 12x20x1 in. and the plate on the bottom was 12x20x1-1/4 in. The plates were prestressed, as on the third level, with eight 1-1/4 in. A193B7 threaded rods. The location of the north reaction assemblage is illustrated in Fig. 2.42. The plate under the slab was welded to a 20x7x2 in. plate oriented at 90 degrees to form a tee member. The tee member was pin connected to one end of two 30x5-1/4x1-1/2 in. horizontal flat steel bars. As seen in Fig. 2.43, the flat bars were located inside two 60 in. long A36 channels (C15x33.9) which were prestressed to the reaction floor. The other end of the horizontal flat bars were pin connected to the channels. The horizontal forces were transferred from the slab into the tee member and into the horizontal flat bars. The bars transferred the loads into the channels. The flat bars were pin-connected on either end and were instrumented as load cells. The horizontal reaction forces were transferred through these two pairs of bars and were monitored through the load cells. Figure 2.44 is a picture of a reaction on the first level.

The reactions at the base of the column were formed by casting the column directly on a steel plate which rested on a neoprene pad. The neoprene pad was stiff under vertical loads but provided little restraint to lateral loads. The columns were restrained from lifting vertically off the floor by a 1-1/4 in. threaded rod which went through the slab in the drop panel and connected to the base reaction.

2.5.2 Beam Reactions. Reactions providing vertical deflection restraint were placed at the ends of the beams to model the restraints of a continuous beam. The reactions were provided by structural steel struts between the beams and

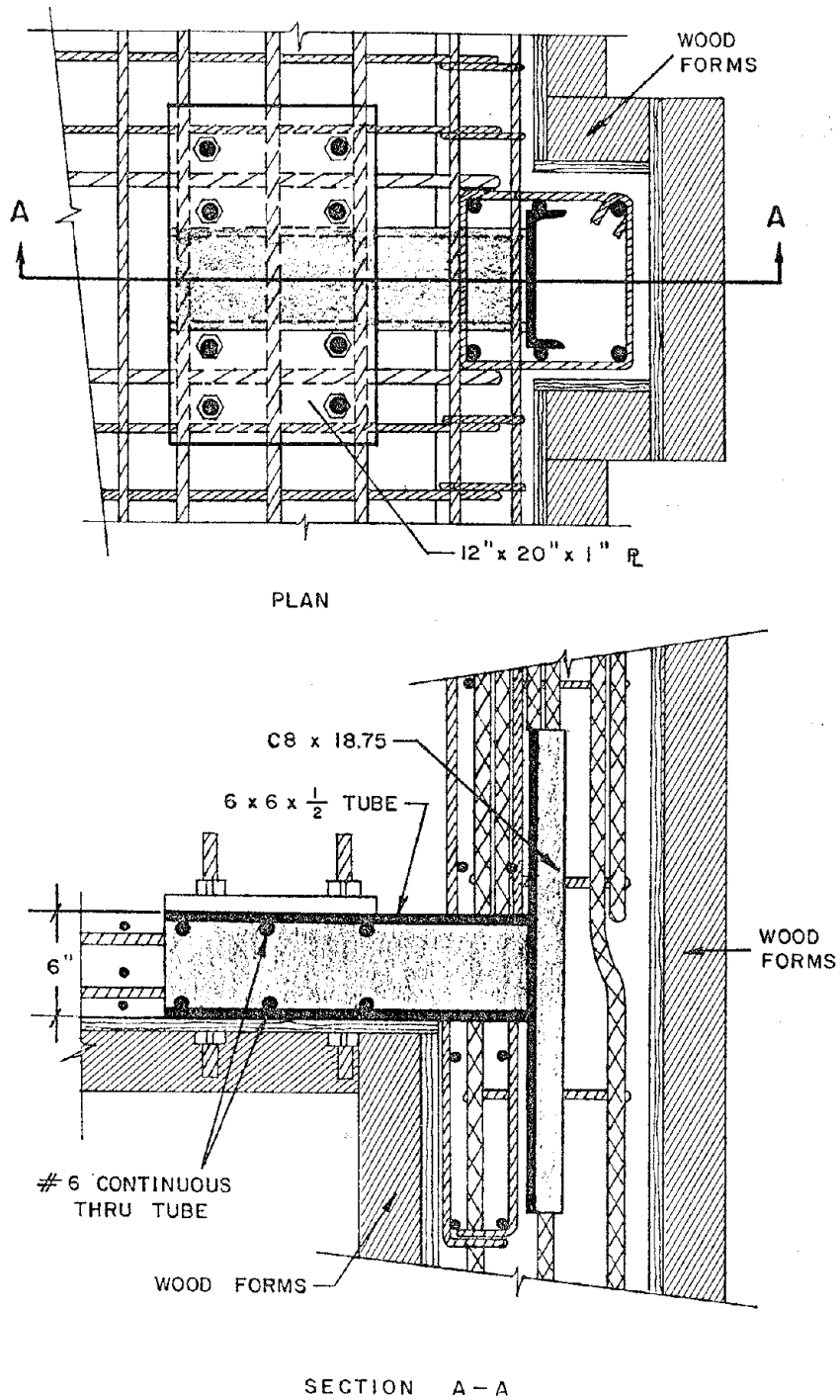


Fig. 2.41 Structural steel assembly embedded in drop panel - column area, shown in formwork before placing concrete

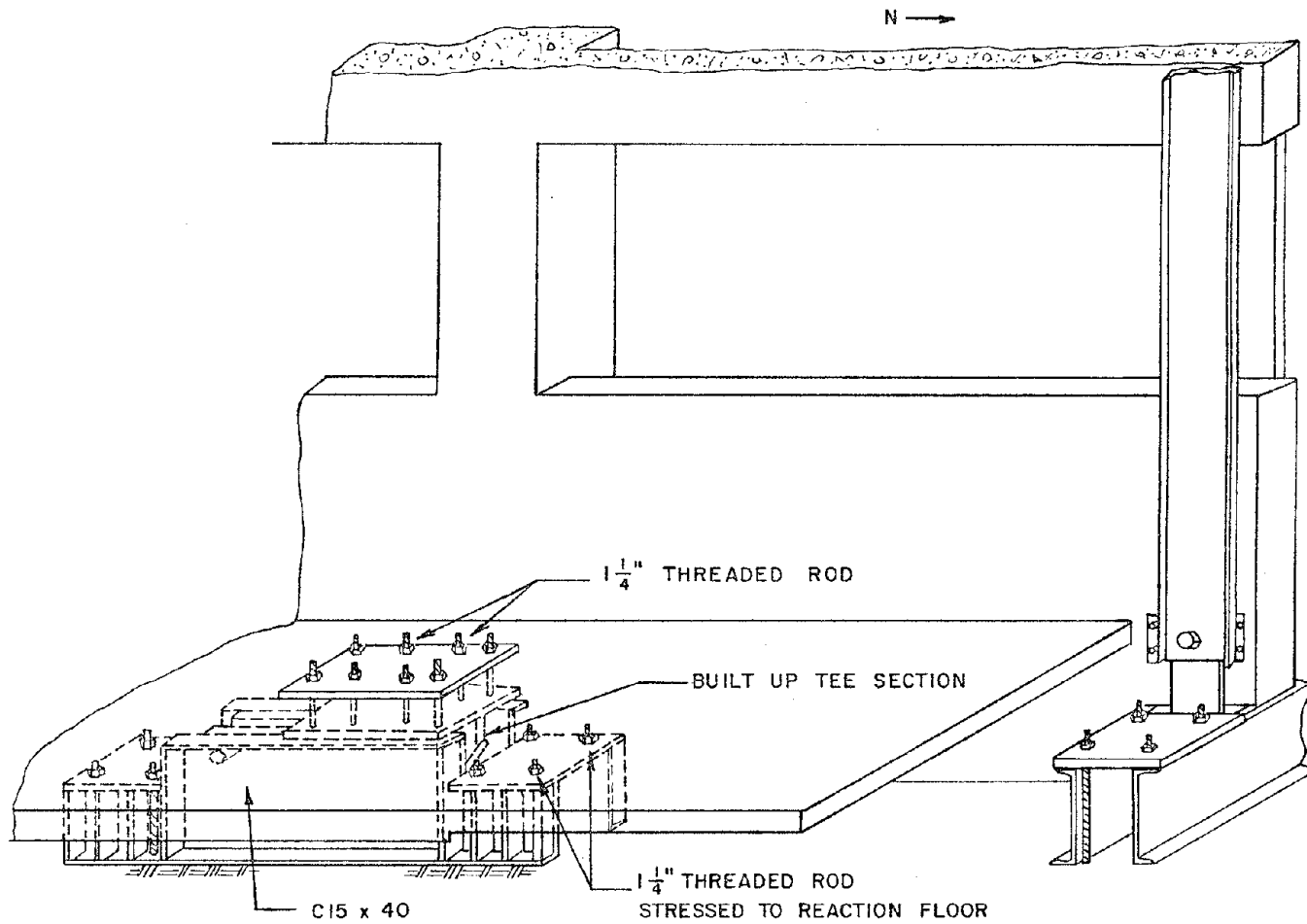


Fig. 2.42 Reaction assemblage under first level slab

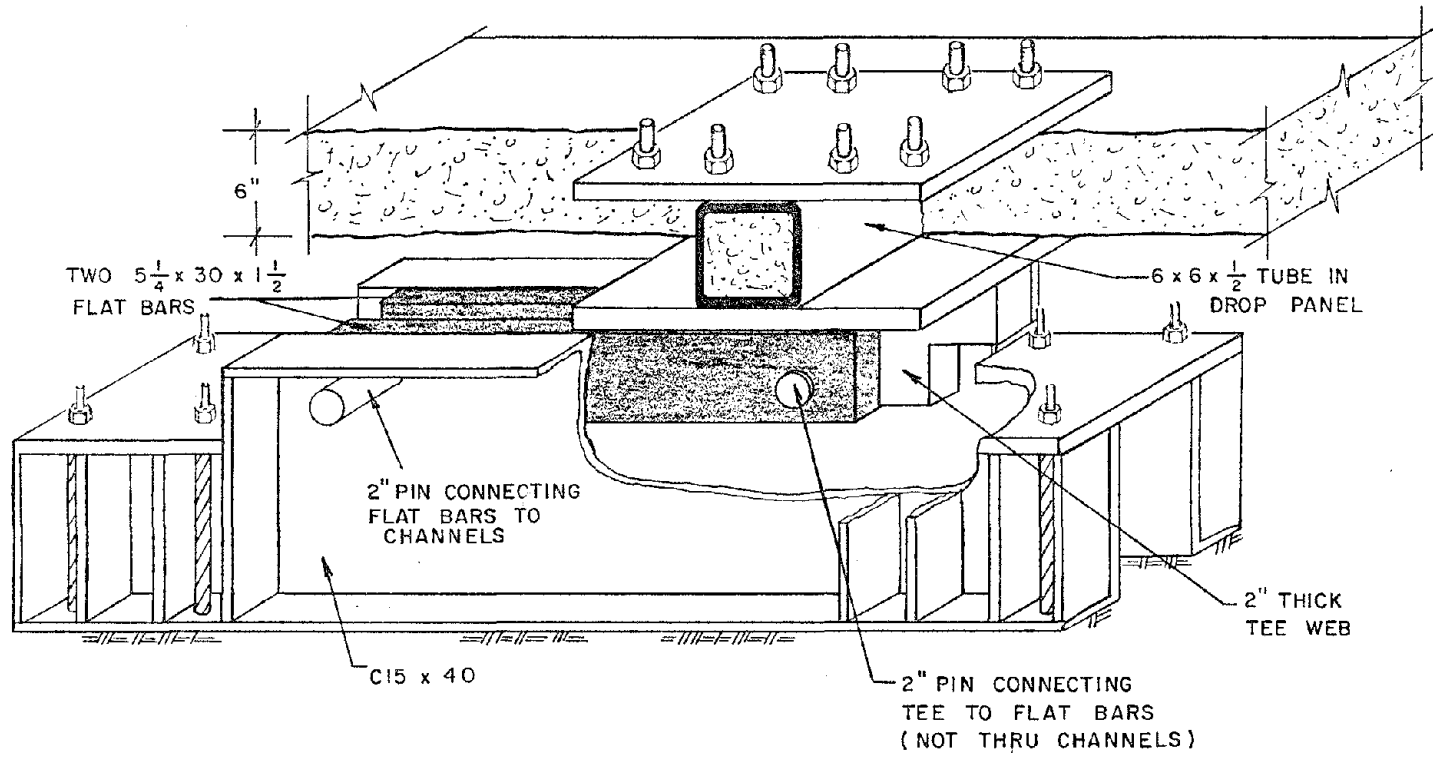


Fig. 2.43 Reaction assemblage

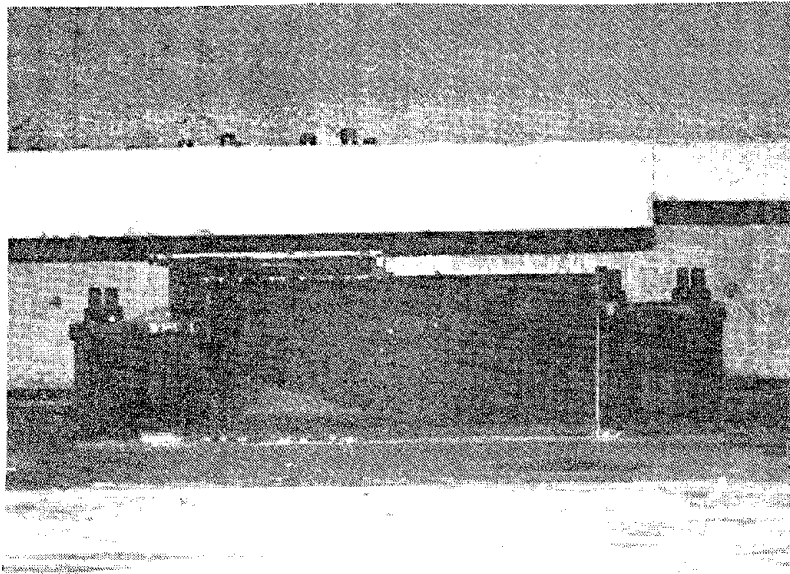


Fig. 2.44 Reaction assemblage and drop panel on first level



Fig. 2.45 Test frame with boundary restraints

connecting together to a builtup member tied to the reaction floor. The struts were pin connected to the ends of the beams to provide vertical restraint but allow rotation and lateral deflection of the beams. The struts consisted of a set of A36 channels (C8x13.75), one on either side of the spandrel beam. The struts were connected to the floor reaction by two 5x1-1/4 in. steel plates ( $F_y = 50$  ksi) 24 in. long. The 5x1-1/4 in. plates were pin connected to two channels (C10x25) which were bolted to larger channels (C12x30) tied to the floor. Each set of struts was instrumented as a load cell to measure the force in the struts. The struts are visible in the picture in Fig. 2.45 and are drawn and labeled in Fig. 2.46.

2.5.3 Out-of-Plane Bracing. The out-of-plane bracing was provided to add stability to the frame and to act against the small forces produced by eccentricity of the loading and reaction points with respect to the frame. The braces are indicated in Fig. 2.47. The braces on the first level were pipe sections with 2 in. outside diameter. These braces were located 8 in. above the floor. They connected to a 3/4 in. diameter threaded rod embedded in the center of the column on one end. On the other end they connected to a 3/4 in. diameter threaded rod which was connected to a reaction assembly tied to the reaction floor.

The braces at the top level were box sections built up from structural steel angles (L3x3x3/8). On one end they were pin connected to a box section bolted to the spandrel beam at the edges of the piers. The other end of the braces were pin connected to steel columns supporting the laboratory crane rails and roof.

2.5.4 Data Acquisition. The instrumentation for the tests was designed to yield information on behavior of the original frame, behavior of the pier strengthened frame and the interaction between the piers and original frame. The number of channels of data were set by the limits of the data acquisition system. A Compupro computer was used for data acquisition and reduction purposes. A 100 channel high-speed system, the Accurex, was used to monitor the analog output of the instrumentation and to convert it to a digital format. The system had the capability to monitor 71 quarter-bridge channels, used for strain gages, and 27 full-bridge channels; used for load cells, displacement transducers and pressure transducers. The data were recorded on disks and a hard copy printed at the test site.

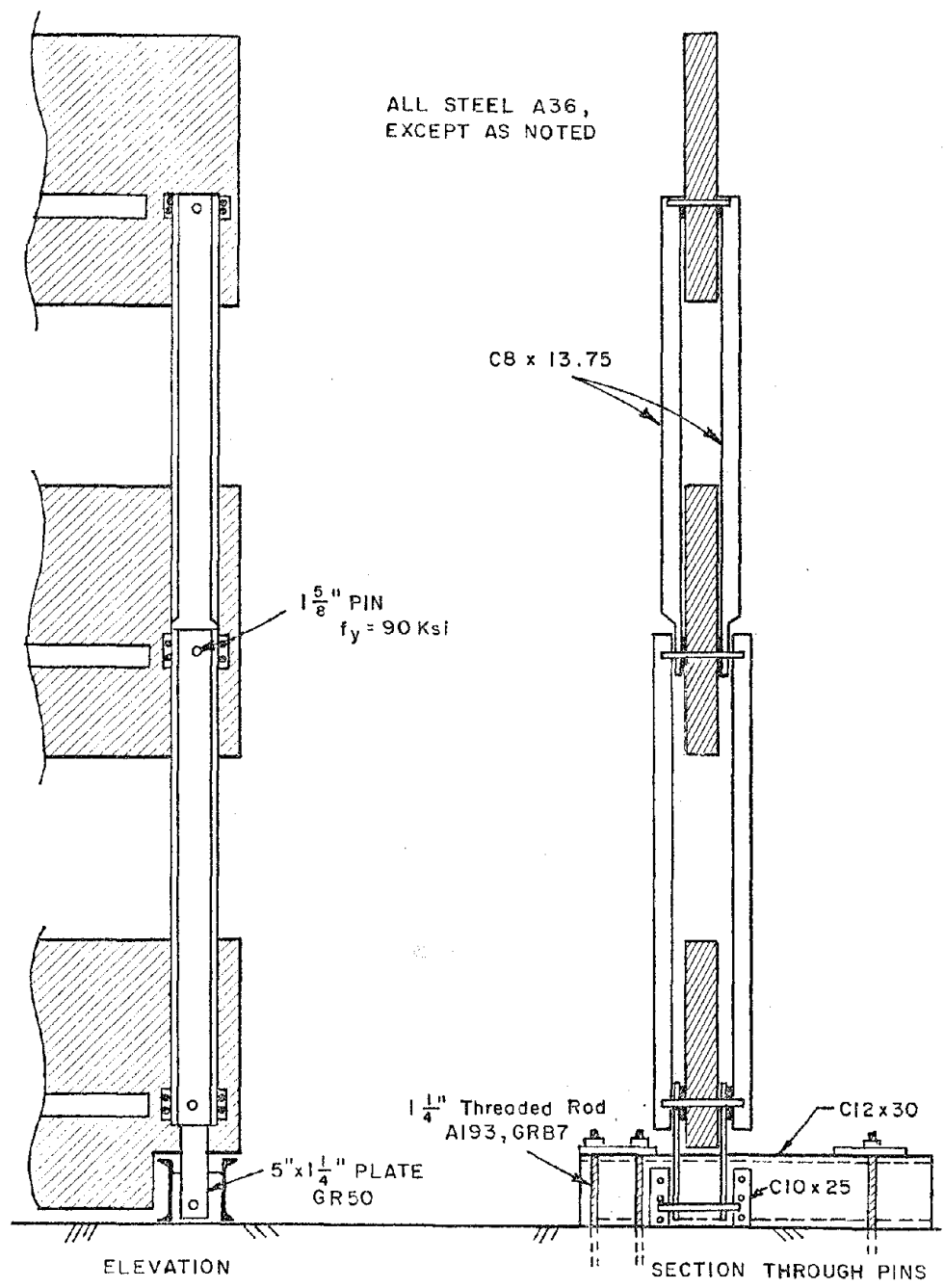


Fig. 2.46 Steel struts to provide vertical deflection restraints at ends of beams

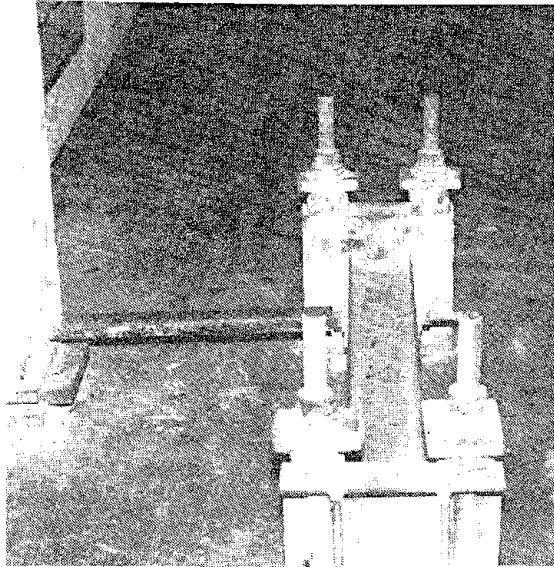


Fig. 2.47 Out-of-plane brace at first level



Fig. 2.48 Out-of-plane braces at third level

The strain gages were mounted on reinforcing bars at the critical sections of members of the frame. The approach taken in instrumenting the pier was to heavily instrument a pier over one story height and to instrument longitudinal bars at selected critical sections. A total of 96 strain gages were mounted; 69 gages in the north end of the frame, including the heavily instrumented pier area, were connected to the Accurex scanning system, and the remaining 26 gages were connected to switch and balance units which were read manually. The locations and channel numbers of the strain gages are shown in Figs. 2.49 through 2.51. The load cells were located on the vertical struts at the beam ends and on the horizontal bars providing the base reactions. The locations and directions of the load cells are shown in Fig. 2.52.

The linear voltage displacement transducers (LVDTs) were connected to the Accurex system. The LVDTs were used to measure global deflections (relative to the reaction wall) of the frame and to measure slip between new and existing concrete. The six displacement transducers used to measure the vertical deflections of the top of each spandrel beam and the horizontal deflection of each beam at the slab level were mounted on the south end of the frame with orientations indicated in Fig. 2.53. Dial gages were used to provide a manual check on selected channels. Figure 2.54 shows the LVDT and dial gage measuring vertical deflection of the first level beam. Figure 2.55 shows the LVDT and dial gage measuring horizontal deflection of the first level beam. The locations of the ten displacement transducers used to measure slip are also shown in Fig. 2.53. These LVDTs were mounted, as pictured in Fig. 2.56, with the LVDT epoxied to the original frame and a reference block epoxied to the new concrete. The relative movement, or slip, between these two points was measured.

The applied load was monitored by a pressure transducer connected to the hydraulic line to the loading rams at the top level. A multimeter was used to monitor the load on the frame at all times. The load (voltage output) was monitored by the Accurex and on an X-Y plotter which provided a continuous plot of the load versus lateral deflection of the third level beam. This plot made it possible to monitor the performance of the frame at all times.

2.5.5 Test Procedure. The equipment for running the tests and monitoring the data was located on the northeast side of the frame and is pictured in Fig. 2.57. The hydraulic pump, not visible in Fig. 2.57, was controlled manually. The activation

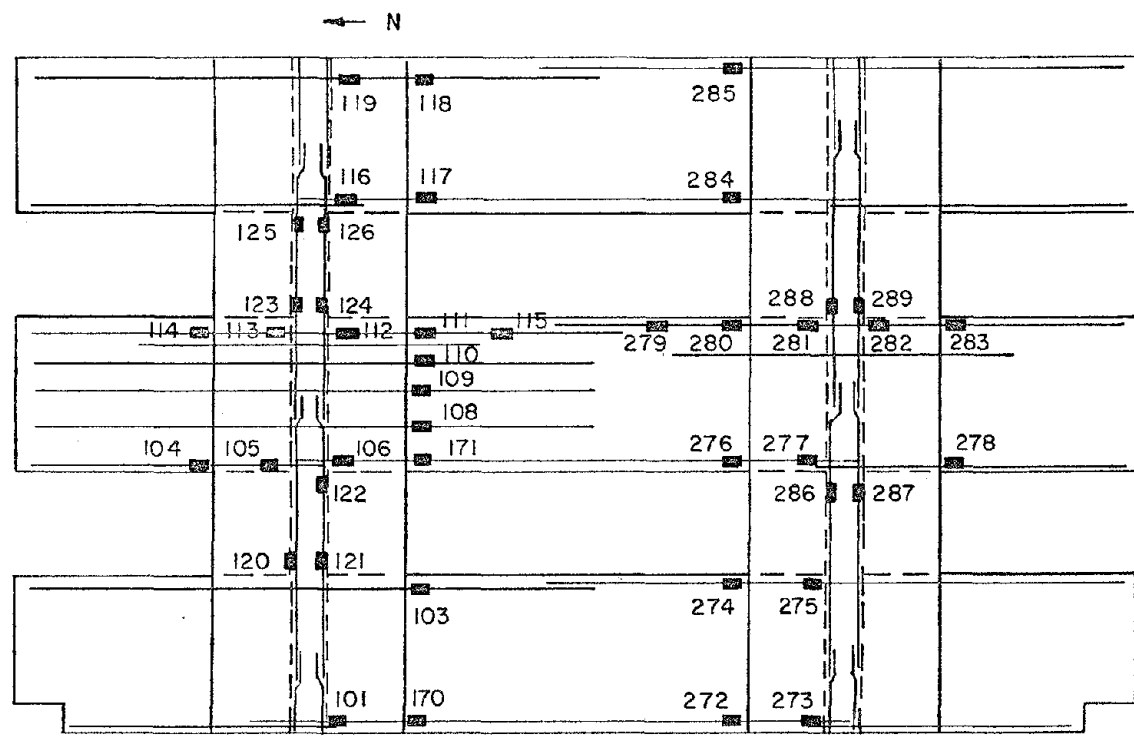


Fig. 2.49 Strain gage locations in the original frame

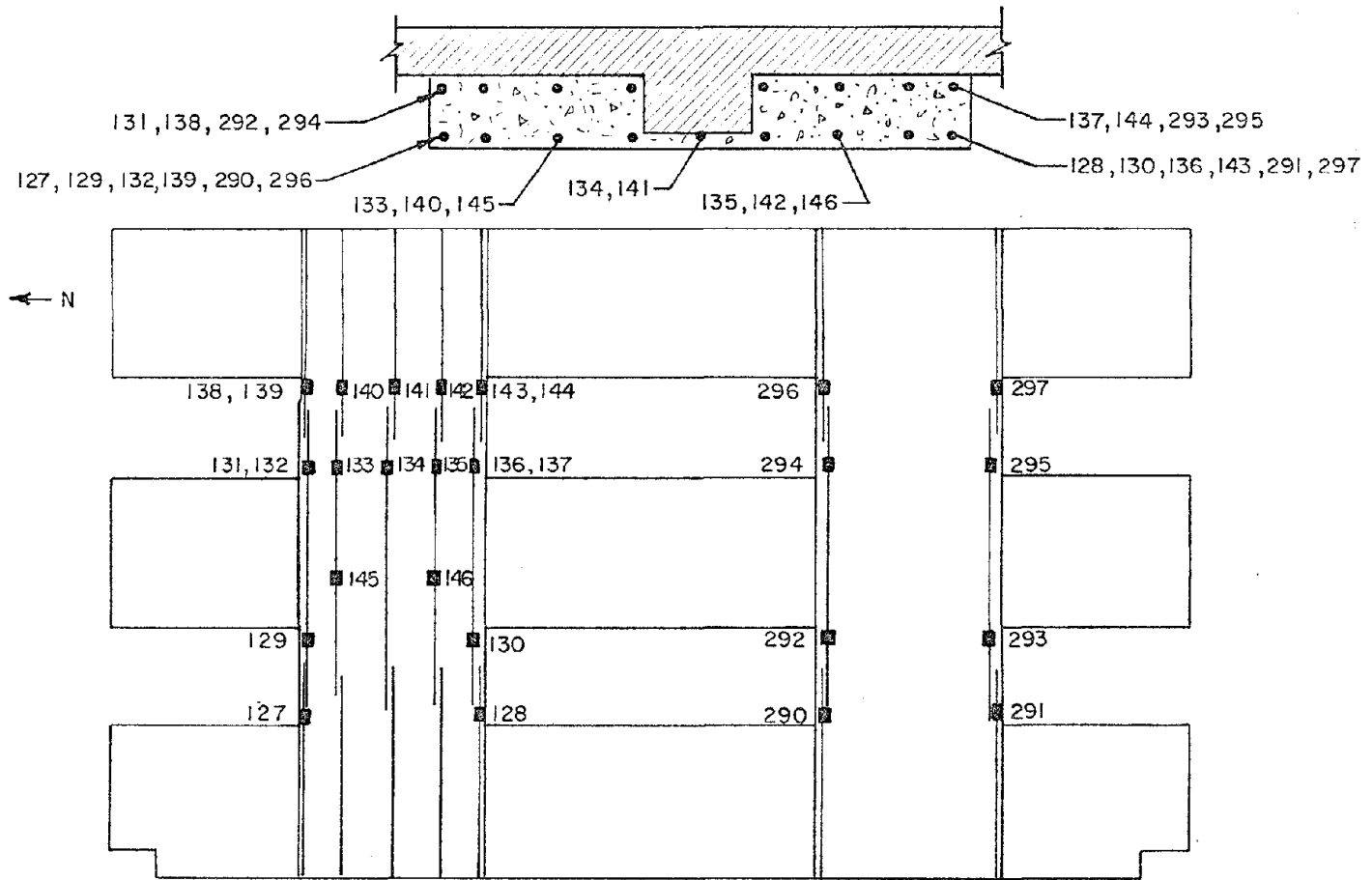


Fig. 2.50 Strain gage locations on the longitudinal reinforcement in the pier

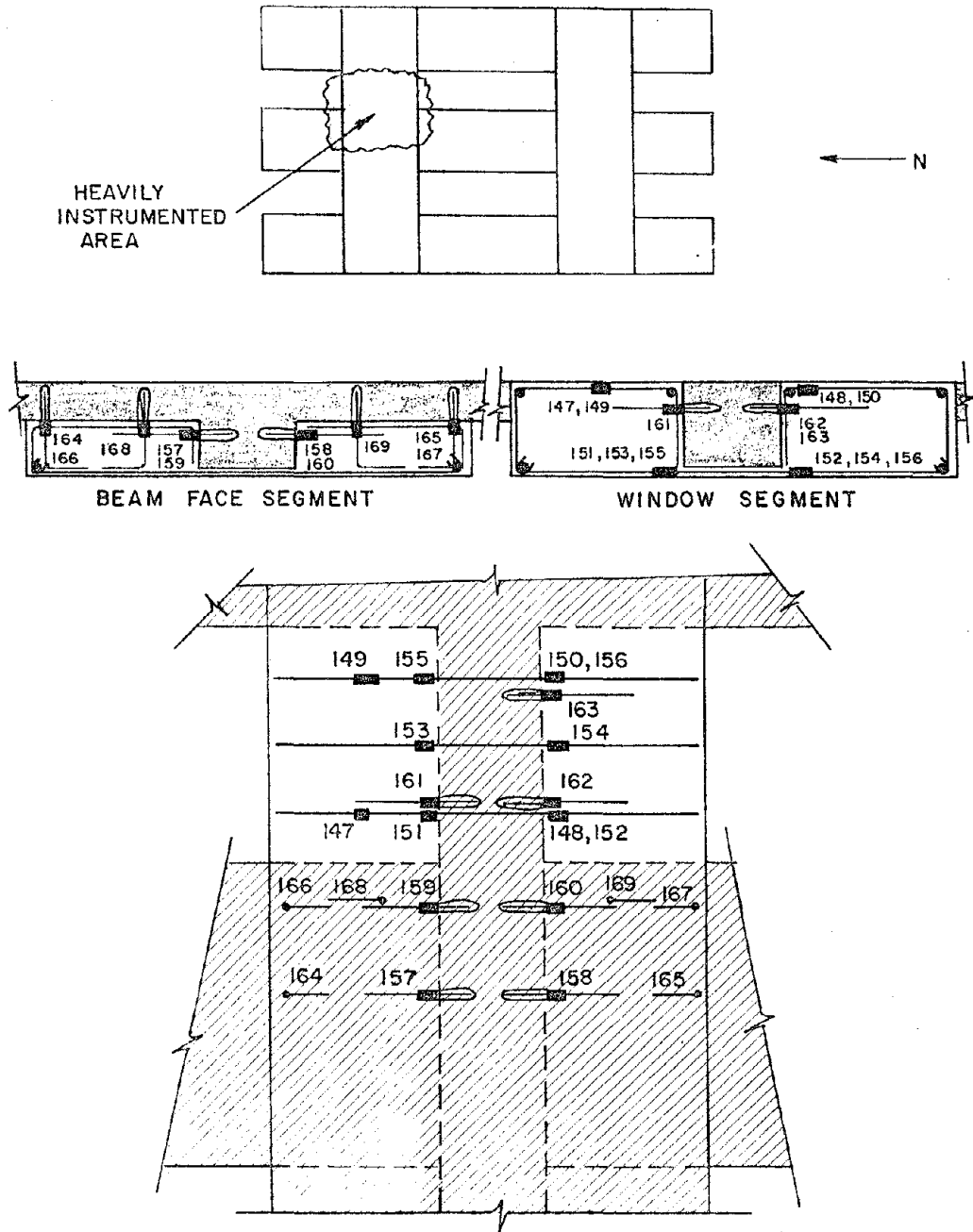


Fig. 2.51 Strain gage locations on dowels and transverse reinforcement in the pier

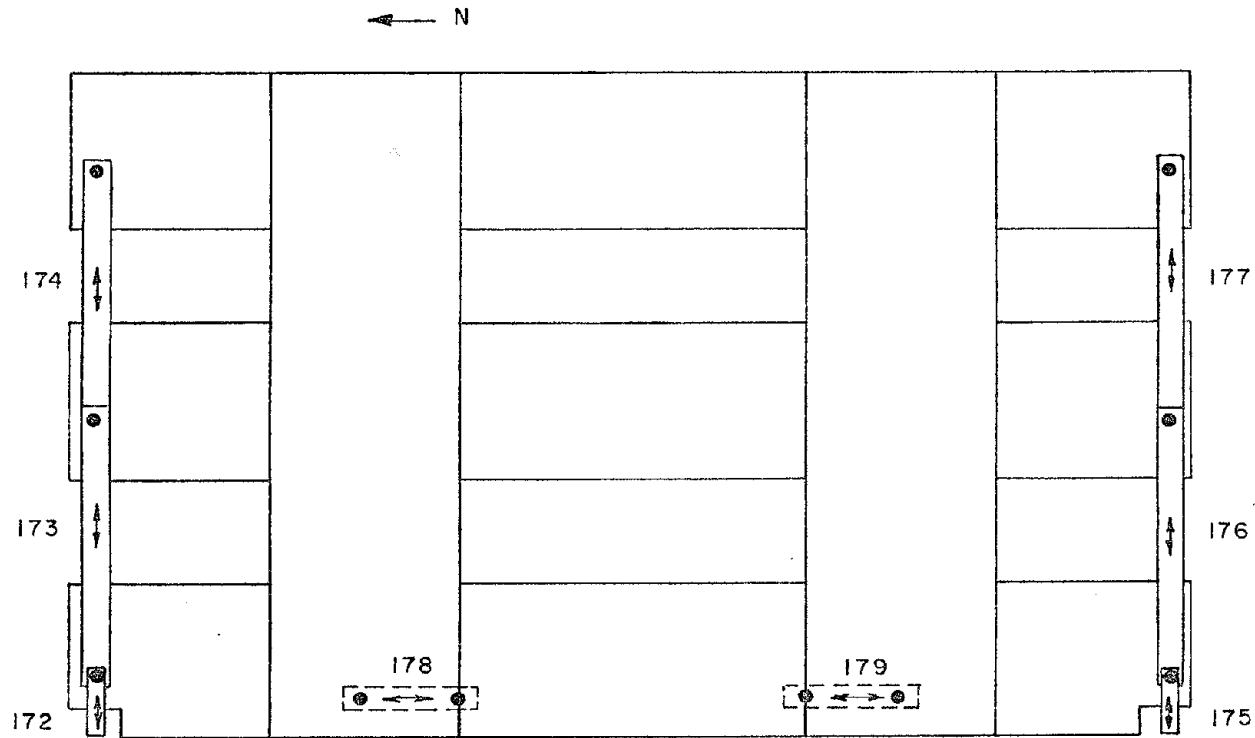


Fig. 2.52 Locations of load cells in the boundary restraints

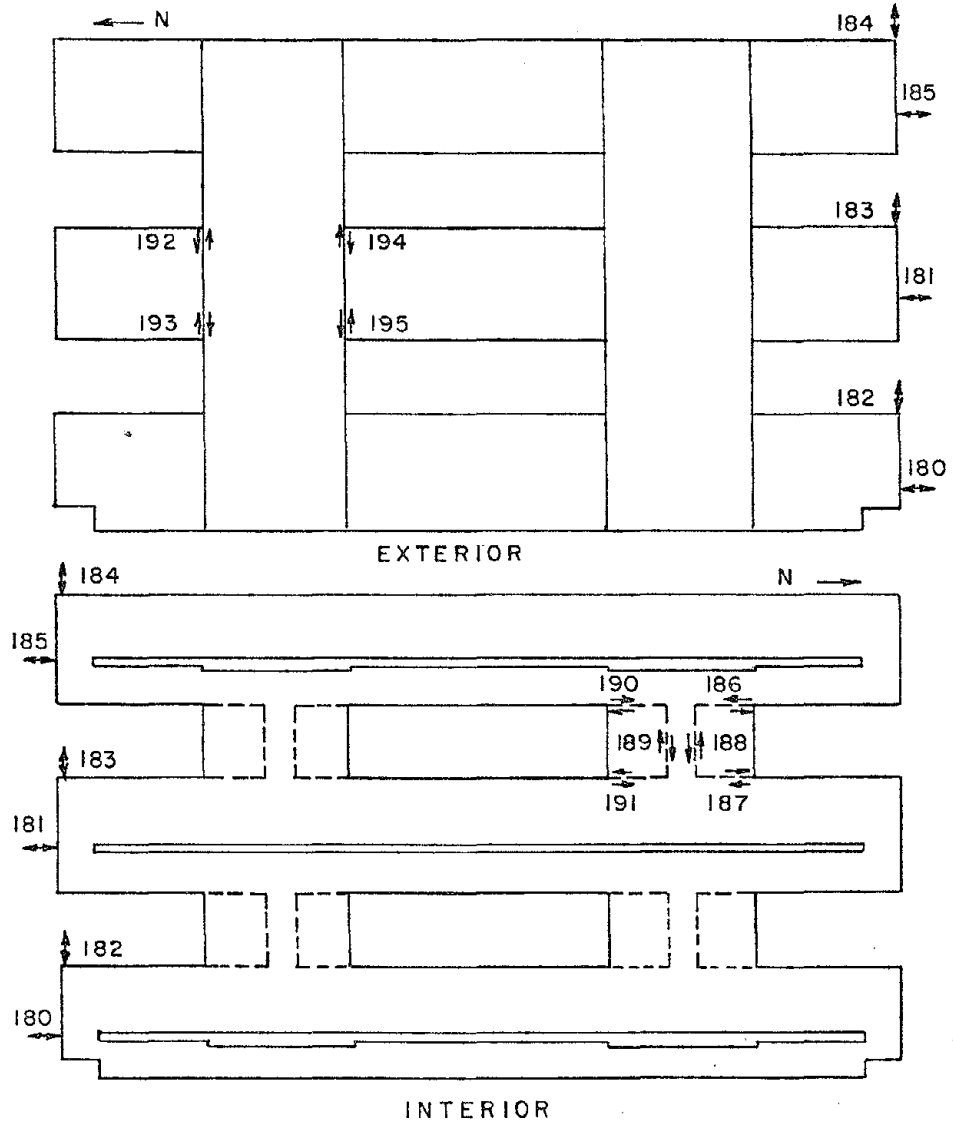


Fig. 2.53 Orientation and Location of LVDTs

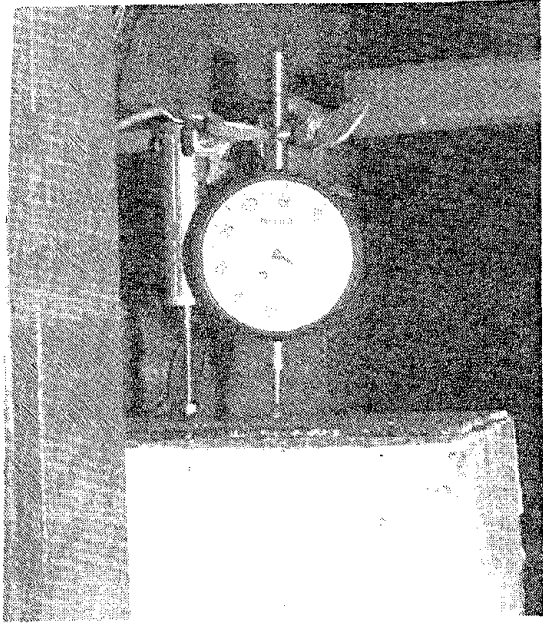


Fig. 2.54 LVDT (channel 182) and dial gage measuring vertical direction of the first level beam

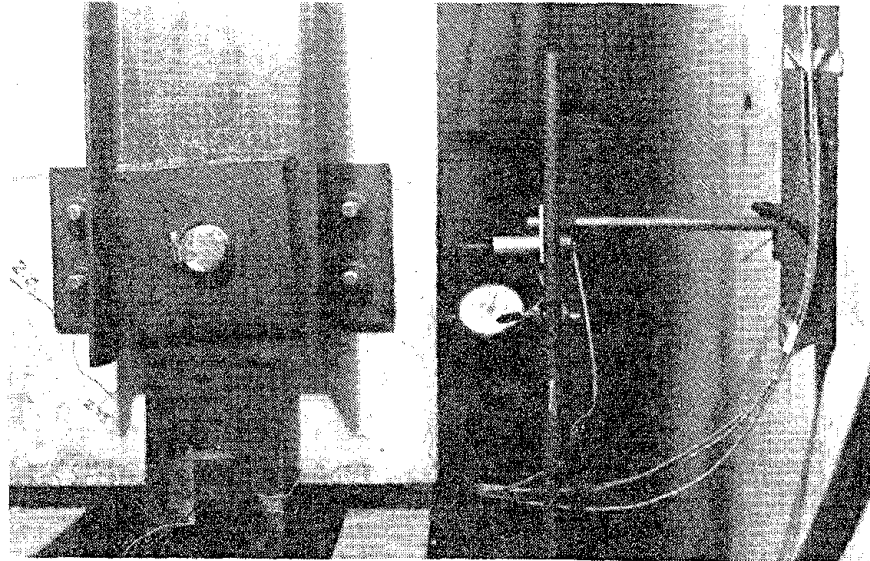


Fig. 2.55 LVDT (channel 180) measuring horizontal deflection of the first level beam

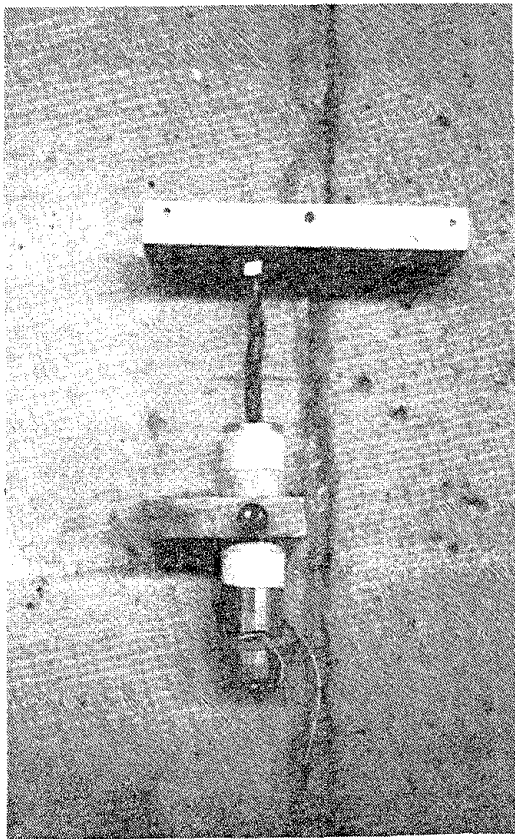


Fig. 2.56 LVDT (channel 188) used to measure slip between the original column and the pier

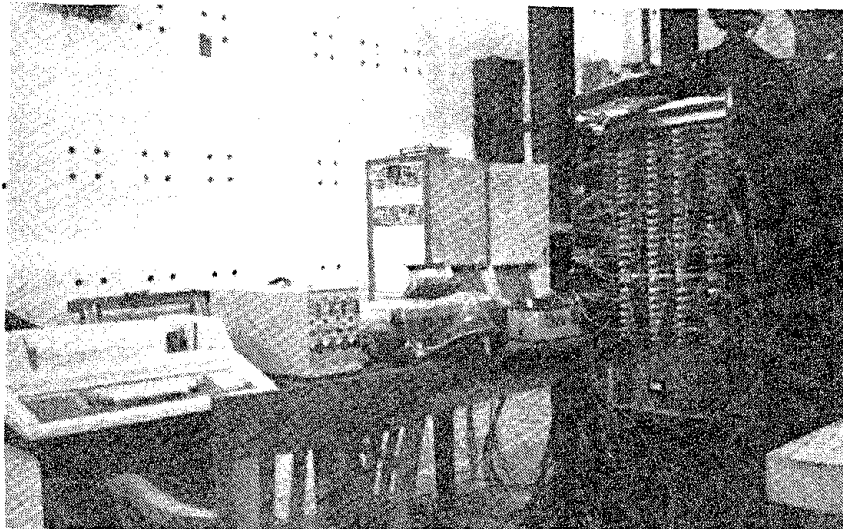


Fig. 2.57 Data acquisition equipment by northeast corner of frame

of the hydraulic ram pairs was controlled by valves located on the third level of the frame.

The test involved reversed cyclic (static) lateral loads introduced in the third level slab. The frame was loaded in sets of three cycles to a predetermined drift level. Each cycle was initiated by loading in the north direction. A cycle of load was accomplished by loading the frame in the north direction to a given level of drift, then unloading by releasing the pressure in the hydraulic rams. The ram pair was retracted and deactivated. The other pair of rams was then activated and the frame was loaded in the south direction to the same level of drift. This load was released and the rams were retracted in preparation for the next cycle.

## CHAPTER 3

### RESULTS OF PIER STRENGTHENING

#### 3.1 Test of Existing Frame Model

The unstrengthened frame model was tested to determine its lateral stiffness for comparison with the strengthened frame. Two cycles of load were applied to a predetermined drift. Unless otherwise specified, drift will refer to the lateral deformation of the frame between the third and first slab levels. Percent drift will refer to deformation between the third and first slab levels over the height between those levels, 160 in. The drift level was very low, approximately 0.05%, to prevent a shear failure of the columns. The approximate shear capacity of each column, calculated using actual material strengths, was 31 k. The lateral loads were well below the limiting value of 31 k per column. This test also provided an opportunity to check the performance of the instrumentation and data acquisition systems.

The frame was loaded in two cycles. The frame was loaded to a drift between the third slab level and the first slab level of approximately .08 in. or 0.05%. The lateral load necessary to produce this drift was 32 k or 16 k per column. This was below the calculated shear capacity of 31 k per column. The plot of lateral load versus drift between the third and first slab level for the two cycles of the existing frame test is shown in Fig. 3.1. There was little change in the response of the frame in the second cycle of loading. At a total applied load lateral load of 32 k, the first cracking occurred. Hairline flexural cracks approximately 4 in. long were noted in the beams at the beam-column joint.

#### 3.2 Test of Strengthened Frame Model

3.2.1 General. The strengthened frame was tested under four sets of three cycles of lateral load to four different drift levels. The deformation history of the strengthened frame during the test is illustrated in Fig. 3.2. The first set of cycles was to 0.05% drift to compare the strengthened frame's lateral stiffness to that of the existing frame. Following sets of cycles were to a low (0.125%), medium (0.25%) and high (0.5%) level of drift. These three sets of cycles gave a good indication of the

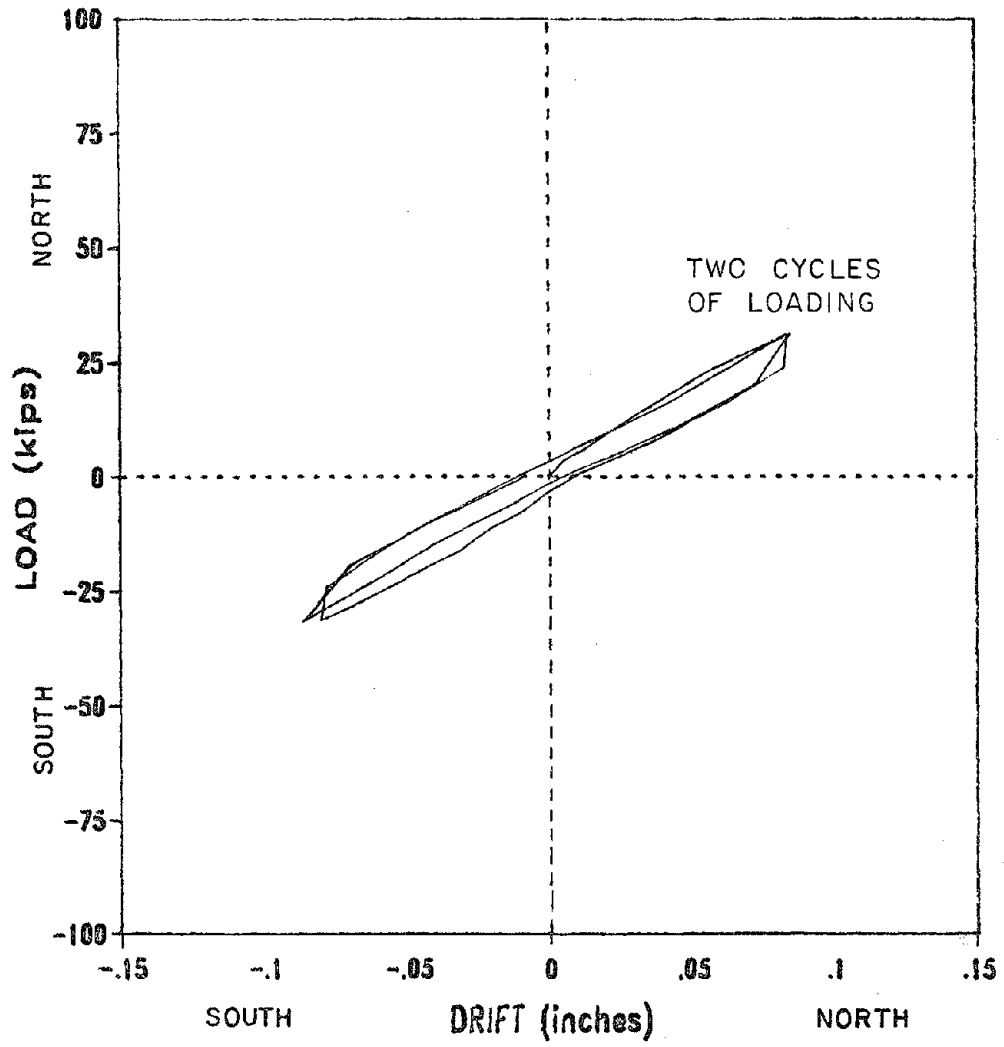


Fig. 3.1 Load vs. drift for test of existing frame model

# DEFORMATION HISTORY

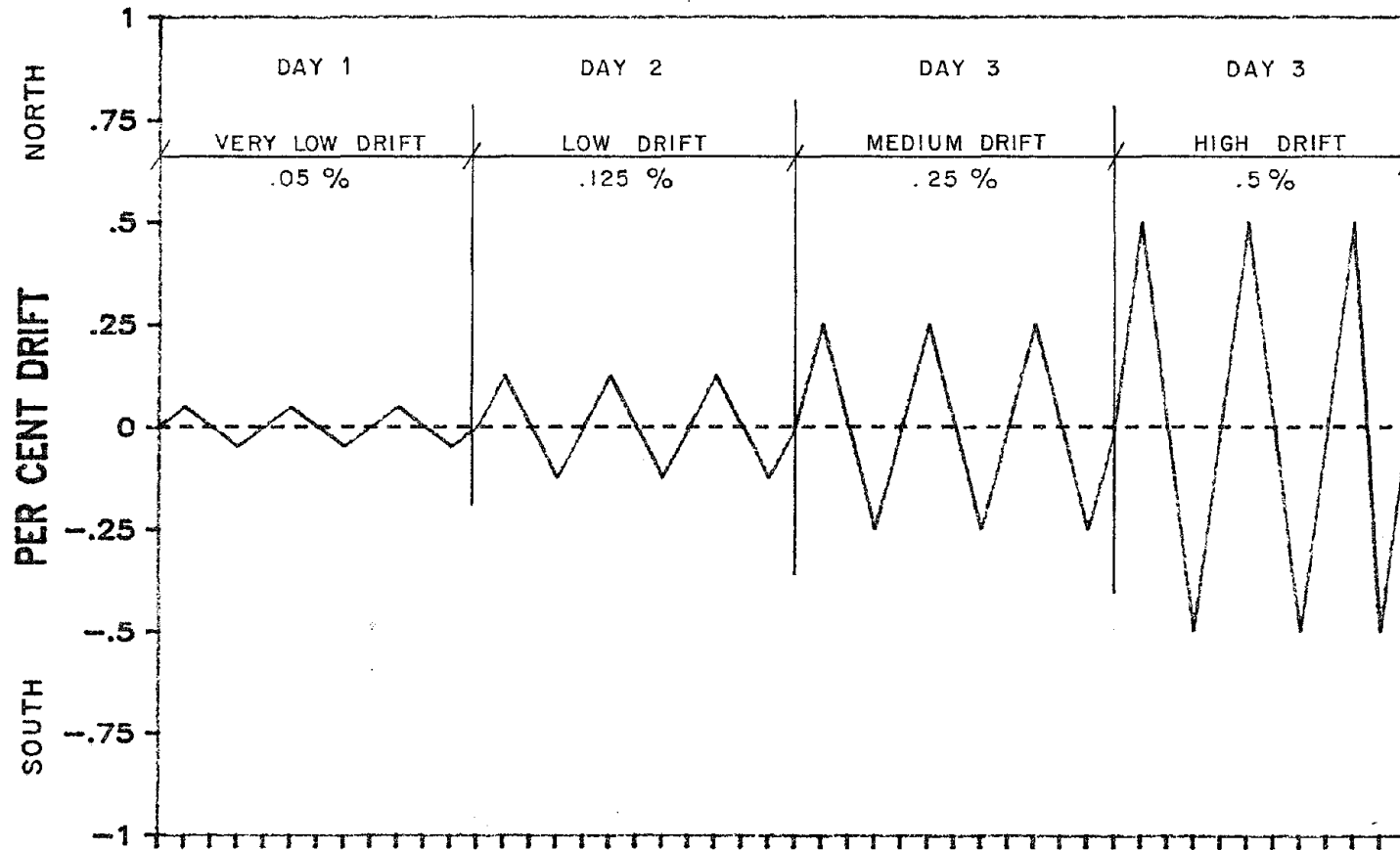


Fig. 3.2 Deformation history of the strengthened frame model

envelope of the load versus drift behavior of the strengthened frame.

It was essential to establish the failure mechanism and strength of the frame without producing damage that would directly affect the test of the steel bracing system which was to follow the pier strengthening test. The pier strengthening was designed to develop the flexural capacity of the beams. The expected failure was a flexural failure of the beams in the region of the pier beam joint. A failure of the beams in this region would have had little effect on the behavior of the steel strengthened frame. However, damage in the columns could have had an effect on the behavior of the frame. For this reason, it was decided to load the pier strengthened frame to a high enough drift level to create severe distress in the beams but very little distress in the columns.

3.2.2 0.05% Drift Cycles. The strengthened frame was subjected to three cycles of 100 k lateral load in each direction. The maximum drift resulting from the 100 k lateral load was approximately .08 in. (0.05% drift) when loaded in the north direction and .12 in. when loaded in the south direction. There was slightly more flexural cracking in the beams than appeared during the existing frame test. These hairline cracks originated in the beams at the beam-pier joint and in the continuous bay approximately 1 to 1.5 ft from the edge of the pier. This corresponds to the location of the cutoff point of the additional reinforcing bars in the negative moment region of the beams mentioned in Chapter 2.

This first set of three cycles of load revealed that the strengthened frame had an initial lateral stiffness that was approximately three times that of the existing frame. This is illustrated in Fig. 3.3 which shows a lateral load versus drift plot for the existing frame and the strengthened frame for the 0.05% drift cycles. The plot of Fig. 3.3 also revealed that the strengthened frame did not behave identically under the two directions of loading. The strengthened frame was stiffer, approximately 30% stiffer, under loading in the north direction of subsequent cycles than under loading in the south direction. This was assumed to be due to two conditions of the test. First, the boundary constraints could have had provided different stiffness in the two directions of loading. The connections of the struts on the beams, the out-of-plane braces and the loading frame were not equally "snug" in all locations. Second, each cycle of loading was initiated in the north direction. The frame had already been subjected to load and possibly seen distress

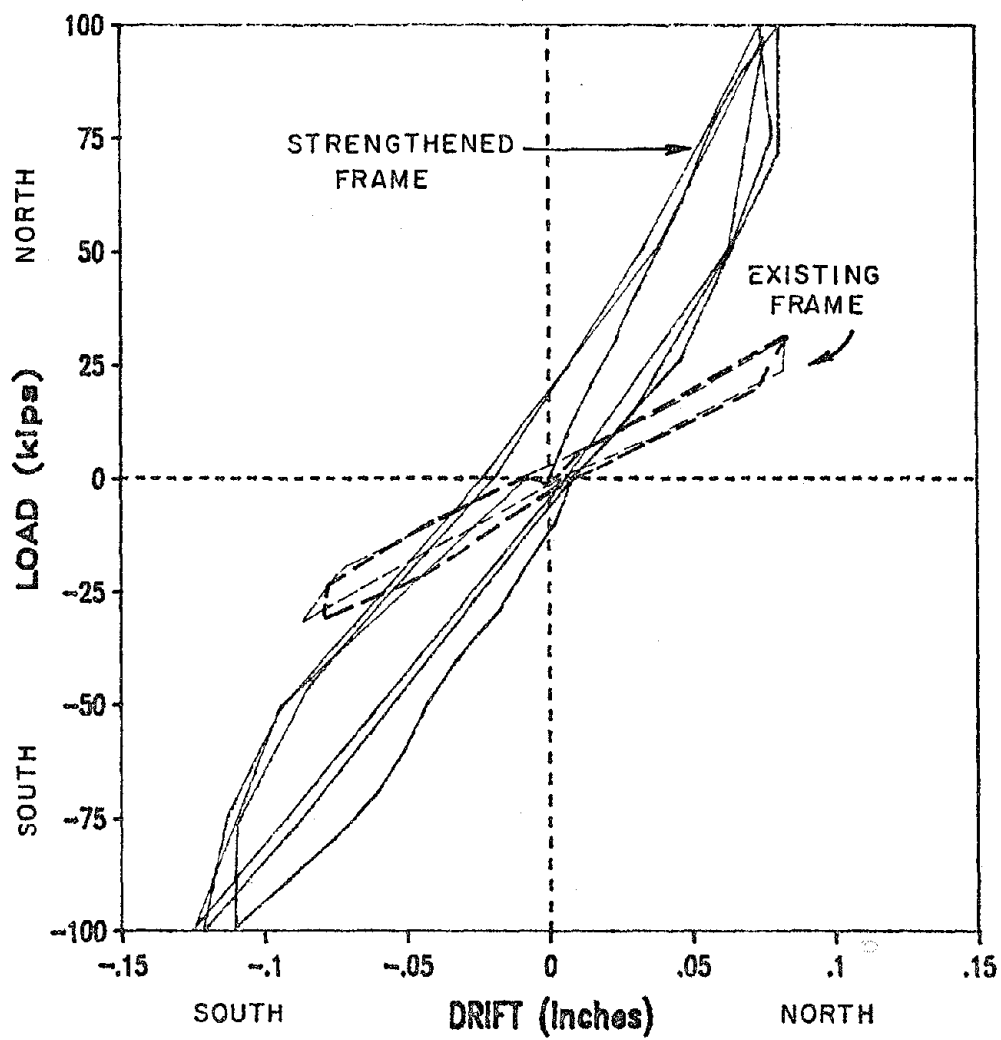


Fig. 3.3 Load vs. drift for the strengthened frame and existing frame models for cycles to 0.05% drift

when it was loaded in the south direction. This could have caused the frame to be less stiff in the south direction.

3.2.3 0.125% Drift Cycles. In the three cycles to 0.125% drift the frame was loaded by applying three cycles at 150 k lateral load in each direction. The maximum drift resulting from 150 k lateral load was .16 in. for loading in the north direction and .22 in. for loading in the south direction. Figure 3.4 shows the lateral load versus drift for the 0.125% drift cycles. The plot of load versus drift is scaled for comparison with similar plots for the following cycles of the test. In the second two cycles of the plot of Fig. 3.4 there is a change in stiffness producing an "s" shaped curve. The change in stiffness was assumed to be the result of cracks caused by loading in one direction closing under loading in the other direction and producing an increase in stiffness.

The crack pattern resulting from the three cycles to 0.125% drift is illustrated in Fig. 3.5 for the exterior and interior of the frame. Cracks were not marked under the first level slab at any time during the test. Except for very slight hairline flexural cracks in the first level of the pier, all cracking was concentrated in the spandrel beams. The cracks in the beams were located, in general, in the area between the face of the beam-pier joint and approximately 2 ft from the joint. The largest cracks originated in the top of the beam at about 9 in. to 1 ft 6 in. from the joint where the discontinuous reinforcing in the negative moment region terminated. Some approximate crack widths under peak loads are noted on Fig. 3.5 for the widest cracks.

The effect of the noncontinuous negative reinforcement in the beam was also indicated in the yield pattern of the reinforcement in the beams. Fig. 3.6 shows the locations of reinforcement strain in the spandrel beams indicating yield. Strain gage 115 (at the cut off point) reached yield while strain gage 111 (at the pier face) reached only one-half yield. At the section where the discontinuous negative moment reinforcement ended, the negative moment was not as high as the moment at the joint but the reinforcement was considerably less.

3.2.4 0.25% Drift Cycles. The test was continued by loading the frame to three cycles at 0.25% (medium) drift. During these 0.25% drift cycles, the frame began to lose significant stiffness under repetitive cycles. For this reason and because of the difference in stiffness in the two directions of loading, the peak load varied over this portion of the test.

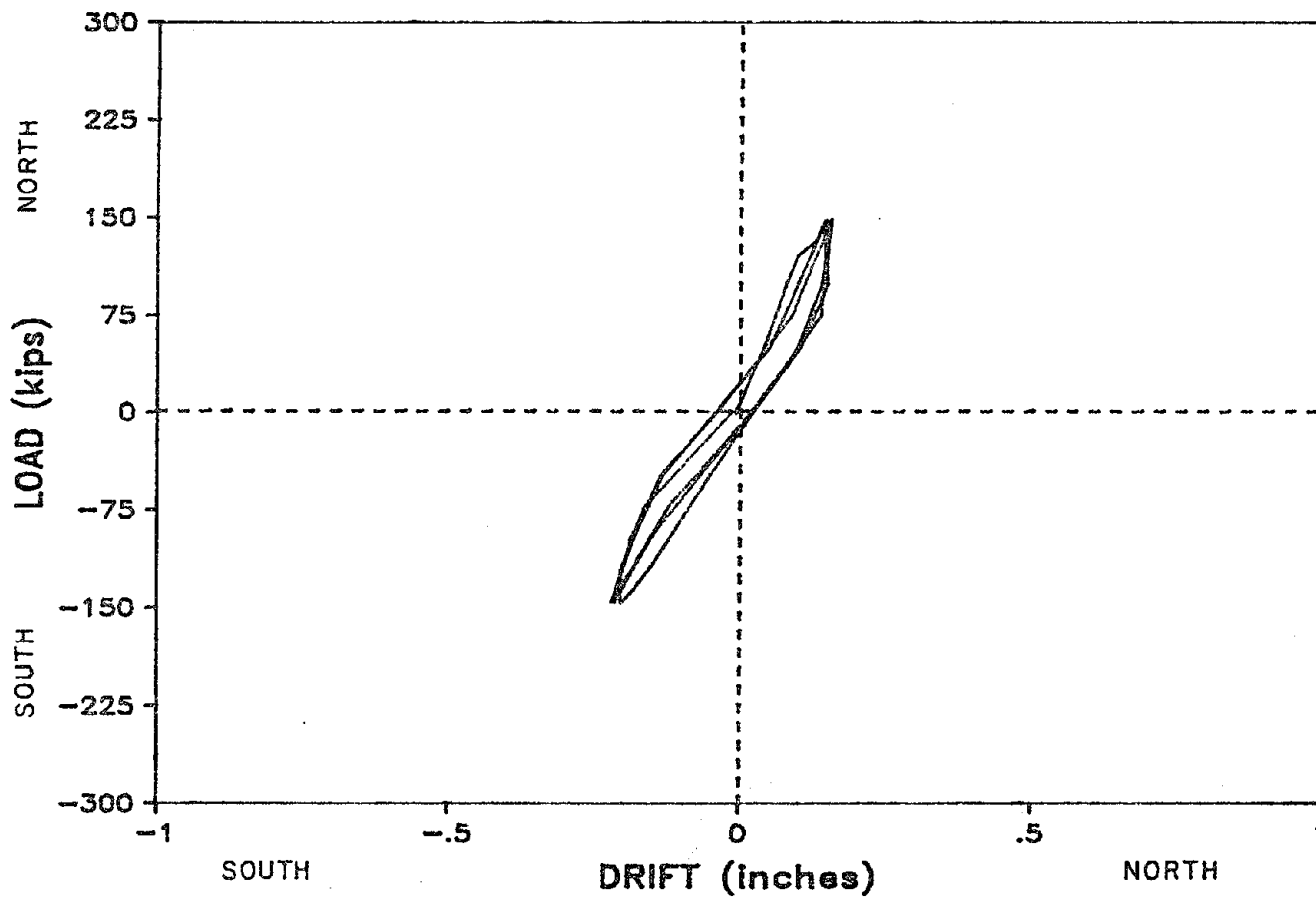


Fig. 3.4 Load vs. drift for three cycles to low (0.125%) drift

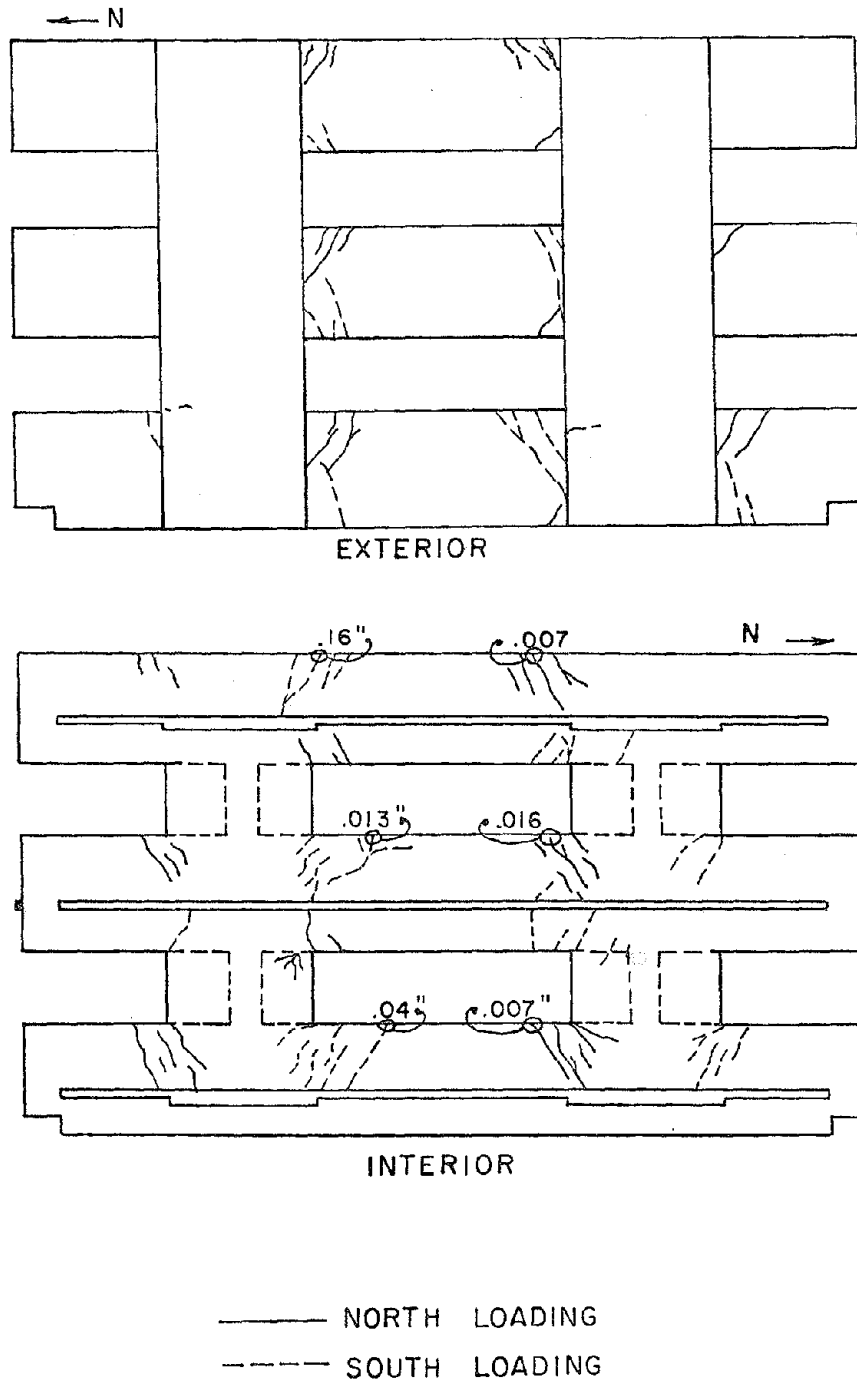


Fig. 3.5 Crack pattern after three cycles to 0.125% drift

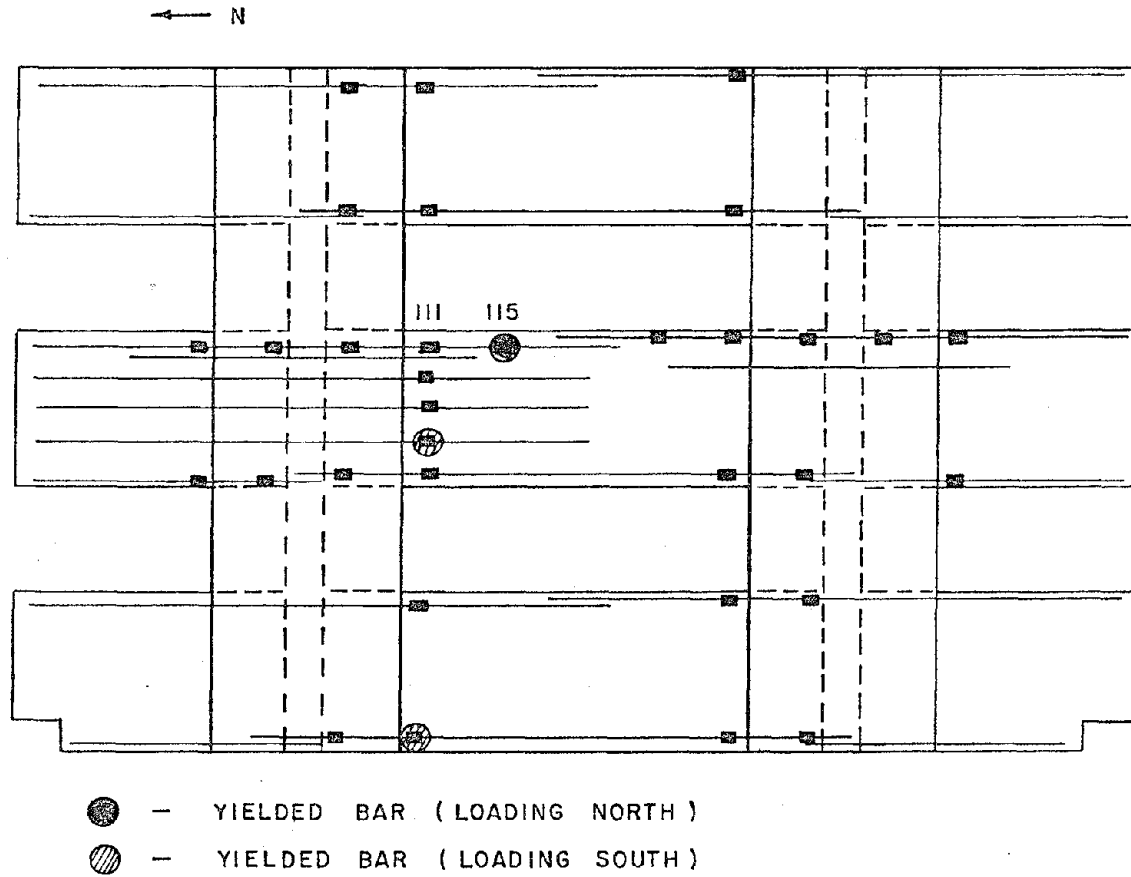


Fig. 3.6 Locations of yielded bars in beams indicated by strain gages after three cycles to 0.125% drift

The peak loads and drifts for the three cycles are listed in Table 3.1 and the load versus drift plot for the 0.25% drift cycles is shown in Fig. 3.7. In Fig. 3.7 the plots for successive cycles indicated loss in stiffness due to deterioration caused by repetition of the load. This trend is more evident in the frame's behavior under loading in the north direction. The reduction in stiffness and the "s" shape of the load-drift plots were even more evident than in the lower drift cycles.

Figure 3.8 shows the crack patterns resulting from loading to 0.25% drift. The flexural cracks increased in both size and number. The crack widths indicated in Fig. 3.5 for the 0.125% drift widened under the loads causing 0.25% drift. Crack widths at peak loads are indicated in Fig. 3.8. In addition to the flexural cracking of the beams, shear cracking occurred at either end of the first level spandrel beam. Some cracks originated from the structural steel strut connection pin and some from the corner of the 9 in. x 16.5 in. block out at the first level beam. The shear cracks were probably due to the local effects of the loads at the strut connection and the stress concentration created at the corner of the blocked out section.

A few flexural cracks appeared on the exterior of the new column on the third level. In addition, shear cracking occurred on the interior of the column at a lateral load just over 200 k. These cracks are indicated in Fig. 3.8.

The pattern of yielded bars in the beams is indicated in Fig. 3.9. At 0.25% drift, yielding was observed at every instrumented beam-pier joint. Once again, the effect of the negative moment reinforcement was evident in the yield pattern. The bottom row of positive moment steel yielded at each joint location gaged but the only location of negative moment steel yielding was that of channels 115 and 279. Gages on the same bar as gages 115 and 279 indicated stresses within 10 to 15 ksi of the approximate yield strength of the bar. Each of the negative moment steel gages at the beam-pier joints indicated stresses within approximately 20 ksi of the yield stress. It was likely that these bars had yielded at the sections at the ends of the extra negative moment reinforcing bars.

3.2.5 0.5% Drift Cycles. The final set of cycles were to a 0.5% (high) drift. The peak loads and drifts for each of the cycles are indicated in Table 3.2. The purpose of the last three cycles of lateral load was to develop the flexural capacity

Table 3.1 Loads and Drifts for Cycles to 0.25% Drift

Cycle	North		South	
	Peak Load	Drift	Peak Load	Drift
1	222 k	.32 in.	206 k	.36 in.
2	232 k	.40 in.	193 k	.36 in.
3	228 k	.40 in.	189 k	.36 in.

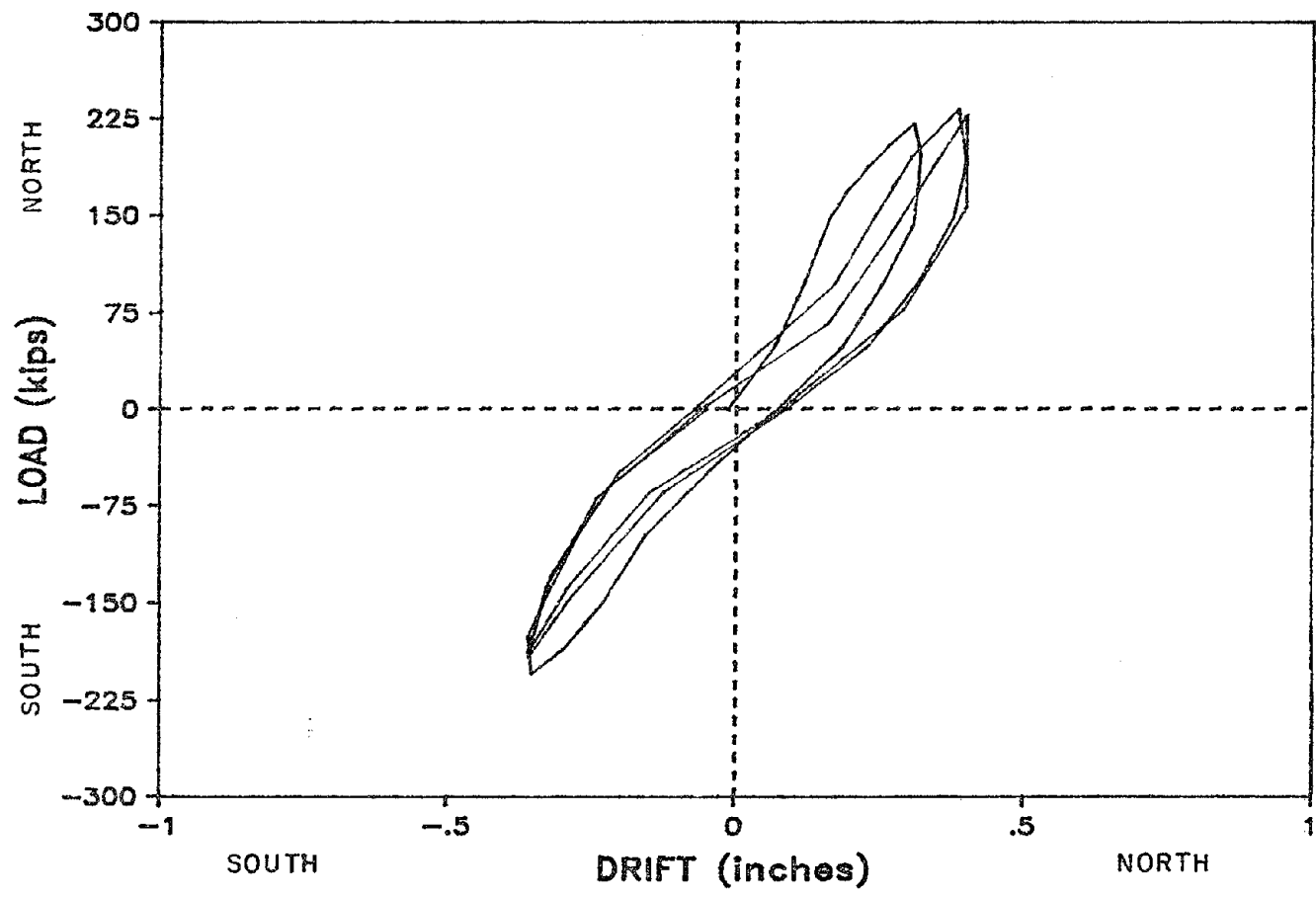


Fig. 3.7 Load vs. drift for three cycles to medium (0.25%) drift

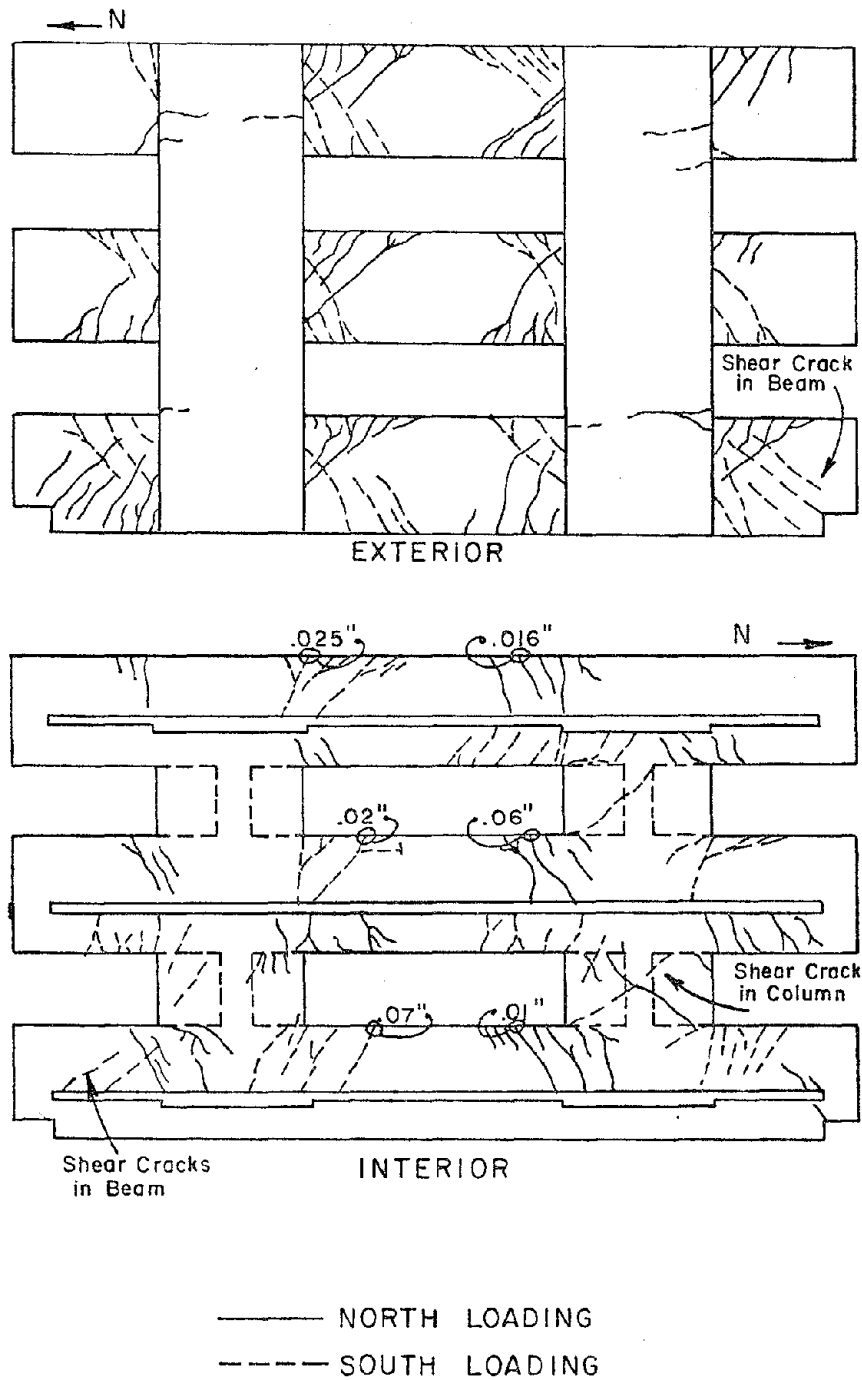


Fig. 3.8 Crack pattern after three cycles to 0.25% drift

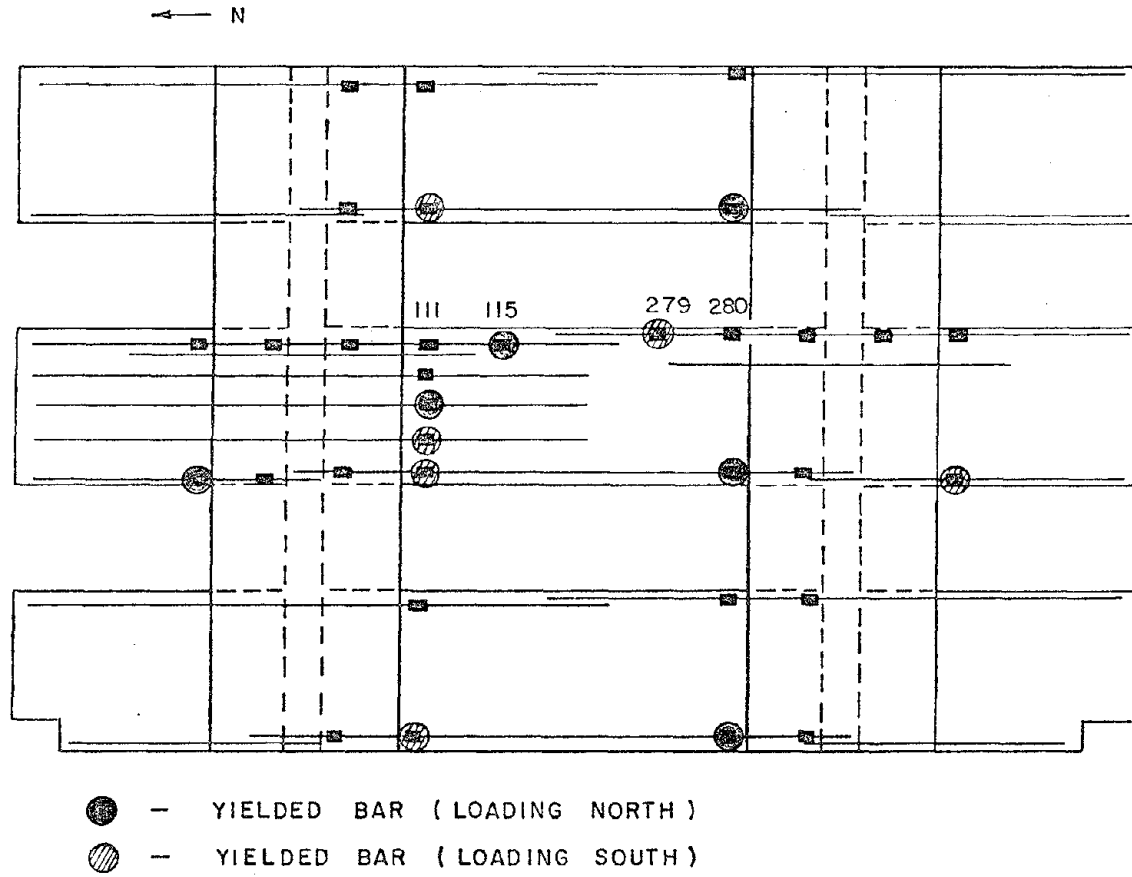


Fig. 3.9 Locations of yielded bars in beams indicated by strain gages after three cycles to 0.25% drift

Table 3.2 Loads and Drifts for Cycles to 0.5% Drift

Cycle	North		South	
	Peak Load	Drift	Peak Load	Drift
1	305 k	.78 in.	266 k	.71 in.
2	286 k	.86 in.	248 k	.72 in.
3	280 k	.87 in.	238 k	.72 in.

of the beams and create a failure without causing excessive damage to the columns of the frame.

The lateral load versus drift plot for the 0.5% drift cycles is shown in Fig. 3.10. The plots for the three cycles of load indicated additional loss in lateral stiffness due to deterioration under repetition of loading. The greatest change in stiffness was between the first and second cycles.

The final crack pattern is illustrated in Fig. 3.11. The crack pattern indicates a great deal of flexural distress in the beams. During the last three cycles of loading, the cracks in the beam grew significantly larger. The flexural cracks reached widths of approximately 1/8 to 1/4 in. at the end of the discontinuous negative moment reinforcing bar. There was some concrete spalling and exposure of rebar at these critical cracks. Figure 3.12 shows the large flexural cracks at the top of the first level spandrel beam, approximately 2 ft north of the south column. There was also some splitting along longitudinal reinforcement in the vicinity of these large cracks in the beam, indicating a deterioration of bond. In addition to large flexural cracks there was an increased amount of shear cracking at the ends of the spandrel beams. Figure 3.13 is a picture of the exterior of the north end of the first level spandrel beam. Although the cracks were marked, some of the cracks with widths of approximately 1/8 in. are visible in Fig. 3.13.

After three cycles to 0.5% drift there was increased cracking in the column in both flexure and shear. The flexural cracks in the new column were on the exterior face. The pattern for these cracks is shown in Fig. 3.11 and the flexural cracks in the exterior of the first level north pier are visible in Fig. 3.13. The increased shear cracking is also indicated in Fig. 3.11. Marked shear cracks are shown in Figs. 3.14 and 3.15. The maximum width of shear cracks was about .02 in.

Figure 3.16 illustrates the pattern of yielded bars as indicated by strain gages. Only longitudinal bars in the spandrel beams reached yield. Even at the maximum lateral loads, the greatest stress seen in the reinforcement in the piers was approximately 50% of yield. The strain gages on the beam reinforcement indicated that the bars had probably yielded across most of the critical sections at the joints. Strain gages 111, 115, 279 and 280 indicated that the negative moment hinging in the beam originated away from the joint at the ends of the discontinuous negative moment reinforcing bar and spread toward the joint. The crack pattern indicated that beam hinging spread

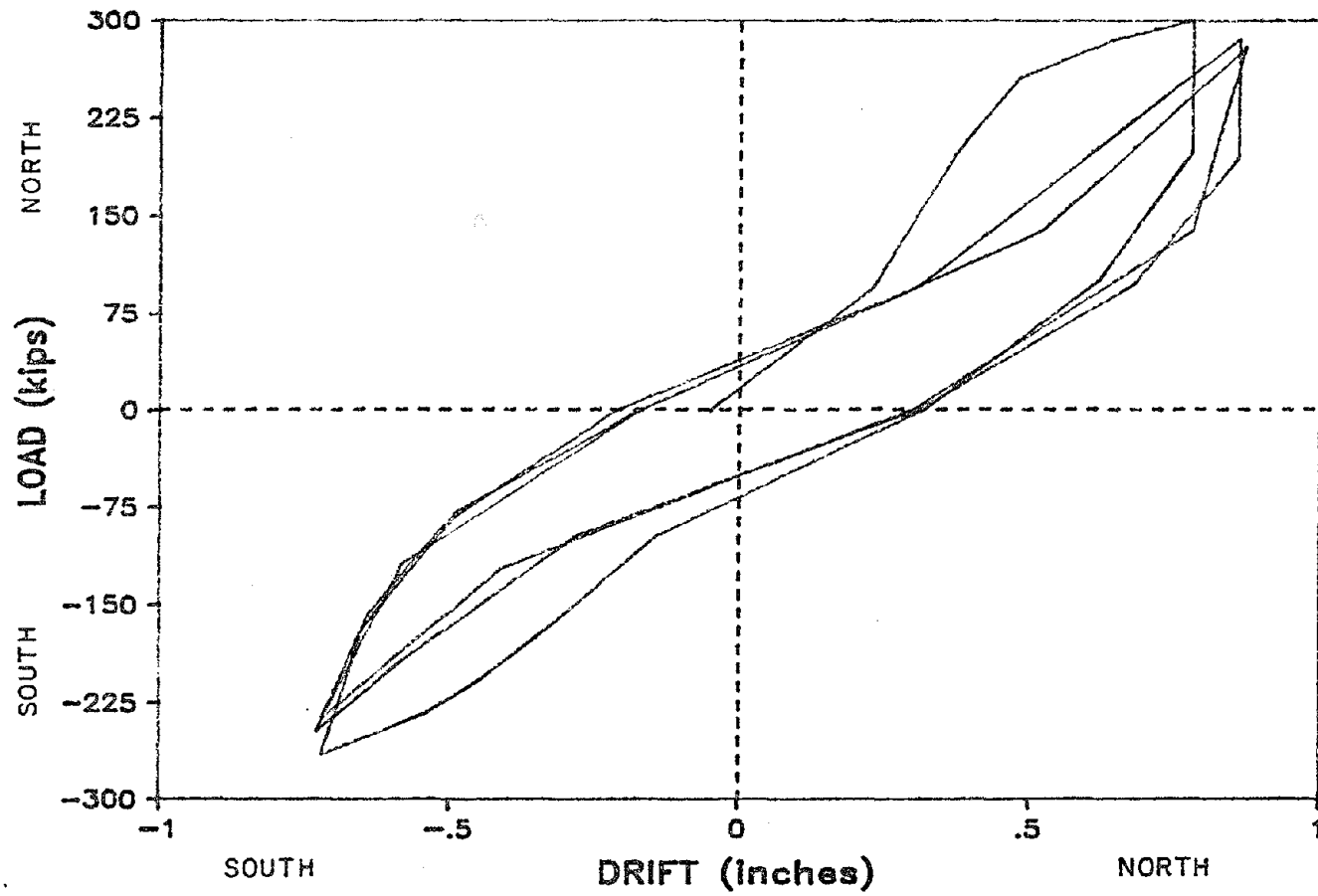


Fig. 3.10 Load vs. drift for three cycles to high (0.5%) drift

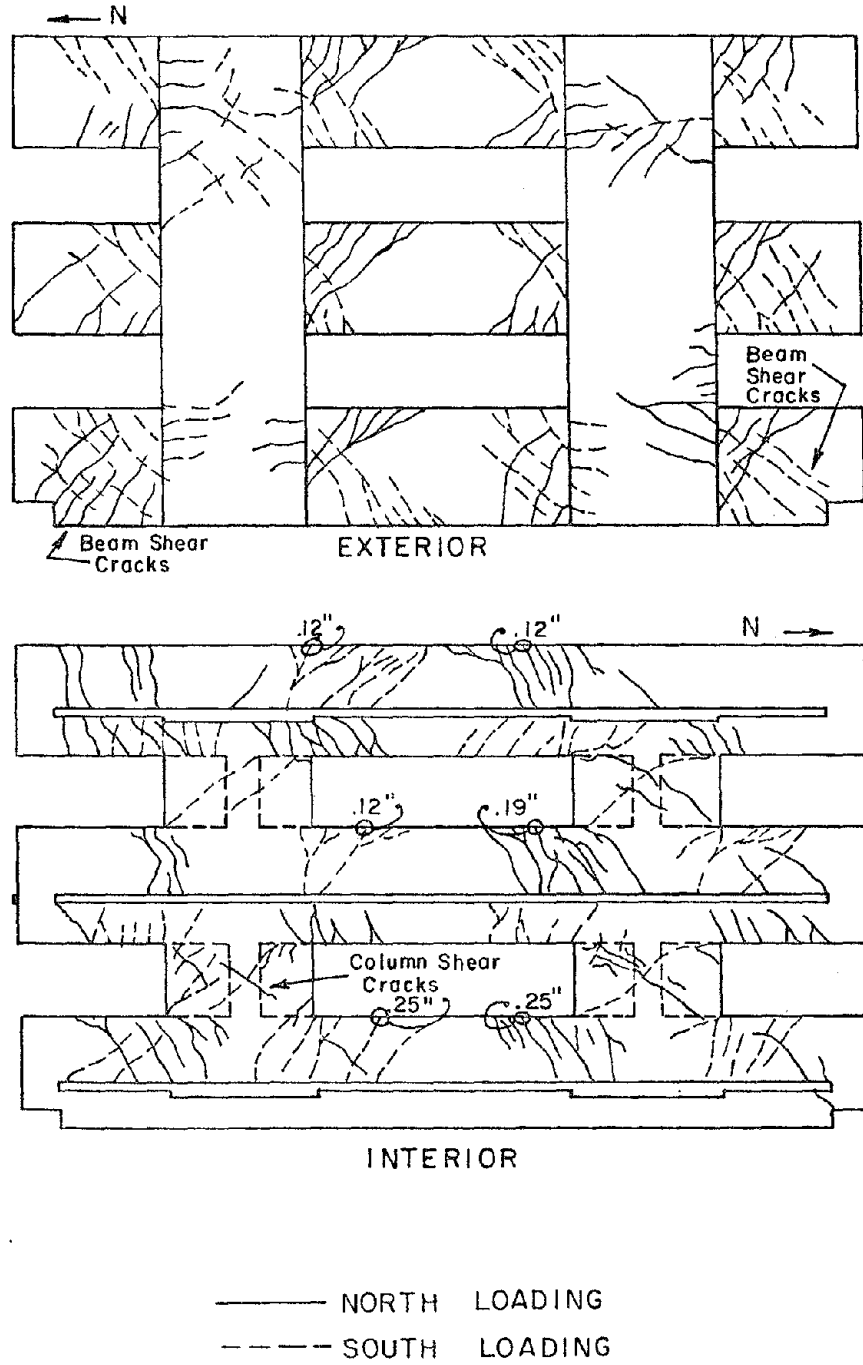


Fig. 3.11 Crack pattern after three cycles to 0.5% drift

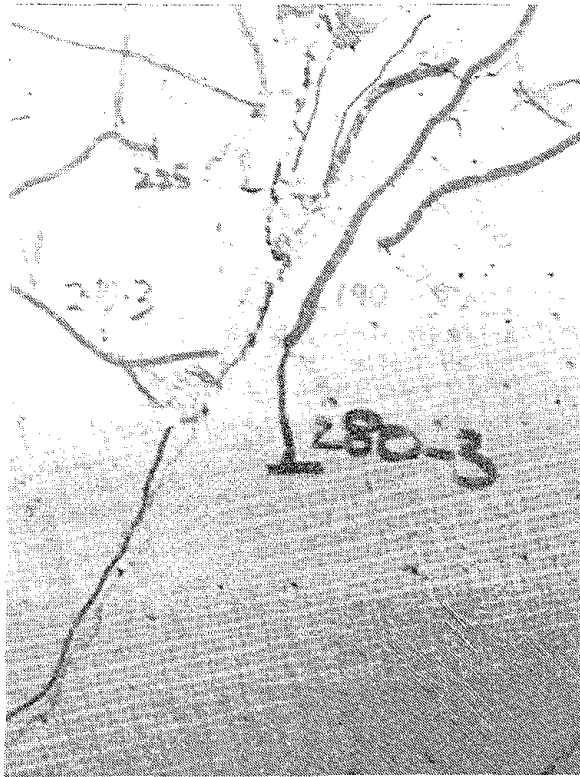


Fig. 3.12 Large flexural crack with some concrete spalling at 0.5% drift. Interior of first level beam, north of south pier

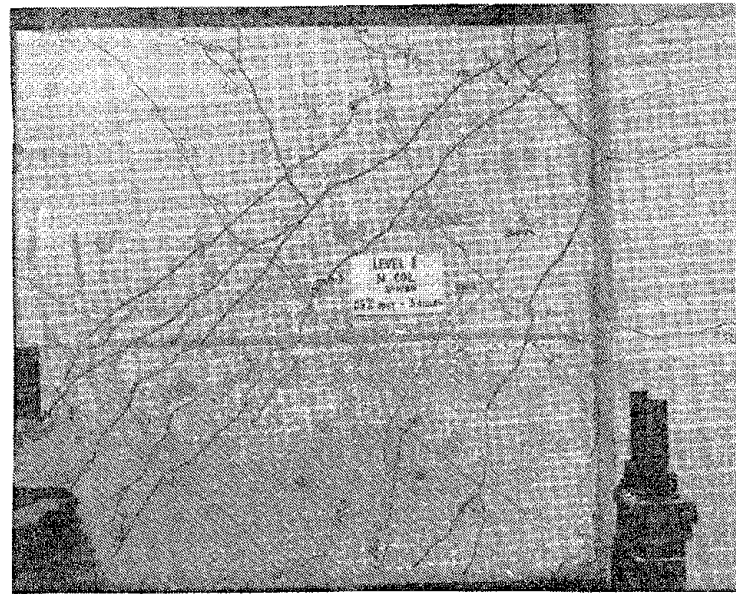


Fig. 3.13 Crack pattern on exterior face of north end, first level beam, 0.5% drift

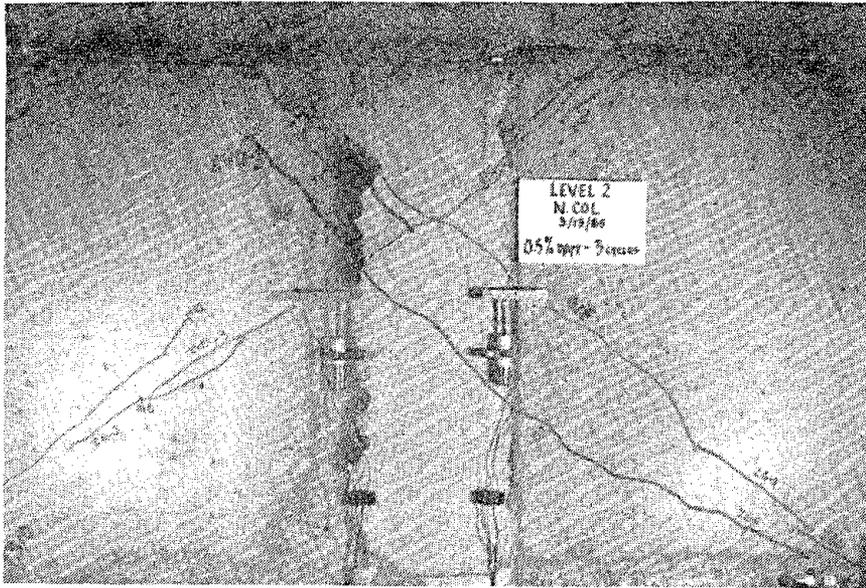


Fig. 3.14 Marked shear cracks on interior of north pier, second level, 0.5% drift

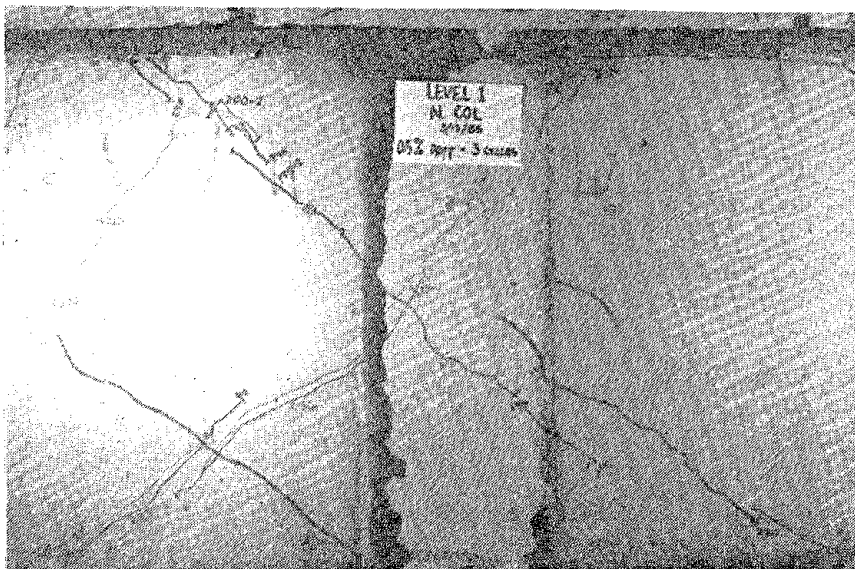


Fig. 3.15 Marked shear cracks on interior of north pier, first level, 0.5% drift

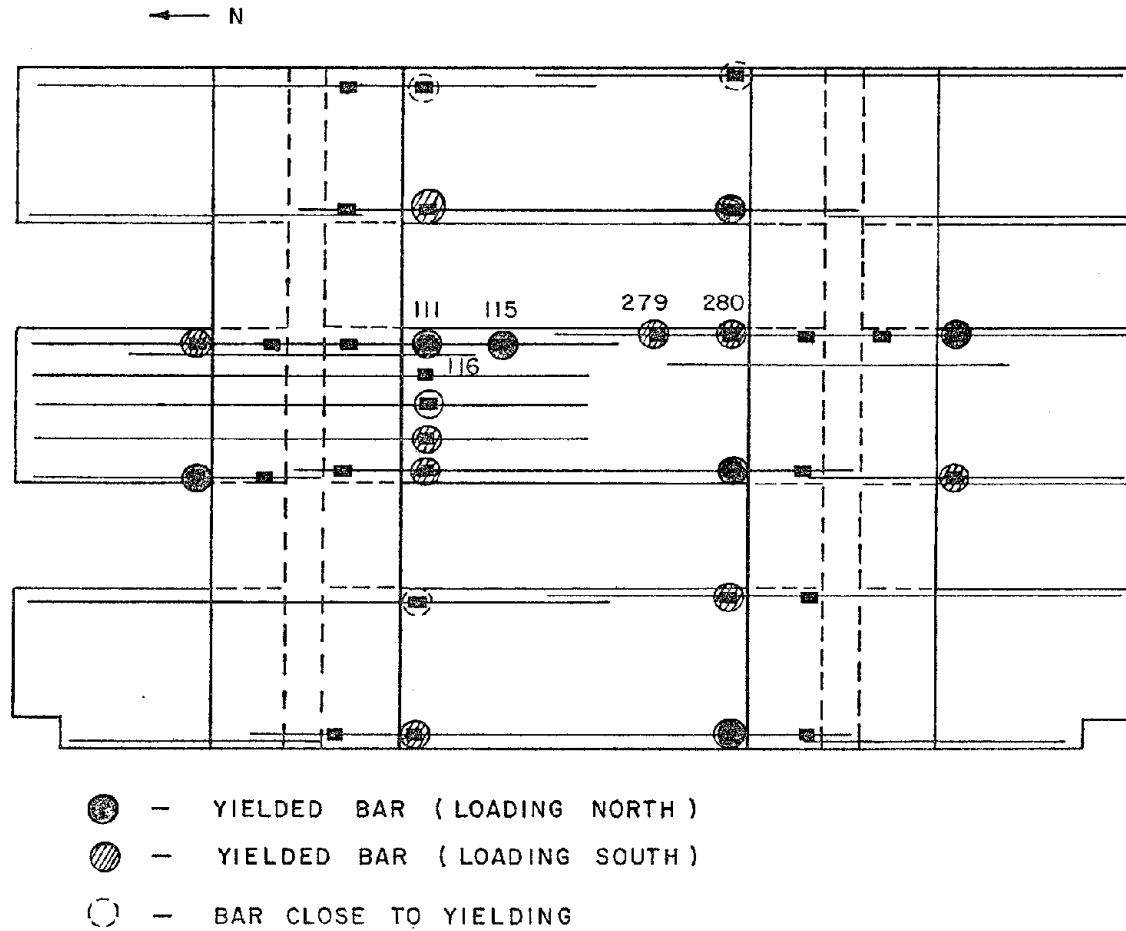


Fig. 3.16 Locations of yielded bars in beams indicated by strain gages after three cycles to 0.5% drift

away from the location of first yield towards the midspan of the beam but there were no strain gages in these locations to verify this.

### 3.3 Summary

The results of the test of the pier strengthened frame gave a good indication of the increased lateral stiffness, increased lateral strength and failure mechanism of the frame retrofitted with reinforced concrete piers. The comparison of the load-drift plots of the existing frame test and the strengthened frame test for 0.05% drift cycles (Fig. 3.3) indicated that the pier strengthened frame was approximately three times as stiff under lateral load as the existing frame.

The crack patterns of the frame and the patterns of yielded bars indicated that behavior was governed by a flexural failure mechanism in the spandrel beams. There were few cracks in the column and none of significant width. The reinforcement in the column was not highly stressed, about one-half yield. The flexural cracks in the beams reached widths of 1/8 in. to 1/4 in. with some concrete spalling observed. The strain gages indicated yield at the top and bottom of each of the beam sections at the pier face. The beam section at the south side of the beam-pier joint at the north end of the second spandrel was gaged throughout its depth. These gages indicated yielded bars throughout the depth of the section (Fig. 3.16). The cracking was also similar at the other section at pier face. Therefore, it is likely that the longitudinal bars throughout the depth of the beams were at or close to yield. The results indicate that the beams were hinging or beginning to hinge at each of the critical beam sections at the joint. The results also indicate that the hinging of the beam under negative moment was significantly affected by the additional, discontinuous reinforcing bars in the negative moment region of the beams.

In addition to flexural cracking there was shear cracking in the beams. The shear cracks occurred at the beam ends of the first and second level beams. The shear cracks in the first level beam had widths between 1/16 in. and 1/8 in. at peak loads. The cracks initiated in the beam at the strut pin hole connections and the corner of the blocked out section of the first level beam. The cracks were probably caused by the local effects of the boundary restraints on the ends of the beams. Similar cracks did not occur at the midspan of the continuous beams of the middle bay.

The nature of cracking in the column was mostly flexural on the exterior and shear on the interior of the frame. The flexural cracks were hairline cracks which began occurring at 0.125% drift levels. The shear cracks were noted at approximately 200 k lateral load (approximately 23% drift) on the frame. These shear crack widths did not grow larger than about 0.02 in. at maximum loads. The shear cracks on the exterior of the pier were hairline cracks which initiated at the peak loads of the test.

The load-drift plots for the last three sets of cycles of loading (0.125% drift, 0.25% drift and 0.5% drift) and an envelope of these plots are illustrated in Fig. 3.17. The load-drift envelope for the two cycles to 0.05% drift of the existing frame test is also illustrated in Fig. 3.17. The envelope of load-drift plots indicated that the strengthened frame began to lose stiffness at 0.25% drift levels. At the 0.5% drift level, the envelope of the load-drift plots was approaching a horizontal tangent indicating that the strengthened frame was near its ultimate load. The calculated lateral capacity of the existing frame was approximately 62 k, two times the calculated shear capacity of one column. The maximum lateral load applied to the frame was 305 k in the north direction. This maximum load was approximately five times the calculated lateral capacity of the existing frame and was not yet the ultimate load of the frame. Had the test not been stopped to prevent excessive damage to the frame, it is likely that slightly higher lateral loads could have been applied.

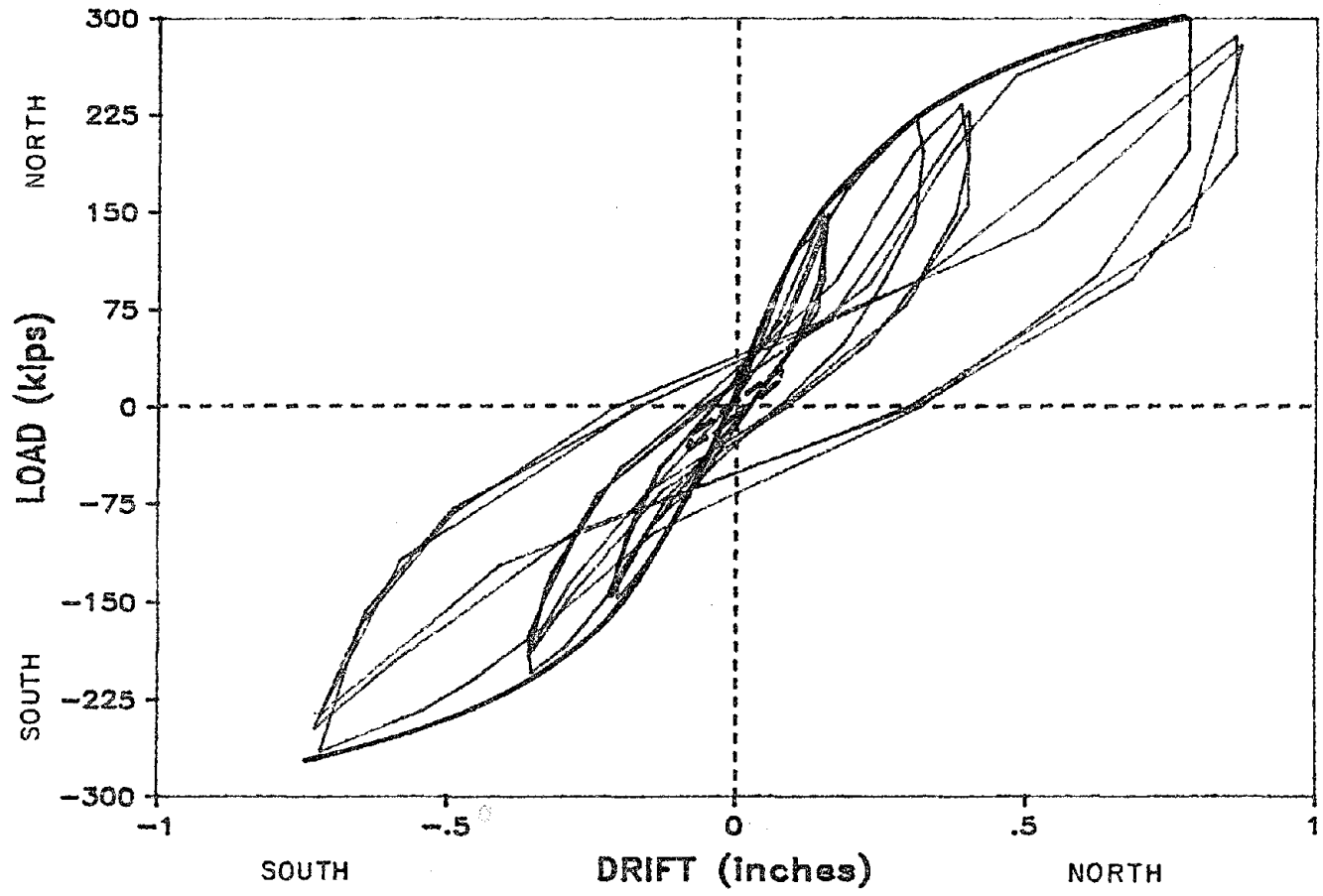


Fig. 3.17 Envelope of Load vs. drift plots for all cycles strengthened frame test

## CHAPTER 4

### ANALYSIS OF PIER BEHAVIOR

#### 4.1 General

The test results discussed in Chapter 3 gave an indication of the lateral strength, lateral stiffness and failure mechanism of the pier strengthened frame. The test specimen was also instrumented to yield information on the behavior of the reinforced concrete piers and their interaction with the existing frame. This instrumentation was located largely at the second level of the north pier, indicated in Fig. 2.51, which was assumed to be a typical joint of the pier strengthened frame. The data from strain gages on the pier reinforcement, strain gages on the dowels and linear voltage displacement transducers (LVDTs) were analyzed. In general, the data yielded information on the flexural and shear behavior of the piers; as well as, information on the behavior of the dowels and the connection between the pier strengthening materials and the original frame.

While analyzing the flexural behavior of the piers, it was important to note that the second level beam-pier joints were the typical joints with two beams and two piers framing into them. The beam-pier joints on the first and third level each had a beam on either side but only one pier framing into the joint. Only the top story of the prototype building would have had joints framed by two beams and one pier. Under lateral loading conditions, the beams contributed moments to the joint which were additive and were balanced by the additive moments contributed by the piers. In the first and third level joints of the model frame there were two beams contributing moments with only one pier section to balance the moments, increasing the moments in the pier at the cross sections at the bottom of the first level window segment and the top of the second level window segment were not modeling moments that would have existed in the pier of the third, fourth and fifth stories of the prototype building. As mentioned in Chapter 2, the pier was designed for the large moments developed at the first level by the lateral forces. However, the joints at the first level were not true models of the first story of the prototype building because the joints were not restrained from rotation as the first story would be restrained by the foundation.

## 4.2 Analysis of Data

4.2.1 Interstory Drift. The linear voltage displacement transducers (LVDTs) 180, 181 and 185 measured the lateral movement of the south end of the first, second and third level beams at the slab level. Figure 4.1 is a plot of the percent of interstory drift between the levels of the frame for the last three cycles of loading. A comparison of the plotted values shows that the percent of interstory drift was approximately the same between the levels at a given lateral load, indicating that the piers strengthened the frame uniformly along its height.

4.2.2 Crack Patterns. The pattern of cracking on the piers provided an indication of their behavior. The pattern of cracking after three cycles of loading to 0.5% drift is shown in Fig. 4.2 for the exterior and interior of the piers of the north and south columns. In general, Fig. 4.2 shows a pattern of flexural cracking on the exterior face of each pier and a pattern of shear cracking on the interior face of the piers between the spandrel beams (the window segment).

The pattern of flexural cracks (Fig. 4.2) on the exterior of the piers indicated that the piers were deformed in reverse curvature, as columns, under lateral load. The flexural cracking indicated that the flexural tension was transferred primarily in the exterior 8 in. of the piers. The majority of flexural cracking in the piers was concentrated near the joints of the first and third levels of the frame. These joints had a two beam - one pier configuration which produced high moments in the piers. Figure 4.3 is a view of the crack pattern of the north pier window segment at the second level. This is the area of the frame which was heavily instrumented. The only visible evidence of flexural tension in the interior of the piers occurred at the top of the window segments of the piers. A flexural crack initiated at the top corners of the interior of the window segments and extended along the new/existing concrete interface. These cracks probably were indicative of poor bond and poor concrete compaction at the top of the window segment rather than high stresses. There was very little hydrostatic pressure on the concrete at this level during casting to promote adequate compaction and good bond between the new and existing concrete at the interface.

The majority of the shear cracking in the piers occurred on the interior face. These shear cracks initiated in the weak plane of the new/existing concrete interface as flexural

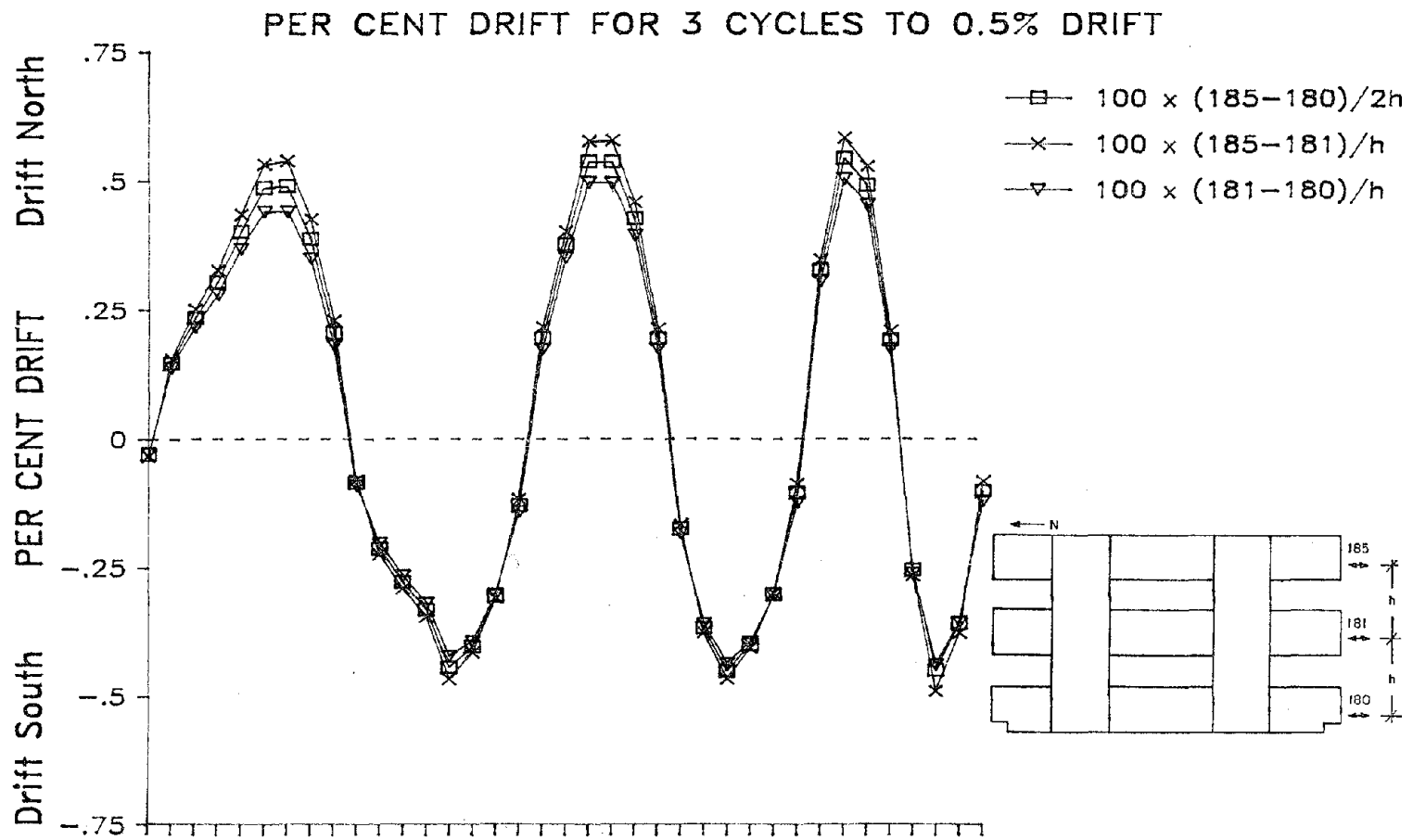


Fig. 4.1 Interstory drift for last three cycles of loading

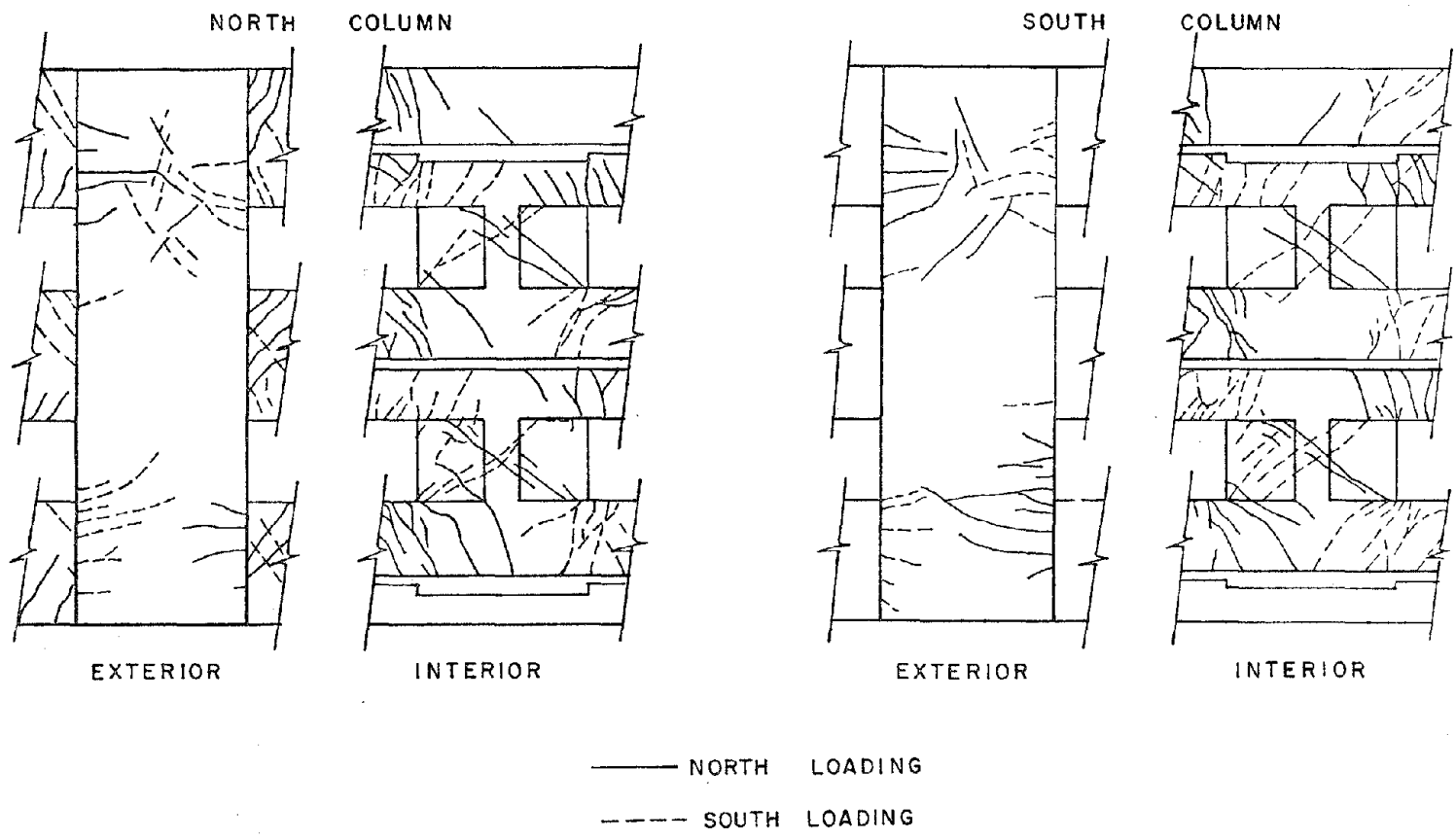


Fig. 4.2 Crack patterns of piers after three cycles to 0.5% drift

TRANSITION FROM FLEXURAL CRACK TO SHEAR  
CRACK UNDER LOADING IN THE OPPOSITE DIRECTION

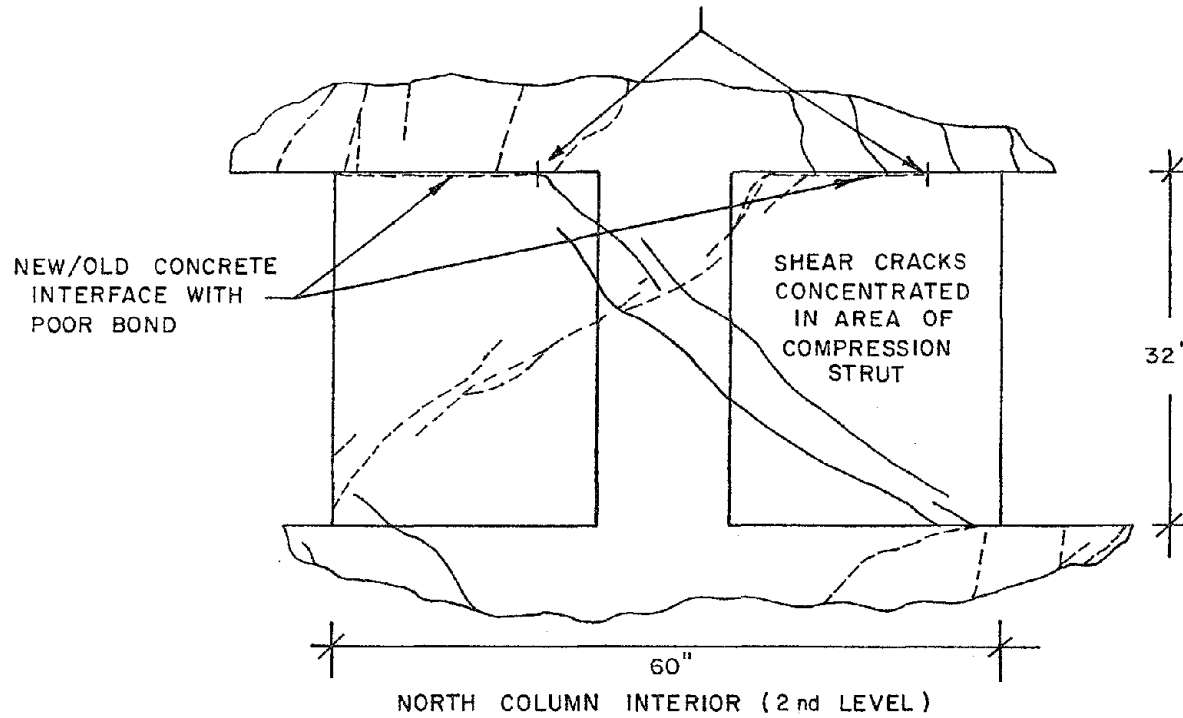


Fig. 4.3 Crack pattern, interior window segment, north pier, second level, three cycles to 0.5% drift

cracks. During loading in the opposite direction, these cracks developed into diagonal shear cracks. The majority of these shear cracks made the transition from horizontal cracks to diagonal cracks at a point near the original column at lateral load levels between 200 and 250 k. At about the same load levels, diagonal shear cracks also initiated in the opposite corner of the interior pier window segment. At higher loads the diagonal cracks crossed the original column and met. Parallel shear cracks also formed. Eventually, at the peak loads of the test, some small diagonal shear cracks occurred on the exterior of the pier. There was a slightly lower level of shear cracking due to south loads, indicating slightly lower shear and stress levels.

The pattern of parallel shear cracks in the interior of the pier supported the concept that a compression strut formed across the interior of the pier window segment as represented in Fig. 4.4. Figure 4.4 shows the assumed areas of stress transfer for north loading conditions. The compression and shear forces were likely transferred from the bottom of the beam into the top of the 5-1/3 in. interior thickness of the pier near the original column of the frame where the diagonal cracks initiated. The parallel shear cracks indicated a concrete strut which transferred these forces through the pier and into the top of the beam at the bottom of the window segment. There was very little cracking in the region of the pier away from the strut, indicating that little force was transferred in that area of the pier. The orientation and width of the compression strut was assumed from the crack pattern of the pier. Had the compaction of concrete been better at the new/existing concrete interface at the top interior of the pier window segment, the shear cracks might have initiated at the top corner of the pier window segment in the same manner as at the bottom corner. Epoxy-grouted dowels into the bottom of the beam would probably serve the same purpose as better concrete consolidation but overhead dowels are difficult to place.

4.2.3 Stresses in Longitudinal Pier Reinforcement. Strain gage data for stresses in the longitudinal reinforcement across the pier cross sections are presented in Figs. 4.5 through 4.8. Each figure shows the stresses for the maximum load in each direction: 305 k north and 265 k south. The stresses in Figs. 4.5 through 4.8 indicated much higher strain gradients across the piers at the bottom of the first level and the top of the second level window segments. The strain gradients correlated with crack patterns observed and were expected considering the joint configuration. The strain

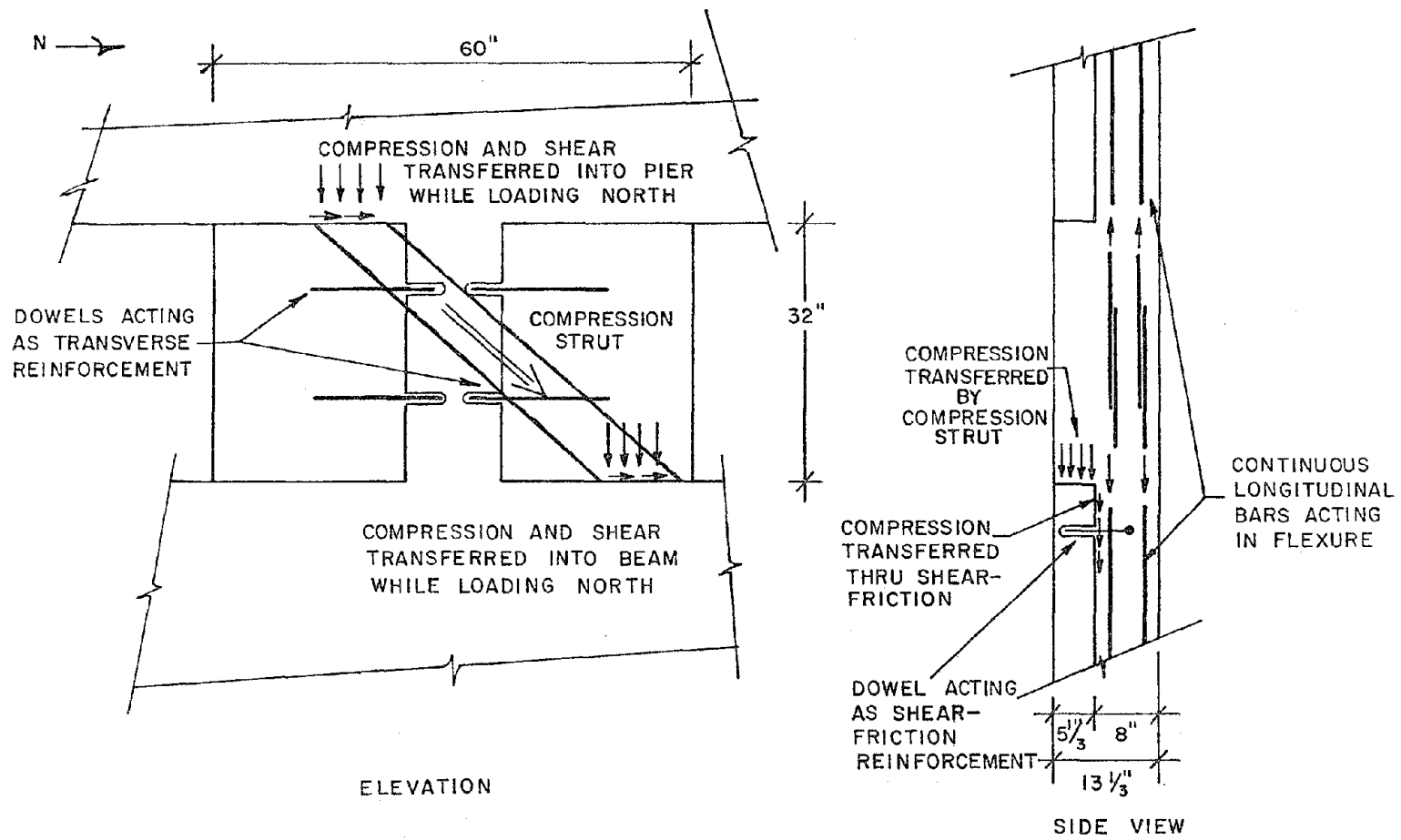


Fig. 4.4 Assumed behavior pattern of window segment under north loading conditions.

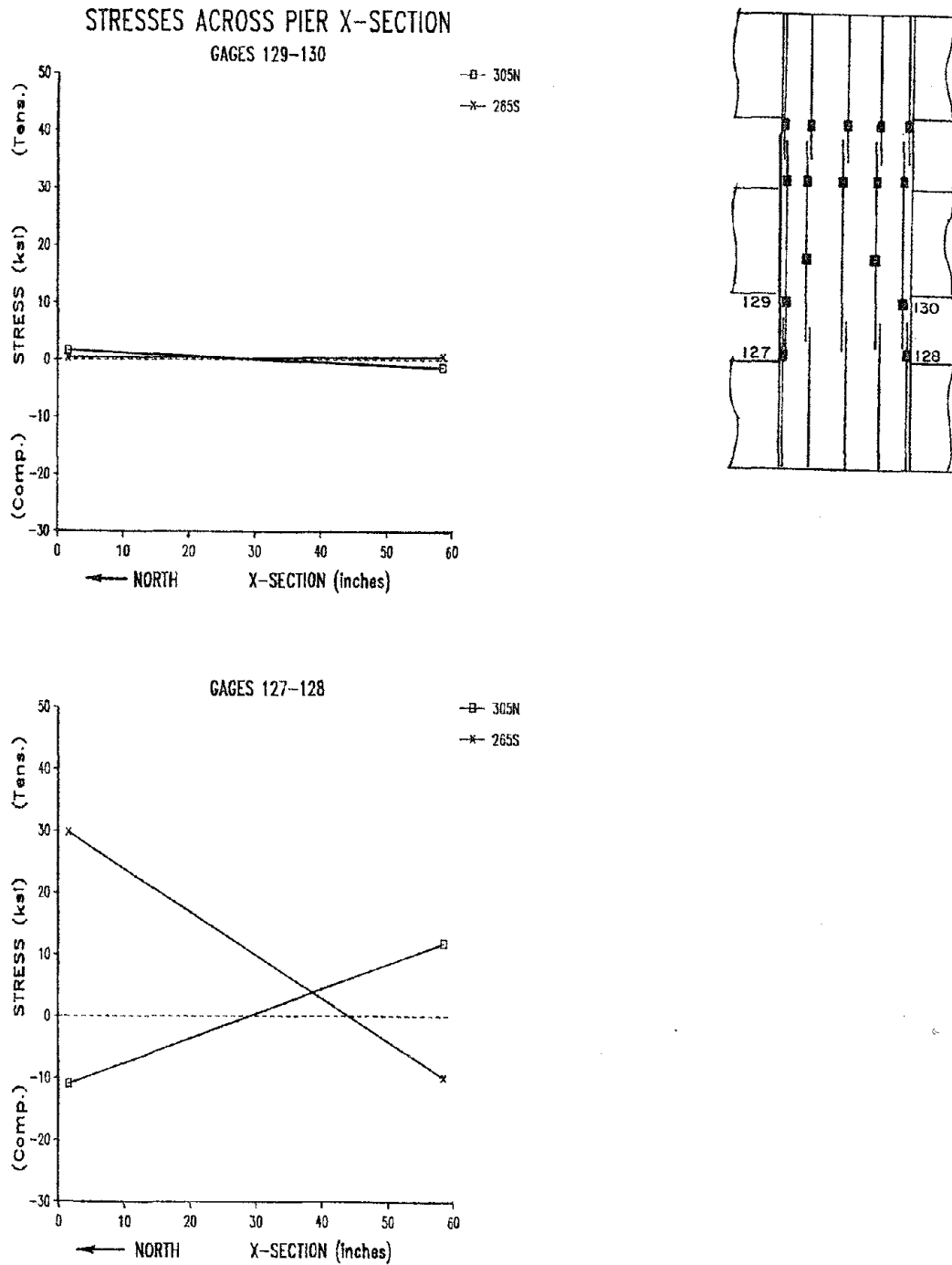


Fig. 4.5 Stress gradients across top and bottom cross sections of north pier, first level

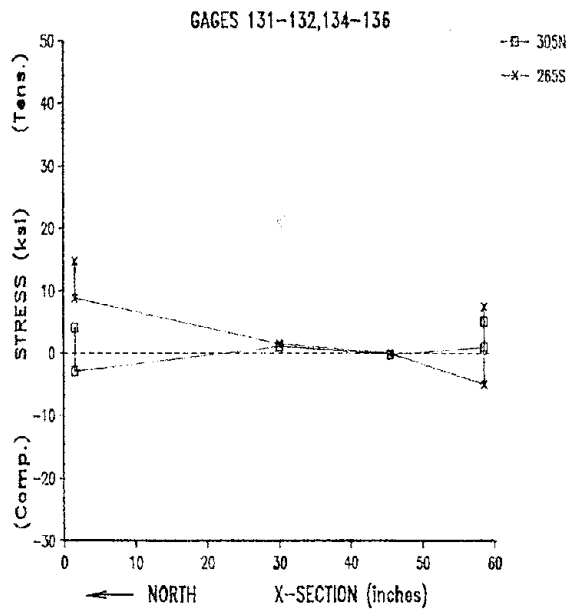
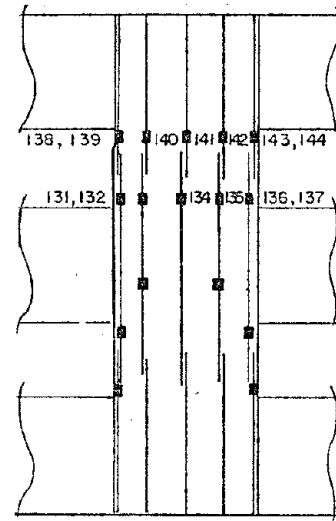
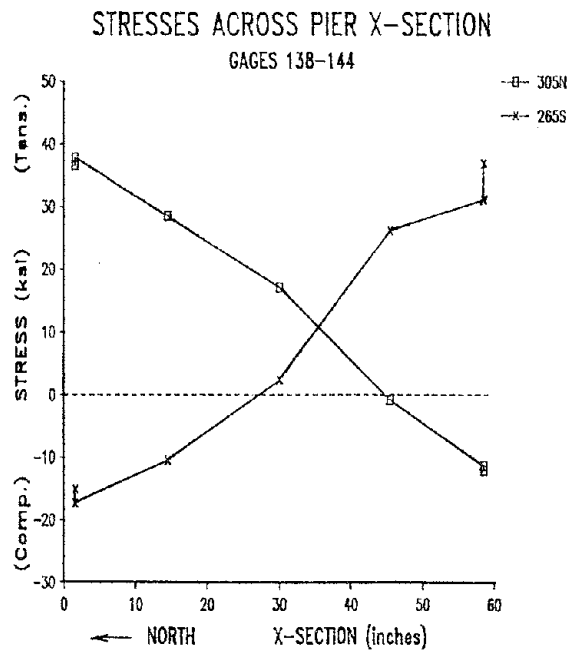


Fig. 4.6 Stress gradients across top and bottom cross sections of north pier, second level

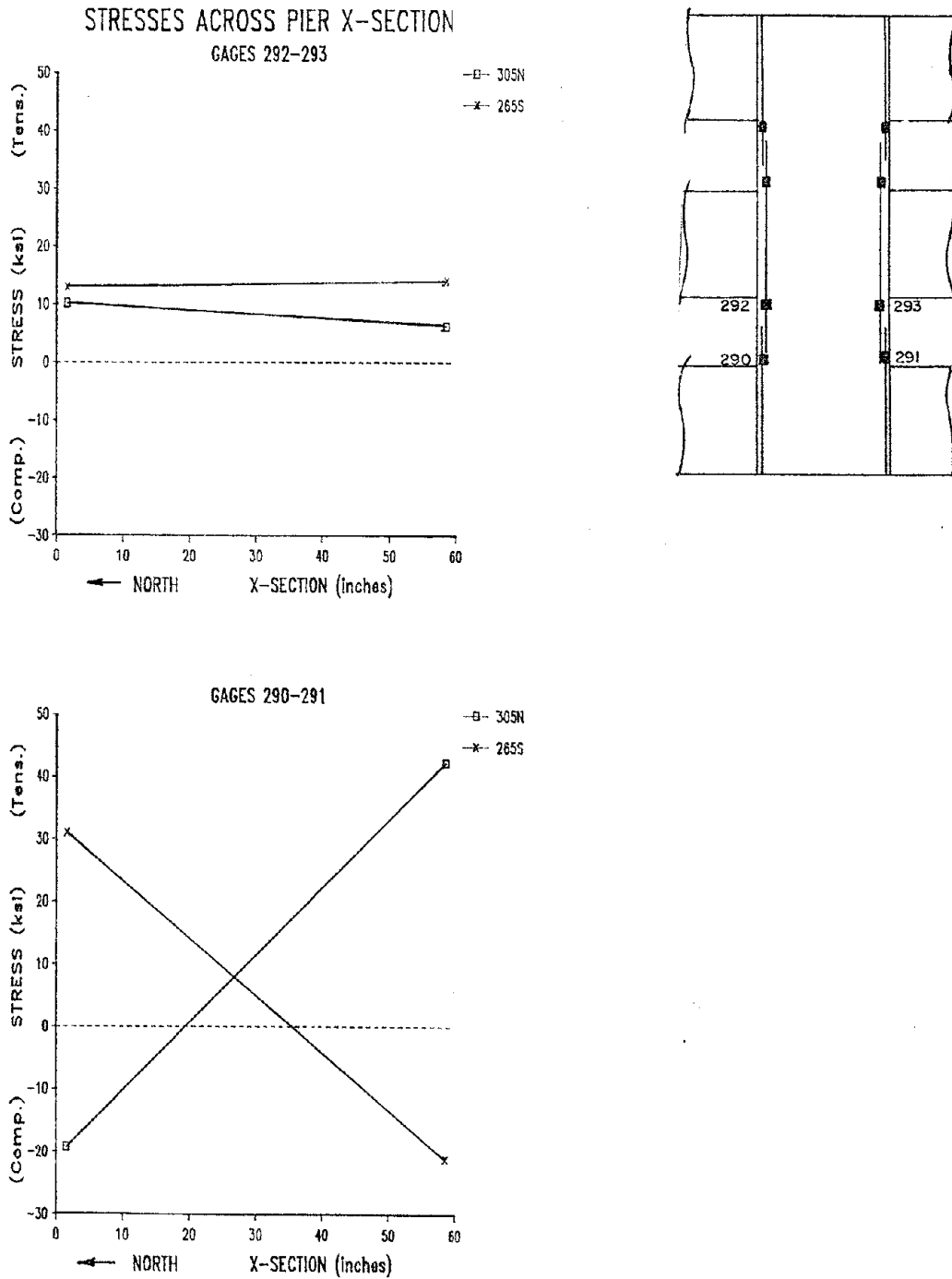


Fig. 4.7 Stress gradients across top and bottom cross sections of south column, first level

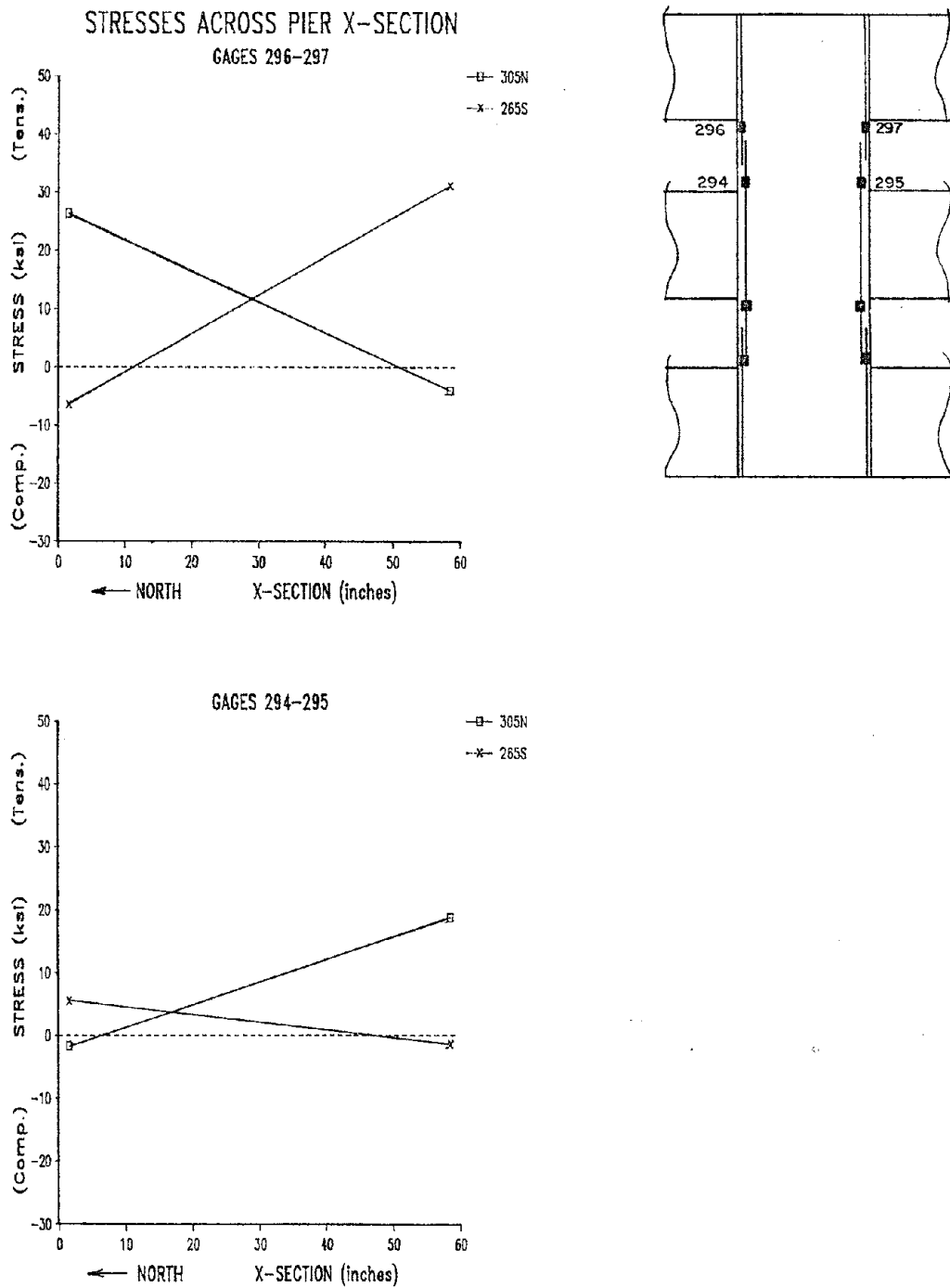


Fig. 4.8 Stress gradients across top and bottom cross sections of south column, second level

gradients also correlate to the nature of flexural cracking of the piers. The appearance and lateral stiffness of the piers suggested that the piers could have behaved as small shear walls and deformed in single curvature. However, the pattern of strains in the longitudinal bars and the crack pattern of the piers indicated reverse curvature of the pier between the spandrel beams. The pier behaved as a column would in frame action.

The stresses plotted in Figs. 4.5 through 4.8 were, determined from strain gages located on the front layer of longitudinal reinforcement in the pier except for strain gages 292 through 295 which were located on the second layer of reinforcement, approximately 5 in. from the front layer. Figure 4.6 is a plot of the two cross sections which had gages on the outside longitudinal bars in both layers of reinforcement (gages 131 & 132, 136 & 137, 138 & 139, and 143 & 144). These plots indicated there was a strain gradient normal to the plane of the frame across the 5-in. thickness between the two layers. This gradient was slight in comparison with the gradient across the width of the pier. It indicated an out-of-plane movement in the pier that was possibly due to the eccentric loading of the frame or the eccentricity of the centroid of the pier relative to the centroids of the original column and spandrel beams.

4.2.4 Slip at the New/Existing Concrete Interface. The relative slip between the pier and the original frame was measured by LVDTs 186 through 195 at the concrete interfaces. The LVDTs were located around the heavily instrumented joint of the north pier as indicated in Fig. 2.53. The data from the LVDTs measuring slip support the concept of a compression strut across the window segment on the interior face of the pier. Figure 4.9 is an illustration of the window segment interior, north pier - second level, with the locations of the LVDTs and the assumed compression struts for each direction of loading. Table 4.1 lists the LVDTs which showed significant slip under the two directions of loading and the direction of slip. The arrows in Fig. 4.9 indicate the direction of positive slip for recording and plotting purposes. A comparison of the information in Table 4.1 with the illustration of Fig. 4.9 indicated that slip occurred, and forces were transferred, in locations and directions expected from the assumed compression strut behavior.

The north loading condition produced compression struts, as shown, which transferred high stresses across the interfaces monitored by LVDTs 190, 188, 187, 192 and 195. LVDTs 190 and 187 indicated a transfer of shear at the top and bottom

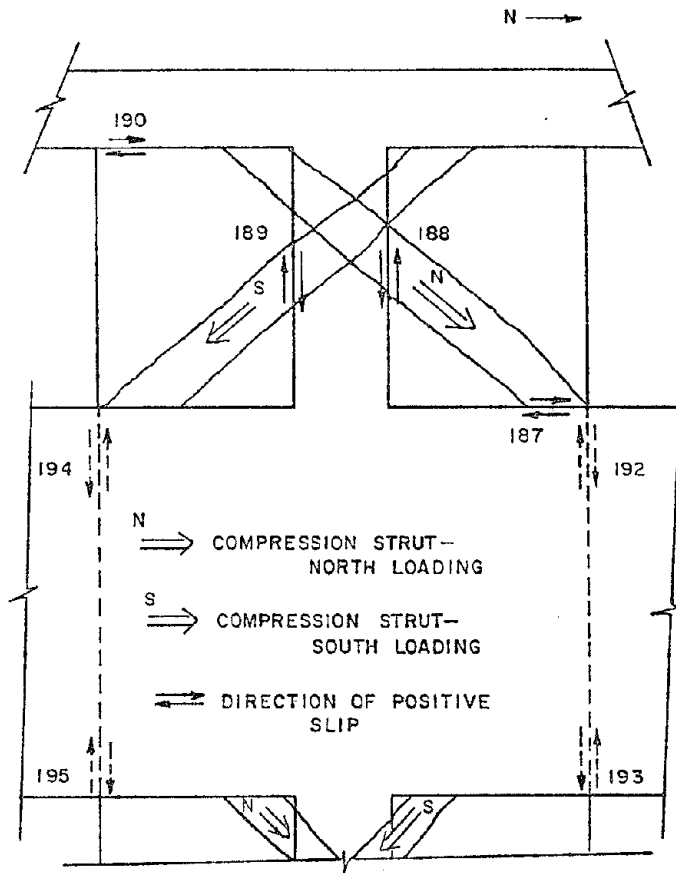


Table 4.1 Slip Behavior

LVDTs with High Slip Under North Loading	Direction Of Slip
190	positive
188	positive
187	positive
192	negative
195	negative
LVDTs with High Slip Under South Loading	Direction of Slip
188	positive
194	negative
193	negative

Fig. 4.9 Locations of LVDTs and compression struts, window segment, north pier, second level

of the compression strut. LVDTs 192 and 195 indicated a transfer of stress across the beam face in the compression zones at the bottom of the second level compression strut and the top of the first level compression strut. LVDT 189 showed high slip due to a shear crack, which formed the compression strut, opening between the LVDT and the reference block.

The lower level of cracking and lower loads due to south loading suggested that the compression strut was not as fully formed as the north loading compression strut. The LVDTs measuring horizontal slip at the ends of the compression strut did not show significant slip. LVDTs 194 and 193 indicated a transfer of stresses across the beam face in the zones of compression at the ends of the compression struts. LVDT 189 showed a high slip due to shear cracking as did LVDT 188.

Figures 4.10 through 4.17 are load versus slip plots for the LVDTs discussed. The plot of Fig. 4.10 for LVDT 190 suggested that there was a gap at the interface at the top of the window segment. Under south loading, the two surfaces moved freely without stress transfer. Under north loading the interface was in the compression zone. There was no slip due to north loading until approximately 250 k load (or 0.29% drift). This indicated that the surfaces were bearing and transferring applied stresses due to shear-friction until the load, 250 k north, was reached at which friction was overcome and slip occurred. The plot of Fig. 4.11 for LVDT 187 indicated a good bond and no relative slip across the interface until the high stresses broke the initial bond at approximately 250 k north.

Figures 4.12 and 4.13 are the load-slip plots for LVDTs 192 and 195 which also showed significant slip under north loads. These LVDTs were located on the exterior of the frame. They showed high slip under north loads when they were located in the compression zones at the ends of the compression struts. Both of these LVDTs showed a sharp increase in slip at the same load as 190 and 187 showed an increase, 250 k north. The plots of 192 and 195 indicated that compression stresses transferred from the top and bottom of the compression struts and across the beam face - pier interface in shear-friction.

Figures 4.14 and 4.15 are load-slip plots for LVDTs 193 and 194 which showed significant slip under south loads. These LVDTs were located on the exterior of the frame in the compression zones at the ends of the compression struts. These LVDTs had a gradual increase of slip in the three cycles of loading to 0.5%. The slip indicated again a transfer of stresses

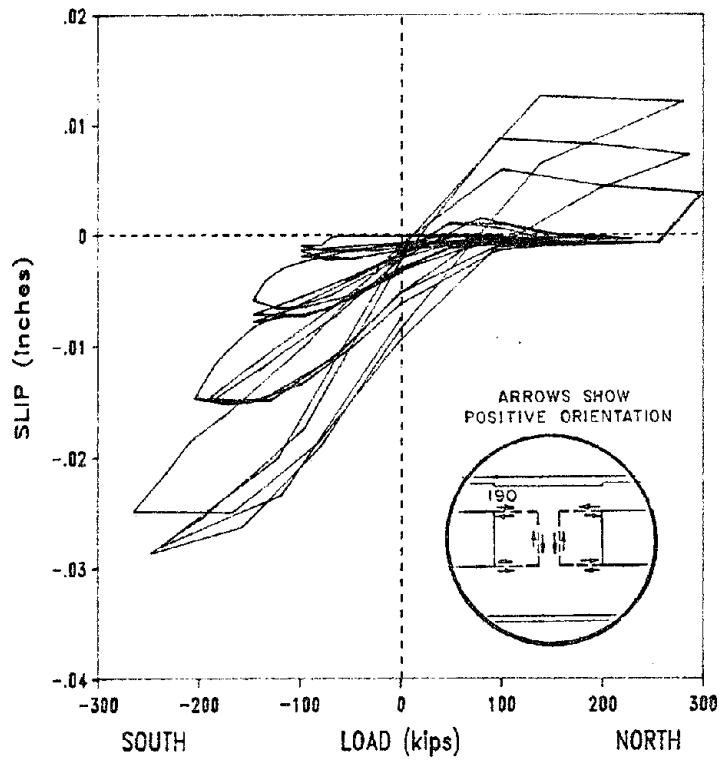


Fig. 4.10 Load vs. slip for LVDT 190

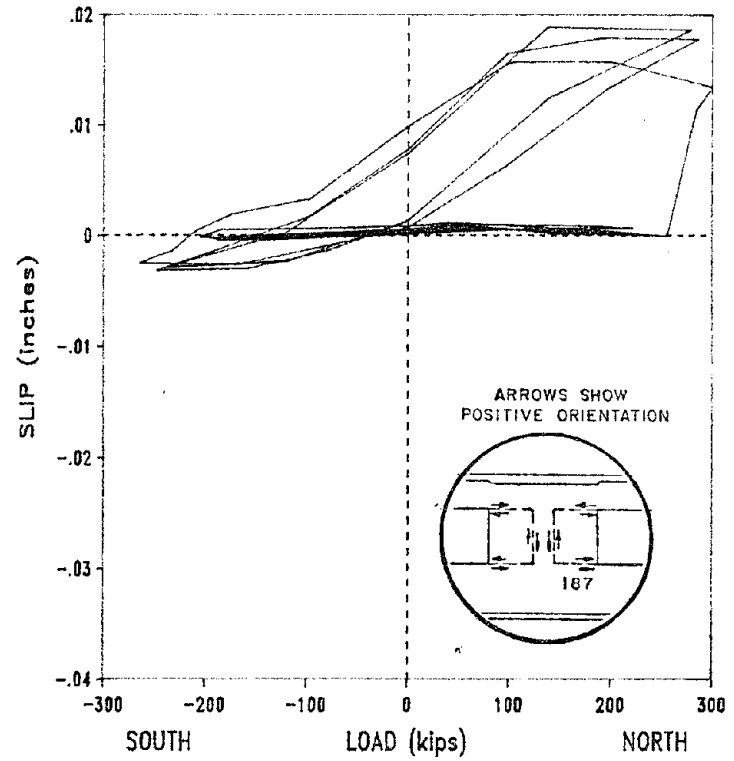


Fig. 4.11 Load vs. slip for LVDT 187

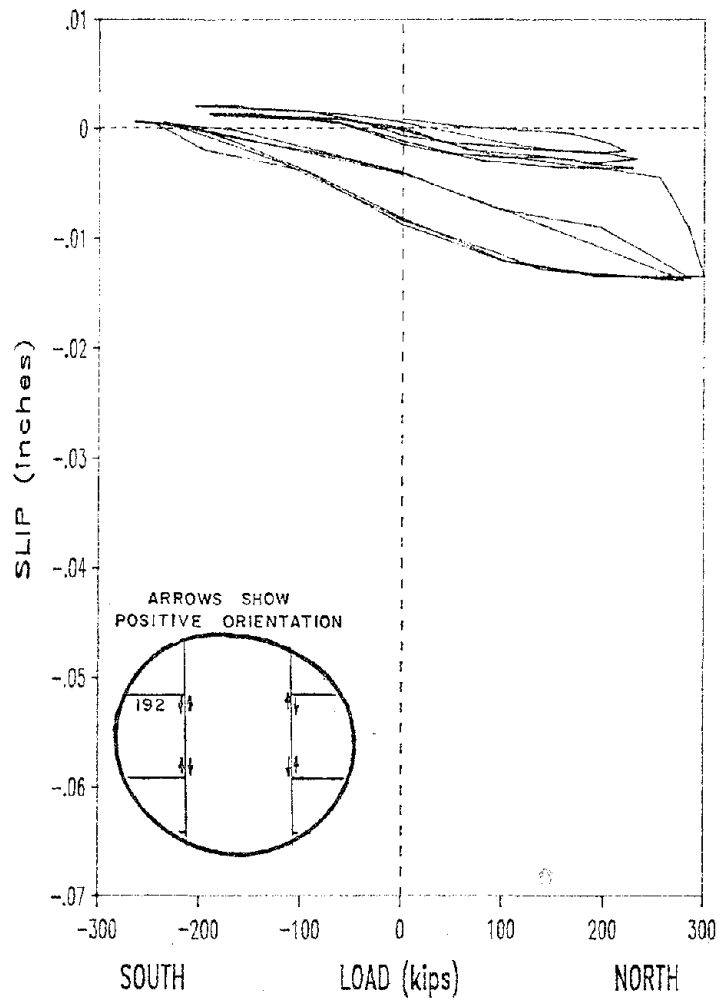


Fig. 4.12 Load vs. slip for LVDT 192.

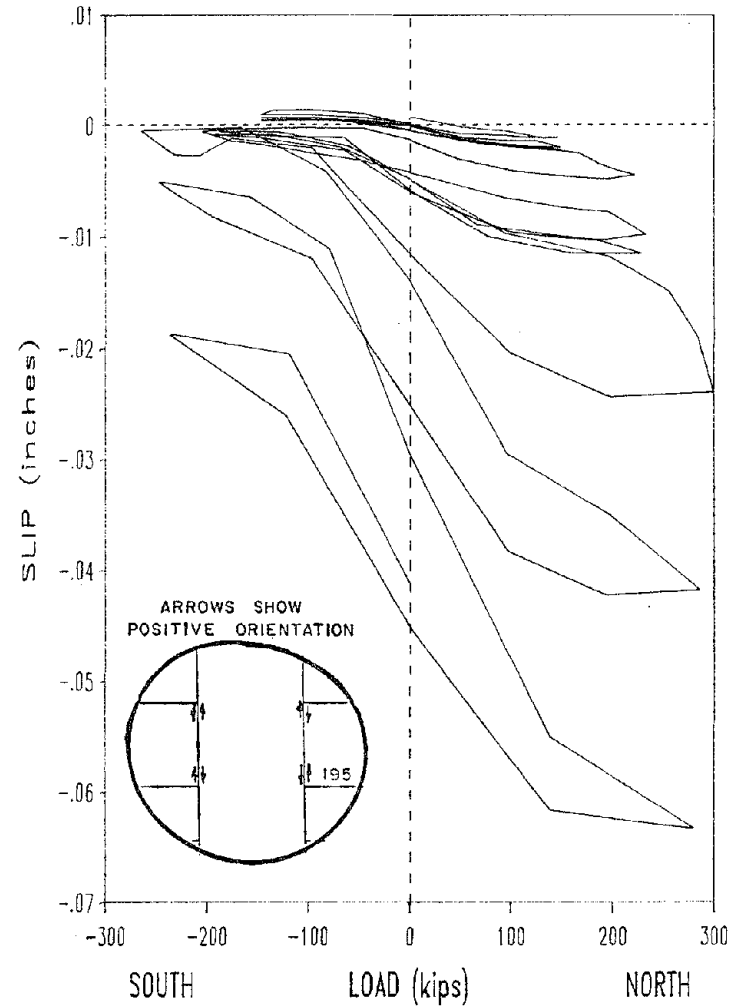


Fig. 4.13 Load vs. slip for LVDT 195.

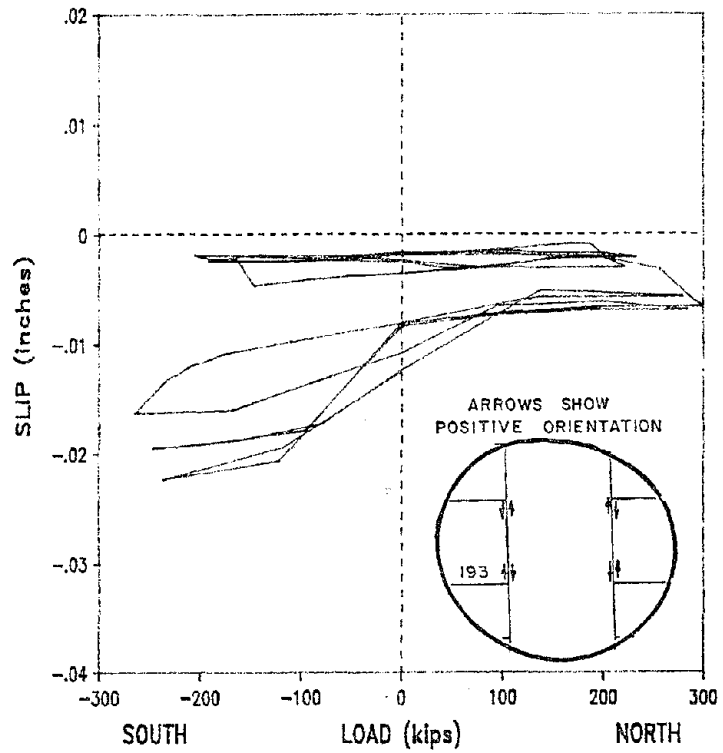


Fig. 4.14 Load vs. slip for LVDT 193

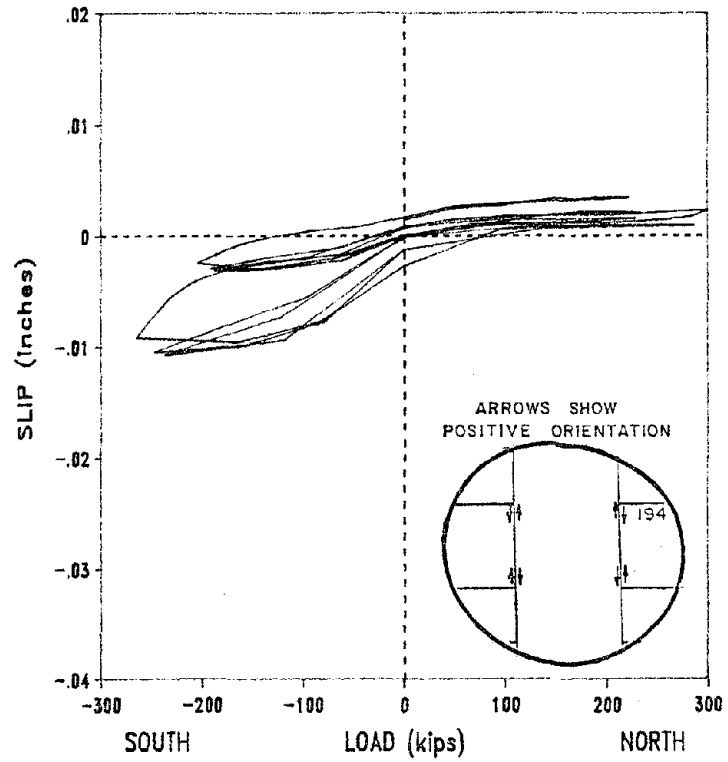


Fig. 4.15 Load vs. slip for LVDT 194

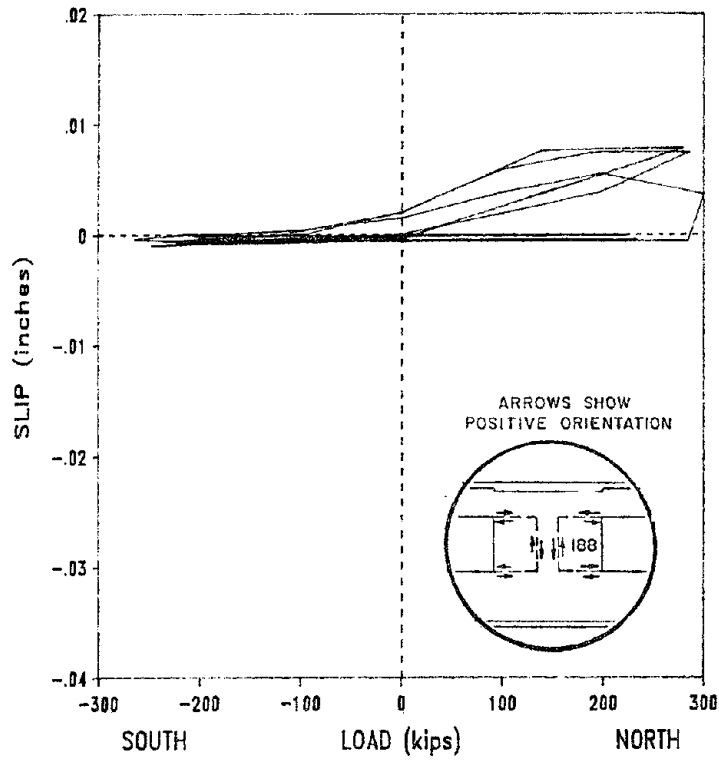


Fig. 4.16 Load vs. slip for LVDT 188

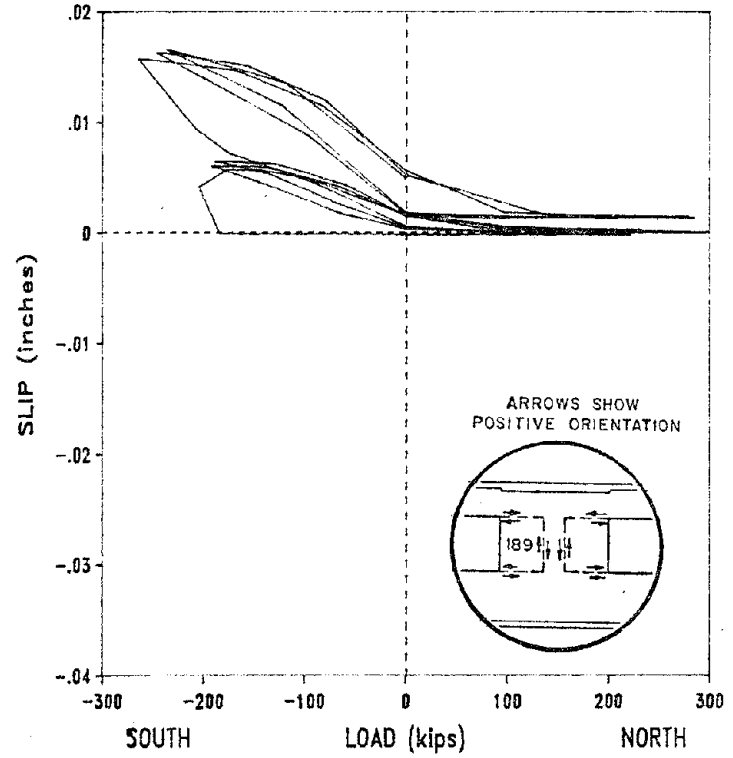


Fig. 4.17 Load vs. slip for LVDT 189

from the top and bottom of the compression strut and across the beam face - pier interface through shear-friction.

The load-slip plots of LVDTs 188 and 189 are shown in Figs. 4.16 and 4.17. They indicated no relative slip until a lateral load, approximately 290 k north for 188 and 210 k south for 189, at which there was a sharp increase in relative movement. The relative movements of 188 and 189 were due to shear cracks opening between the LVDTs and the reference blocks.

4.2.5 Stresses in the Dowels. The dowels were instrumented with strain gages 157 through 169 as shown in Fig. 2.51. The hooked dowels epoxy-grouted into the spandrel beams, which were designed to act as shear-friction reinforcement, were instrumented with strain gages 164 through 169. The shear-friction reinforcement was designed for load levels at which it was assumed high stresses would break the adhesive bond between the new and old concrete. The second phase of this research project necessitated removal of the reinforced concrete piers from the frame. During this process it was discovered that the bond between the new and existing concrete was excellent in most places. Where the concrete could not be cut with a concrete saw, it was necessary to remove the new concrete with a jack hammer. The new concrete showed no signs of cleaving away from the original frame. Therefore, stresses which overcame adhesive bond during the test were assumed to be high.

The data from gages 164, 165, 168 and 169 indicated these dowels were not engaged and generally did not undergo stresses greater than 1 ksi. The dowels of gages 166 and 167 indicated significant stresses as shown in Figs. 4.18 and 4.19. Also shown in Figs. 4.18 and 4.19 are plots of load versus slip for LVDT 192 and 194 for the first cycle at 0.5% drift. LVDTs 192 and 194 were located close to dowels 166 and 167 respectively and a comparison of the load versus stress of the dowel and the load versus slip for the LVDT at that approximate location indicated similar behavior. The tensile stress of the dowel and the slip of the LVDT increased at the same load and in the same direction of loading.

The stresses in dowel 166 increased under north lateral load and increased sharply at a level of about 250 k (approximately 0.29% drift) north. This sharp increase probably occurred when the bond broke around the dowel and the dowel was engaged. The dowel was stressed under north lateral load which produced a compression strut terminating in the area of this dowel. Under south lateral loads, dowel 166 was in the tension

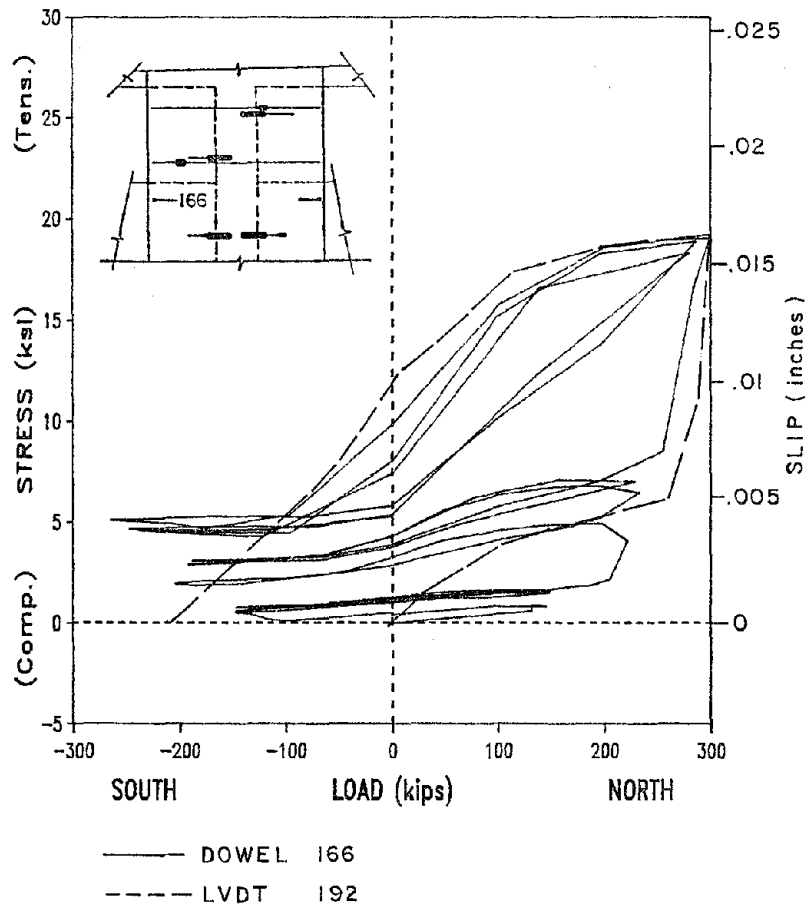


Fig. 4.18 Load vs. stress for dowel 166 and load vs. slip for LVDT 192.

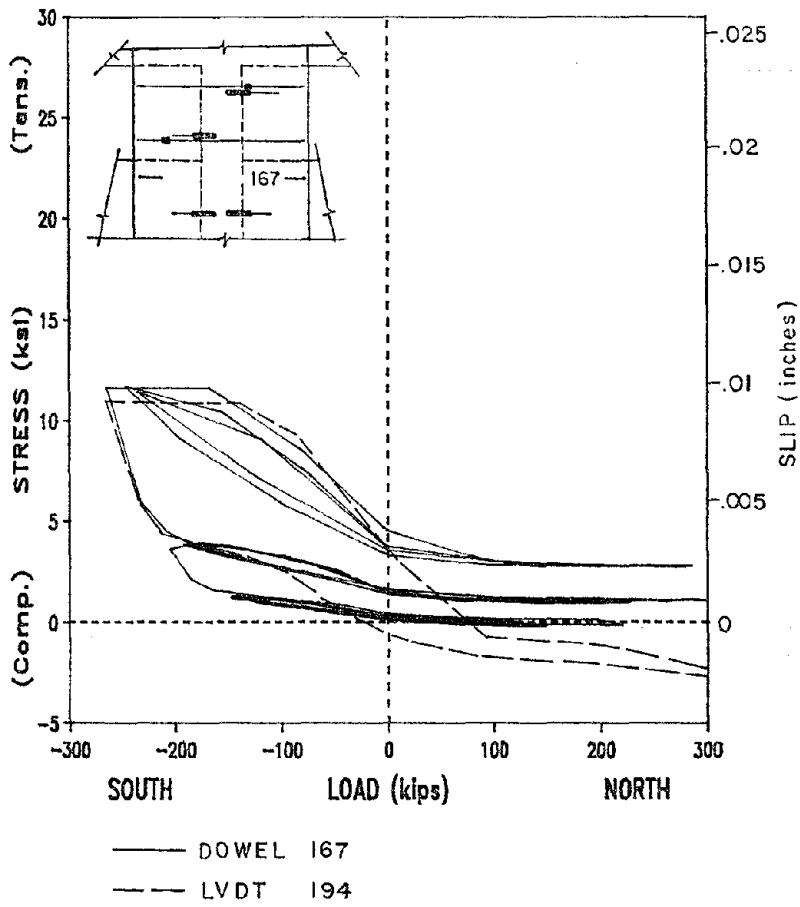


Fig. 4.19 Load vs. stress for dowel 167 and load vs. slip for LVDT 194

zone of the pier and showed no stresses. Gage 167 showed high stresses for south lateral loads when it was in the compression zone of the pier but not for north lateral loads when it was in the tension zone.

The indication was that the dowel was engaged as shear-friction reinforcement and stresses were transferred as indicated in Fig. 4.4 when the dowel was near the compression face of the pier but not when the dowel was near the tension face of the pier. The beam dowels agreed well with the data from LVDTs 192 and 194 and reinforced the assumption that only compression was transferred across the beam-pier interface and tension was transferred only in the exterior 8 in. of the pier.

The fact that the dowels of gages 164, 165, 168 and 169 did not undergo any significant stresses indicated that these dowels were probably unnecessary and could have been omitted. It is likely that the lateral load was near ultimate at the end of the test and yet the dowels of gages 166 and 167 were not stressed above one-third of yield. It is probable that the other dowels would not have developed significant stress at even higher lateral loads and drifts. However the beam dowels were designed as shear-friction reinforcement for the overturning moment at the first level. While these dowels might not be necessary at a typical joint, they might be necessary at the first level where the moments and compression levels would be higher. Also, the compression strut seemed to transfer forces from the top of the window segment close to the original column to the bottom of the window segment at the edge of the pier. It is possible that the dowel picking up load at the bottom of the beam, the top of the window segment, was the dowel closest to the original column and the top of the assumed compression strut. Further experimentation would be needed to prove the accuracy of this theory.

The data from the dowels epoxy-grouted into the original column, strain gages 157 through 163, indicated that these dowels acted as transverse steel and encouraged monolithic behavior between the original column and the pier. The load versus stress plot for the dowels with gages 161, 163, 157 and 158 are shown in Figs. 4.20 through 4.23. The plots of gages 161 and 163 (Figs. 4.20 and 4.21) indicated very little stress in the dowel and then a sharp increase at approximately 250 k north. The dowel then picked up load proportionally with lateral load applied in the following cycles. A comparison of the crack pattern of the interior of the heavily instrumented area (Fig. 4.3) and Fig. 2.51, showing the location of the dowels, indicated

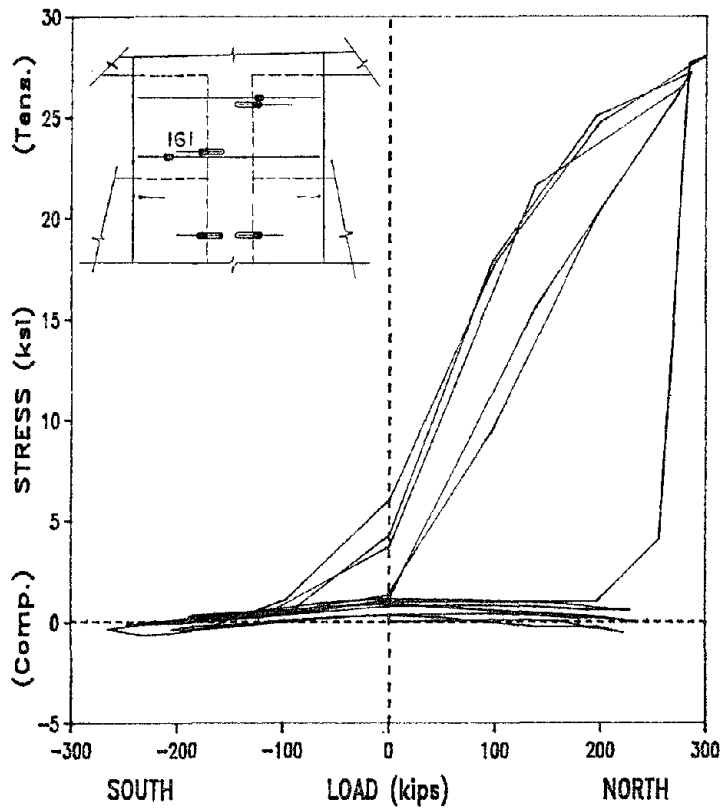


Fig. 4.20 Load vs. stress for dowel 161

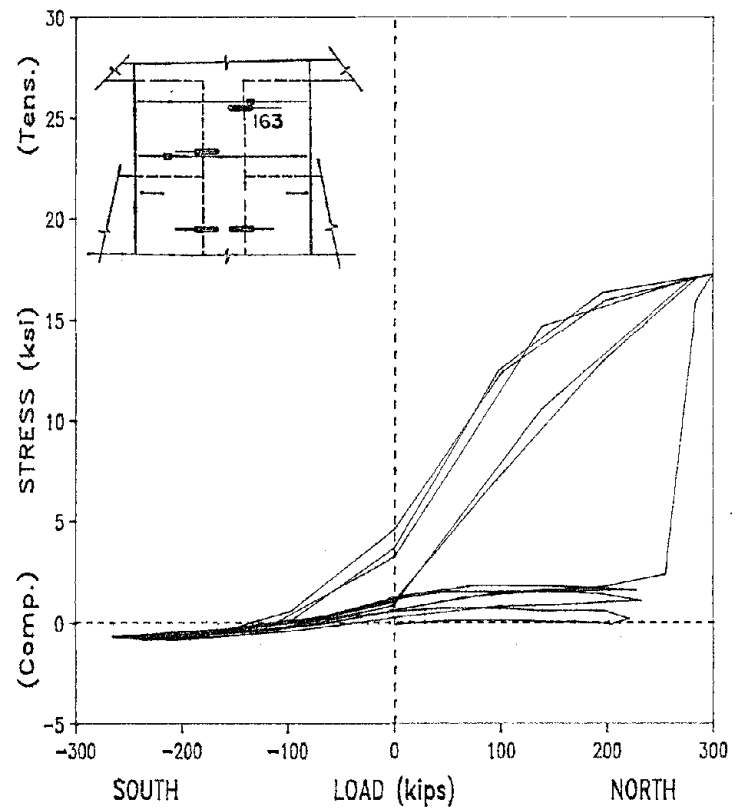


Fig. 4.21 Load vs. stress for dowel 163

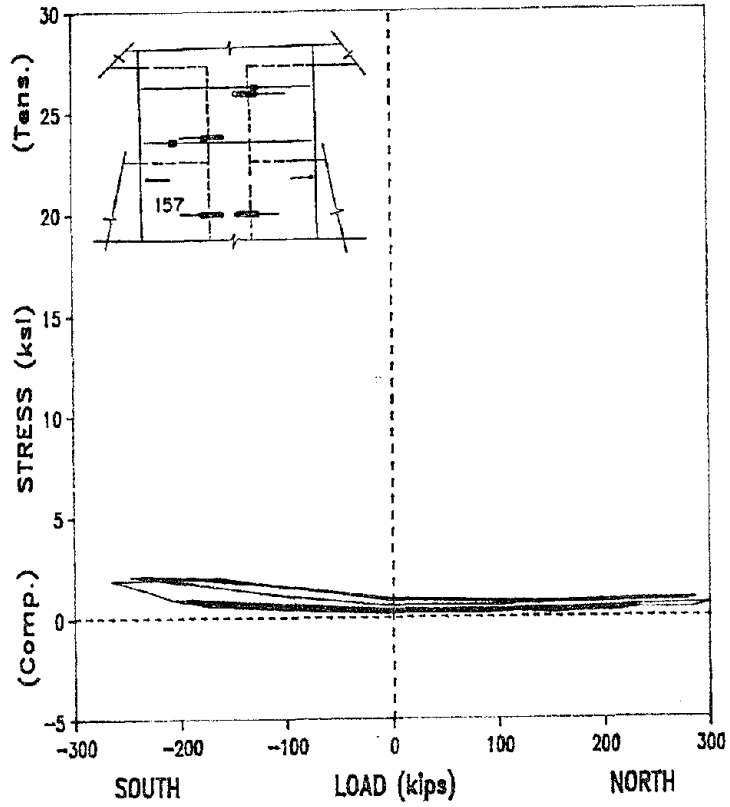


Fig. 4.22 Load vs. stress for dowel 157

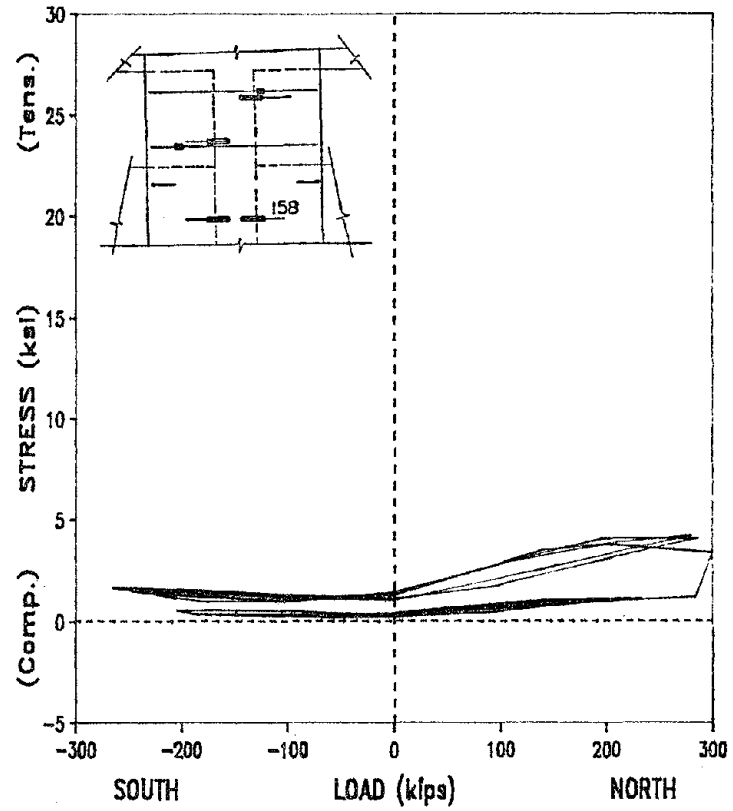


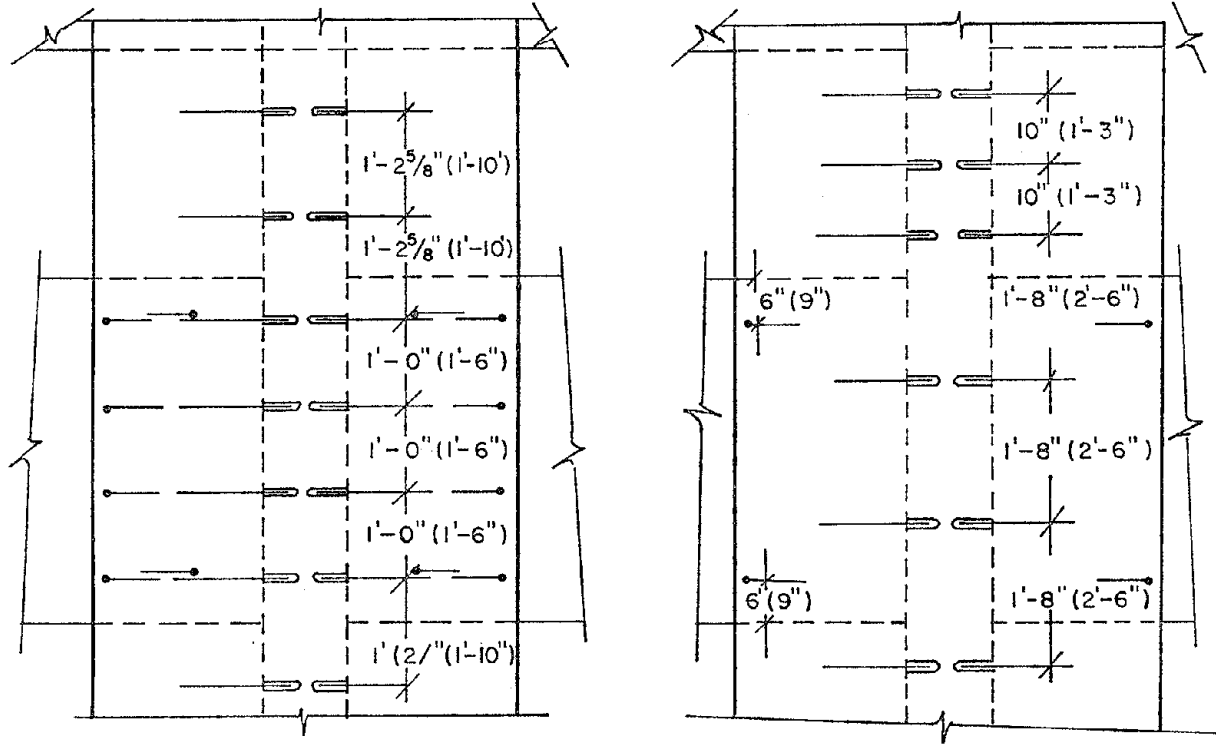
Fig. 4.23 Load vs. stress for dowel 158

that a crack opened up across dowels 161 and 163 as shown schematically in Fig. 4.4. Gage 162 showed no significant stress and no crack opened to cross the dowel.

Dowels 159 and 160 showed no stress; however, dowels 157 and 158 did develop some low stresses. The load versus stress plots for these dowels are shown in Figs. 4.22 and 4.23. The plot for stress in dowel 158 in Fig. 4.23 showed a sharp increase which might indicate a crack. It is doubtful that this increase was due to shear friction action because the dowels above (159 and 160) were in a more likely location for shear-friction transfer but they were not stressed. There were no visible cracks on the exterior of the pier in the locations of these dowels; however, there were some flexural cracks on the interior of the beam at the approximate locations of these dowels. The direction of loading for increased stress in the dowel agreed with the direction of loading under which the cracks opened in the beam. These cracks could have extended into the pier enough to influence the dowels.

The results from the column dowels indicated that they worked in general as transverse reinforcement across cracks. The column dowels in the window segment seemed to be the most critical because major shear cracks occurred in that location. These dowels acted as the only continuity between the pier and the original column in the interior of the pier where the major portion of the shear seemed to be transferred. The column dowels in the beam area did not appear to be as critical. Dowels 159 and 160 developed no significant stress and 157 and 158 developed low levels of stress. Future designs should probably have a closer spacing of column dowels in the window segment, at least as close as the transverse reinforcement in the pier, and a greater spacing of the column dowels in the beam area. A possible design, in which the unstressed beam dowels are eliminated and the spacing of column dowels is changed, is shown in Fig. 4.24.

4.2.6 Stresses in the Stirrups. The stirrups were instrumented with strain gages 147 through 156 as indicated in Fig. 2.51. The stirrups developed no significant stresses until they were crossed by a shear crack which occurred near gages 147, 150 and 156. The load versus stress plots for these gages are shown in Figs. 4.25 through 4.27. Each plot indicated very low stresses in the stirrup until some load in the north direction was reached at which the stresses in the stirrups increased sharply. The stresses fell off and remained low under south lateral loads. The exception was gage 156 (Fig. 4.27) which



a. Original design.

b. Suggested design

Fig. 4.24 Suggested design for dowels

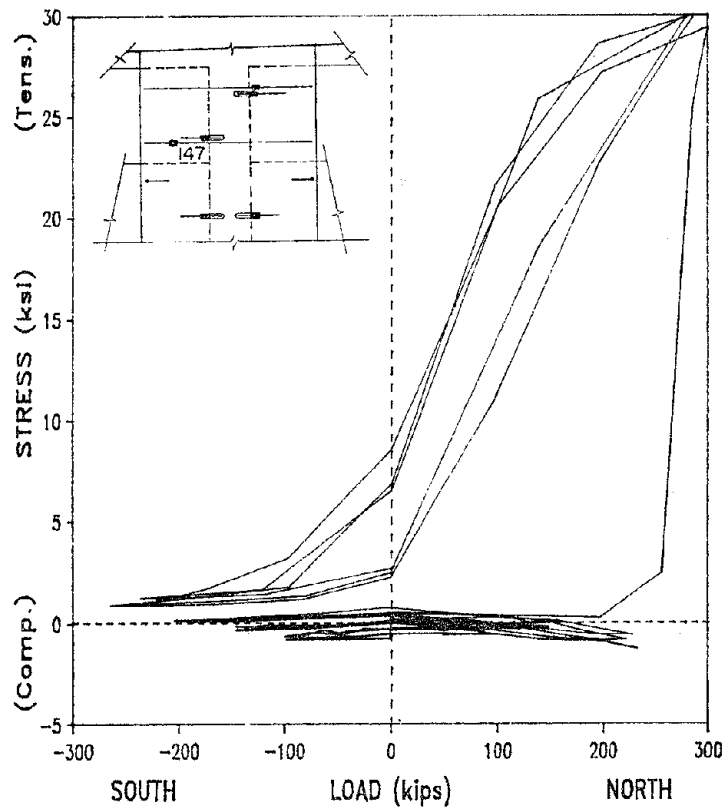


Fig. 4.25 Load vs. stress for stirrup gage 147

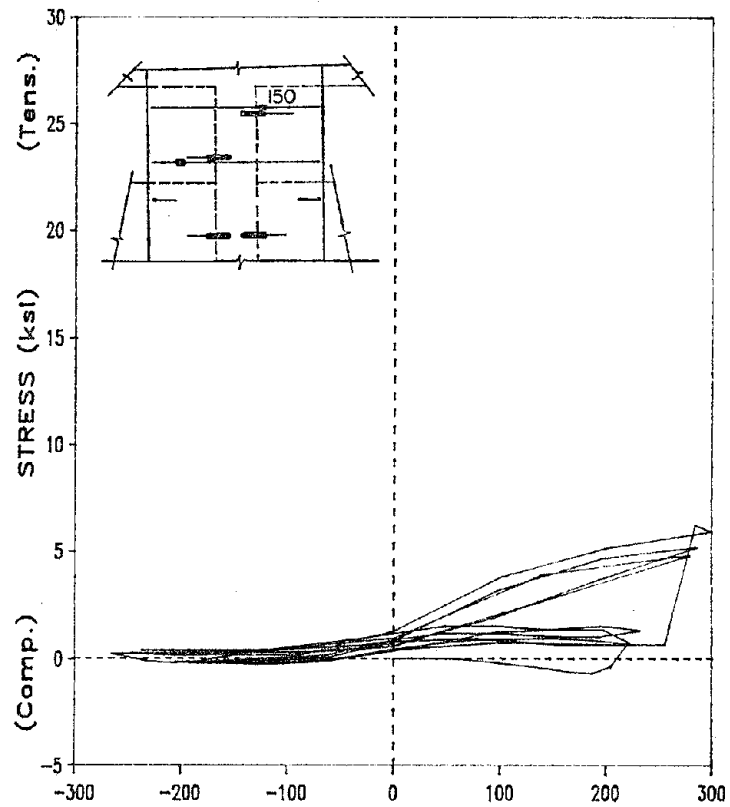


Fig. 4.26 Load vs. stress for stirrup gage 150

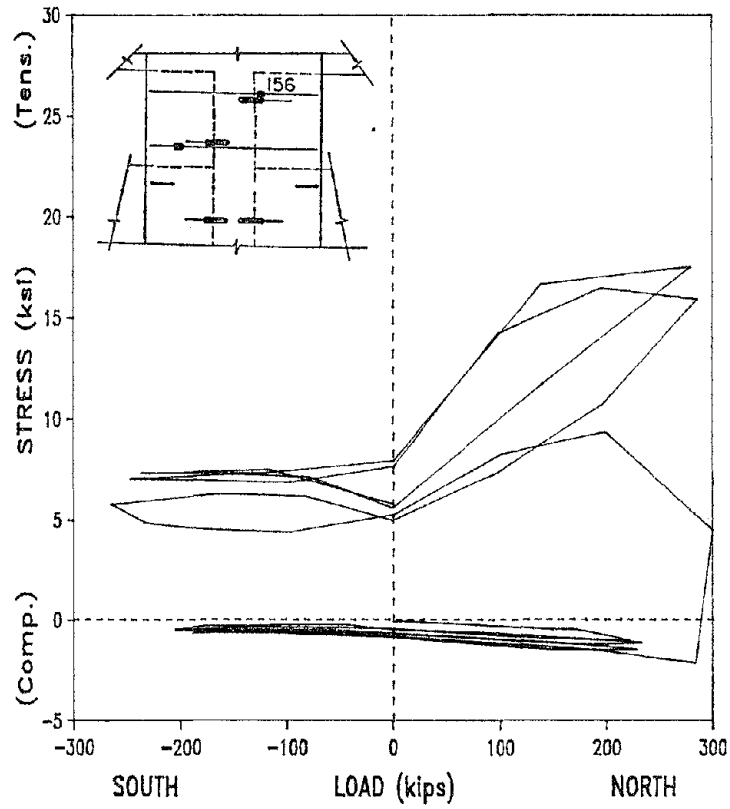


Fig. 4.27 Load vs. stress for stirrup gage 156

retained a tensile stress of 5 ksi while loading in the south direction. Under further cycles of load the stresses increased proportionally to the load in the north direction but remained nearly constant for south lateral loading for each of these gages.

The stirrup data agreed well with the pattern of cracking. Those gages which developed high stresses were in an area of shear cracking. Gages 147 and 150 were on the interior stirrups of the pier and gage 156 was on an exterior stirrup. The indication was that, although the major portion of the shear seemed to be transferred on the interior of the pier the exterior thickness of the pier was subjected to shear which may have increased if the lateral load were increased.

#### 4.3 Summary

Data from the linear voltage displacement transducers (LVDTs) showed interstory drift to have been almost the same between the three levels of the frame, indicating that the pier behaved uniformly along the height of the frame. An analysis of the data from strain gages on the pier reinforcement and dowels and the LVDTs measuring relative slip led to the conclusion that the pier behavior was a combination of flexural behavior across the exterior 8 in. thickness and a compression strut across the interior 5-1/3 in. thickness of the pier.

Both the flexural cracks and the longitudinal reinforcement indicated reverse curvature in the pier between spandrel beams, indicating column frame action as opposed to shear wall action. The flexural tension behavior of the pier was indicated by the pattern of flexural cracks across the exterior of the pier which did not extend beyond the 8 in. exterior thickness. The stresses in the continuous longitudinal reinforcement across the pier cross sections also showed flexural tension across the exterior of the pier. There was no continuous longitudinal reinforcement across the interior 5-1/3 in. of the pier window segment which was keyed between the spandrel beams. The absence of dowels at the top and bottom beam-pier interfaces of the window segment precluded transfer of tension there. The data from the slip LVDTs and beam dowels indicated no significant transfer of stresses along the beam face in a tension zone, so all of the tensile stresses should have been transferred through the exterior 8 in. thickness of the pier.

The pattern of shear cracking across the interior of the pier suggested a compression strut formed in the interior of the window segment of the pier. It was concluded that the poor bond at the top interface of the window segment contributed significantly to the width and orientation of the compression strut. The crack patterns indicated that major shear transfer occurred through a compression strut on the interior of the pier. The slip across the beam-pier interface at the top and bottom of the pier window segment, as seen in Figs. 4.10 through 4.11, indicated the shear was transferred across those interfaces in the areas of the top and bottom of the assumed compression strut. The data from LVDTs measuring slip across the beam face-pier interface and the gages measuring stresses in the corner beam dowels indicated a high transfer of stresses through shear-friction in compression zones and no transfer of stresses through shear-friction in tension zones at the top and bottom of the compression struts.

The data from the epoxy-grouted dowels indicated that, of the dowels gaged, the corner beam dowels developed forces due to shear-friction and the column dowels developed high forces due to shear cracking. The difficulty in removing the piers after testing suggested very good bond at most of the new/existing concrete interfaces. The most important column dowels seemed to be those in the window segment of the pier which developed high forces due to shear. A change in design for the dowels is suggested. Dowels could also be epoxy-grouted into the top and bottom of the spandrel beams in the pier area. These dowels would serve to transfer tension across the interior of the pier as well as shift the orientation of the compression strut, probably widening it. However, these dowels would cause difficulty in construction. The pier is conservatively designed for flexure and it is probably not necessary to increase its capacity with such dowels. The compression strut did not show signs of developing concrete crushing at lateral loads near ultimate. Also, careful compaction of concrete during casting might improve stress transfer at the top of the window segment of the pier.

## CHAPTER 5

### CALCULATED CAPACITIES

#### 5.1 General

The test of the strengthened reinforced concrete frame was stopped before the frame reached its ultimate capacity to prevent excessive damage to the frame. For this reason, a comparison of the test results to calculated capacities may not provide a quantitative evaluation of the calculations; however, in this chapter the calculated capacity of the strengthened frame is compared to the loads applied. The calculated nominal shear capacities of the pier were compared to maximum applied shears. The calculations in this chapter will deal only with the two-thirds scale model. In Chapter 2, calculations were provided for the full-scale prototype frame.

#### 5.2 Ultimate Load of Strengthened Frame Model

The ultimate capacity of the pier strengthened frame was estimated by assuming an idealized failure mechanism as seen in Fig. 5.1. Load,  $P$ , was assumed to cause failure and a drift of  $\Delta$  at the third level. The failure mechanism was assumed to be the result of hinging of each of the beams at the pier faces. The piers were assumed to be infinitely stiff and to rotate about their bases through an angle  $\theta$ . The beams were assumed to undergo straight-line deflection. Each beam had an angle of rotation,  $\phi$ , at the hinges because of the symmetrical nature of the frame. The plastic hinge moments were assumed to be the ultimate negative and positive moment capacities of the beams at the joints. These ultimate capacities were calculated using ACI-318 83 and the approximate material strengths ( $f'_c = 4000$  psi and  $f_y = 60$  ksi). The ultimate load,  $P$ , was calculated using work methods. The external work of the mechanism was

$$\text{External Work} = P\Delta$$

$$\Delta = 13.33 \text{ ft} \sin\theta$$

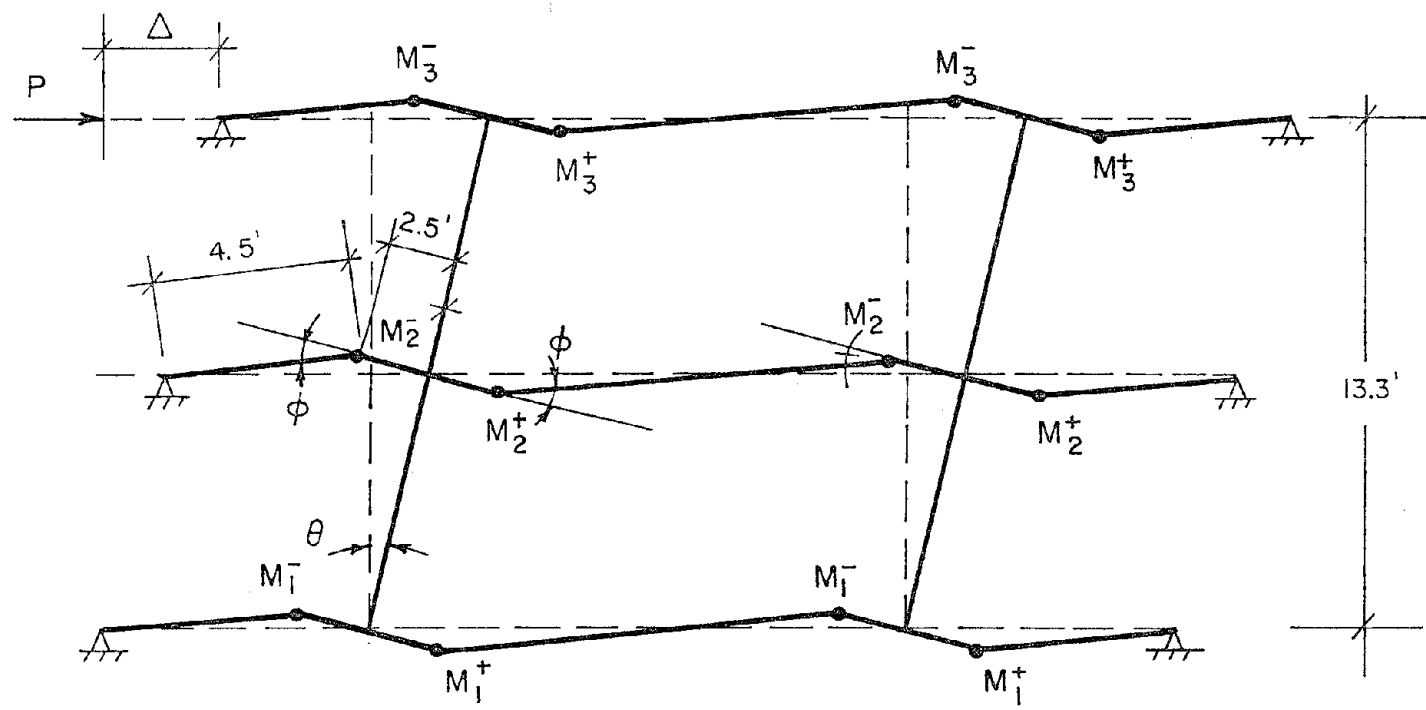


Fig. 5.1 Idealized failure mechanism for all beams hinged and infinitely stiff columns

For small angles

$$\sin \theta = \theta$$

therefore

$$\text{External Work} = P (13.33 \theta)$$

The internal work of the mechanism was the sum of the products of the plastic moments and their angle of rotation,  $\phi$ .

$$\text{Internal Work} = (2M^-_3 + 2M^+_3 + 2M^-_2 + 2M^+_2 + 2M^-_1 + 2M^+_1)\phi$$

The negative moment reinforcement in the beam was alike in the second and third levels of the frame. However, the discontinuous negative moment reinforcement differed in size and length in the first level beam. The positive moment reinforcement was the same in all three beams.

$$M^-_3 = M^-_2 = 249 \text{ k ft}$$

$$M^-_1 = 295 \text{ k ft}$$

$$M^+_3 = M^+_2 = M^+_1 = 162 \text{ k ft}$$

Illustrated in Fig. 5.2 is the relationship between the angles of rotation and for the assumed failure mechanism.

$$\phi = 1.56 \theta$$

The ultimate load,  $P$ , was obtained by setting the external work equal to the internal work. The resulting ultimate lateral load was approximately 300 k.

A second failure mechanism was analyzed assuming the negative moment hinges in the beams occurred at the sections where the discontinuous negative moment reinforcement was cut off. These sections were 1 ft 6 in. away from the pier face for the first level beam and 9 in. away from the pier face for the second and third level beams. The same assumptions of straight-line deflections of the beams between hinges were made. The

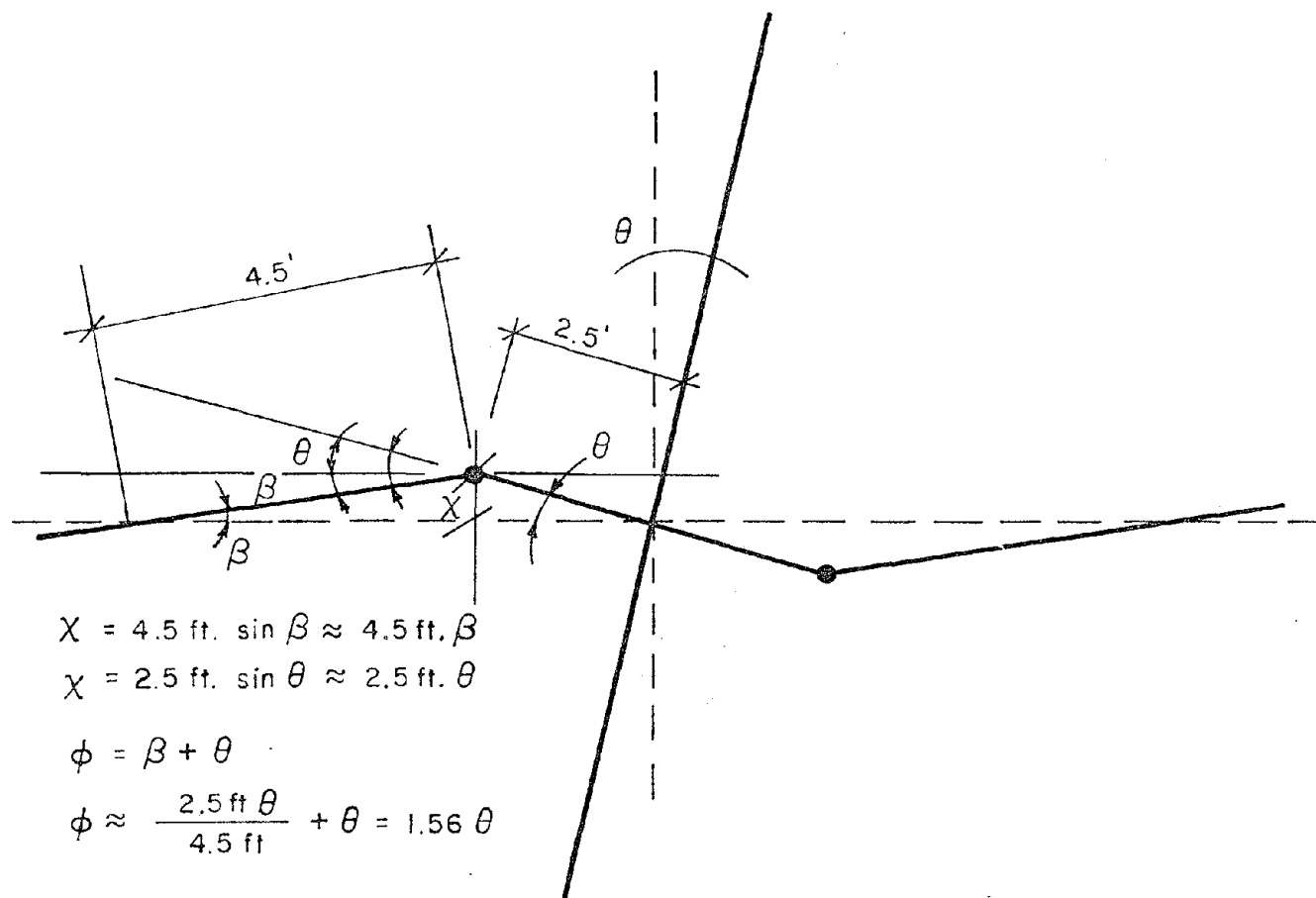


Fig. 5.2 Relationship between angles of rotation  $\phi$  and  $\theta$

cross sections of the beams were alike and symmetrical. All moment capacities were the same as the positive moment capacity.

$$M = 162 \text{ k-ft}$$

The angle of rotation,  $\phi$ , was no longer the same for each beam.

The relationships between the  $\phi$  values and the angle of rotation,  $\theta$ , of the column were the following:

$$\phi^-_3 = \phi^-_2 = 1.86 \theta$$

$$\phi^-_1 = 2.33 \theta$$

$$\phi^+ = 1.56 \theta$$

The ultimate load, P, obtained from this analysis was 261 k. This was below the value for the previous analysis; therefore, this was the critical failure mechanism and load, P = 261 k, was the predicted failure load of the frame. These results agreed well with the crack patterns and bar stresses discussed in Chapter 3 which led to the conclusion that the beams developed hinges under negative moment at the section at the cut off point of the discontinuous negative moment reinforcement.

It is likely that the negative moment reinforcement in the hinging beam was undergoing strain hardening. This was indicated by extremely high strain gage readings and by the large (1/8 in. to 1/4 in.) flexural cracks which opened at the critical sections at the cut off points of the discontinuous bars. Calculations were made to determine the amount of strain hardening necessary to develop the 305 k lateral load applied, given the failure mechanism of negative moment hinging away from the pier face. The result of the calculations was a strain hardened stress,  $f_{sh}$ , of 90 ksi (50% greater than yield) in the top layer of reinforcement in the beam. The tested ultimate strengths of the reinforcement were approximately 50% greater than yield.

In Chapter 3, it was concluded that the beams had hinged at 0.5% drift with maximum loads of 305 k north and 266 k south. The load versus drift plot of Fig. 3.28 indicated the plot was approaching but had not reached a horizontal tangent which would have indicated ultimate load on the frame. The conclusion was

that the beams had hinged but they had not reached their full rotational capacity and the loads had not reached the ultimate capacity of the frame.

Figure 5.3 is a bar graph comparing the calculated capacity of the existing frame model, 62 k; the calculated failure load of the strengthened frame without strain hardening,  $P = 261$  k; the calculated failure load of the strengthened frame with strain hardening, 300 k; and the two maximum loads applied to the frame, 305 k north and 266 k south. The maximum applied loads corresponded well with the calculated failure load from the failure mechanism analysis. The pier strengthening increased the lateral strength of the frame to over five times the calculated lateral strength, 62 k, of the existing frame model. The test results did not lead to conclusions of the available ductility because of the necessity of stopping the test before excessive damage of the frame occurred.

### 5.3 Nominal Shear Capacities of Model Pier

There was some question concerning the method to calculate the nominal shear capacity of the reinforced concrete pier. The nominal shear capacity was calculated by three different methods and the results were all compared to the applied maximum shear in the piers. The window segment was the assumed area of shear transfer and the section considered included the original column. The material strengths used were the actual material strengths ( $f'_c = 3060$  psi and  $f_y = 74$  ksi).

The first method of calculation referred to ACI 318-83 Sec. 11.3, "Shear strength provided by concrete for nonprestressed members", and Sec. 11.5, "Shear strength provided by shear reinforcement". This was also the method used to calculate the nominal shear capacity of the full scale pier referred to in Chapter 2. It was found that provisions for compression in the pier did not significantly affect the resulting nominal shear capacity. Therefore, the equation used to calculate the capacity was

$$V_c = 2 \sqrt{f'_c} b_w d \quad (\text{ACI 11-3}).$$

Using a web width,  $b_w$ , of 13-1/3 in. (thickness of the pier) and a value of 58 in. for  $d$ , the shear capacity of the concrete was calculated at 84.5 k. The equation used to find the shear

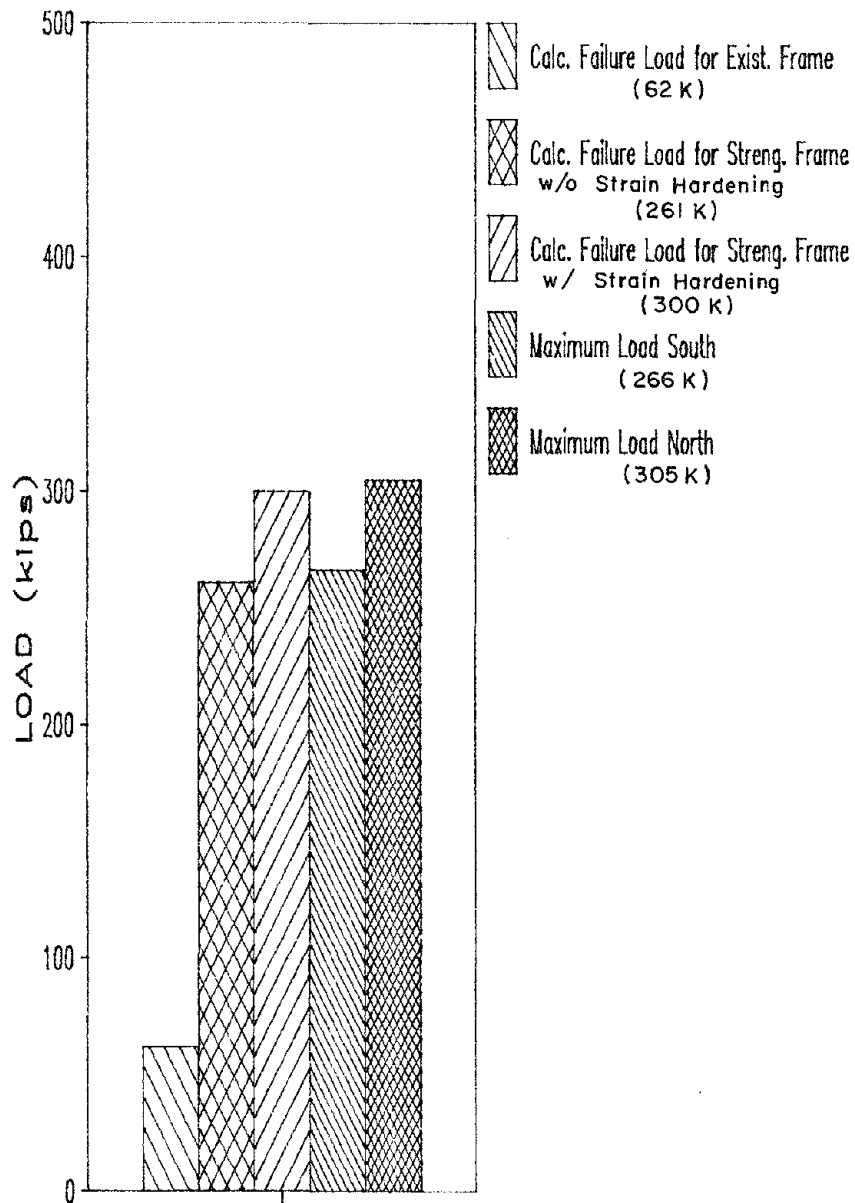


Fig. 5.3 Comparison of model with the calculated failure load of the existing frame model, the predicted failure load of the strengthened frame and the maximum loads on the frame

capacity of the reinforcement was

$$V_s = (A_v f_y d) / s \quad (\text{ACI 11-17})$$

The area of transverse reinforcement was two times the nominal area of the #3 stirrups,  $A_v = 0.22$  in., which were spaced at 9 in.,  $s$ , in the pier. The calculated shear strength provided by the transverse steel was 104.9 k. The nominal shear capacity of the pier was the addition of the concrete shear strength and the steel shear strength,

$$V_n = V_c + V_s \quad (\text{ACI 11-2})$$

which was 189 k (378 k for two piers).

The second approach to calculating the nominal shear capacity of the reinforced concrete pier was to use the provisions in ACI 318-83 Sec. 11-10, "Special provisions for walls." As previously mentioned, the pier was designed using ACI 318-83 Sec. A.5, "Structural walls, diaphragms and trusses." The pier had the proportions of a narrow wall. Therefore, the shear capacity may have approached that given by Sec. 11.10.

The shear strength of the concrete was calculated using

$$V_c = 3.3 \sqrt{f'_c} h d + (N_u d) / 4 l_w \quad (\text{ACI 11-32})$$

The thickness of the wall,  $h$ , was 13-1/3 inches. The assumed compressive force on the pier,  $N_u$ , was 100 k. This was derived as a maximum value from a determinate static analysis of the frame at the maximum load of 305 k north using the values from the load cells on the struts. The horizontal length of the wall,  $l_w$ , was 60 inches. The distance,  $d$ , was  $0.8 l_w$  or 48 inches. The resulting shear strength,  $V_c$ , was 135.4 k. The shear strength of the transverse reinforcement was determined from

$$V_s = (A_v f_y d) / s_2 \quad (\text{ACI 11-34})$$

Once again, the term  $A_v$  term was 0.22 in. and the  $d$  term was 48 inches. The spacing,  $s_2$ , was 9 inches. The resulting strength was 86.8 k and the nominal shear capacity of the pier was 222 k (444 k for two piers).

The other method for calculating the nominal shear strength was to use the equation

$$V_n = A_{cv} (\alpha_c \sqrt{f'_c} + \rho_n f_y) \quad (\text{ACI A-7})$$

where value of 3.0 was used for  $\alpha_c$  because of the low ratio of the clear height ( $h_w = 32$  in.) to the base length ( $l_w = 60$  in.) of the pier. This formula recognizes the higher shear strength of the short, wide walls which form shear cracks with orientations of decreased slope. The nominal shear capacity of the pier according to Eq. 11-7 was 239 k (478 k for two piers).

The bar graph of Fig. 5.4 is a comparison of the calculated nominal lateral shear capacities of the frame with the maximum shear applied 305 k. The discussion of the data in Chapter 3 and 4, indicated that the pier was just beginning to crack in shear and stirrup stresses were less than one half yield in the last three cycles of the test. These last three cycles at 0.5% drift introduced shear into the frame which was 80% of the lowest calculated nominal shear capacity for two piers, 378 k, and was 64% of the maximum calculated nominal shear capacity for two piers, 478 k. The small amount of shear cracking and low stirrup forces suggested that the column was capable of carrying more shear. The conclusion to be drawn from the level of shear distress in the piers was that the two piers probably could have carried the additional 173 k of shear to reach their highest calculated capacity (478 k) and possibly more.

#### 5.4 Summary

The comparison of the test results with the calculated lateral load capacity of the frame indicated that the frame reached its calculated flexural hinging capacity and could have carried more lateral load before reaching its ultimate load-carrying capacity had sufficient drift been imposed to produce strain hardening in the beam reinforcement. The comparison of the results with the calculated nominal shear capacity of the piers indicated that the piers reached between 56% and 80% of their calculated nominal shear capacity. The low levels of shear distress in the pier further suggested that the pier had considerable additional shear capacity.

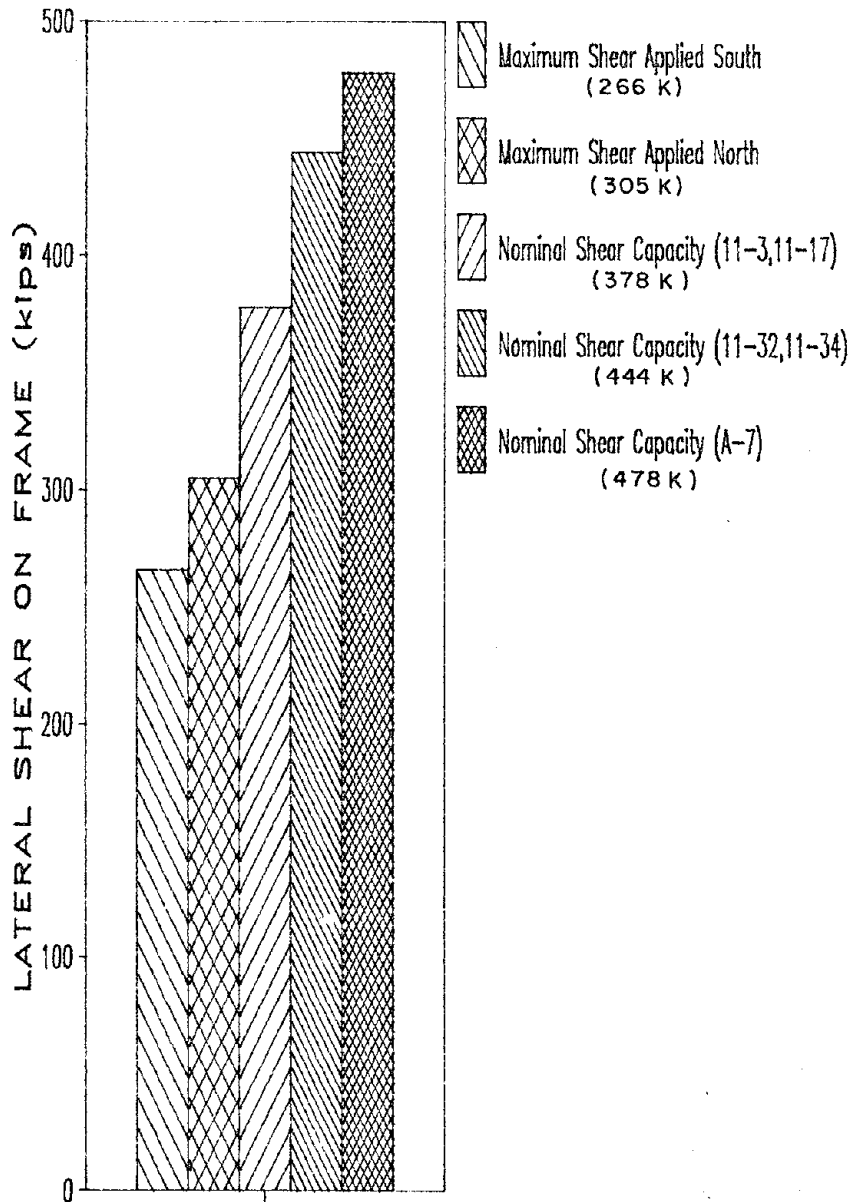


Fig. 5.4 Comparison of maximum shear applied to the piers and the calculated nominal strengths of the piers

## CHAPTER 6

### SUMMARY AND CONCLUSIONS

#### 6.1 Test Program

A two-third scale model of two bays and two stories of an exterior frame of a reinforced concrete building was constructed and tested. The prototype exterior frame had deep spandrel beams which considerably shortened the clear span of the slender columns. The deep beam - short column exterior frame was a popular design for reinforced concrete buildings in California in the 1950s and 1960s. These frames, when evaluated for seismic resistance by modern codes, are often found deficient in ductility and strength due to the relatively low column shear capacity. The model frame was retrofitted with two strengthening schemes and each strengthened frame was tested. The subject of this report was the first of these schemes, reinforced concrete piers cast around the frame's original columns.

The reinforced concrete piers were cast against three sides of existing columns, increasing the width from 12 in. to 60 in. and increasing the thickness from 12 in. to 13-1/3 in. The piers were connected to the existing frame through concrete adhesive bond, increased by sandblasting the existing frame, and through dowels epoxy-grouted into the existing frame. The pier strengthening was designed to increase the column capacities and develop the full flexural capacities of the beams, causing a failure mechanism involving beam hinging.

Testing the existing and strengthened frames involved introducing cyclic lateral deformations. The lateral load was applied to the frame near the columns at the top level and reactions were provided in the same locations at the bottom level. Boundary constraints were applied to the frame to model the continuous nature of an exterior frame.

The existing frame was tested under two cycles of loading to approximately 0.05% drift. The strengthened frame was tested under twelve cycles of loading; three cycles each to approximately 0.05%, 0.125%, 0.25% and 0.5% drift. The strengthened frame was slightly stiffer under north lateral load than south lateral load. The maximum loads in each direction were 305 k north and 266 k south. The test was stopped to avoid

excessive damage to the columns which might have affected the test of the second strengthening scheme. It was stopped at 0.5% drift because fairly wide cracks were evident in the beams and the load versus drift plot of the frame indicated the frame was approaching its ultimate load.

## 6.2 Results of Pier Strengthening

6.2.1 Constructibility and Aesthetics. The construction of the reinforced concrete piers could be carried out on an actual building with no major difficulties. The construction would interfere with the normal operations of different portions of the building for short periods and would diminish the window space of the strengthened exterior frame. The reinforced concrete piers seemed congruous with the reinforced concrete frame and they also seemed to give the frame an appearance of balanced strength and stiffness.

6.2.2 Performance of Strengthened Frame. An evaluation of the existing frame indicated that the weak link of the frame was the shear strength of the column. The piers greatly strengthened the columns in both shear and flexure. The result was flexural hinging of the beams at loads creating little distress in the piers. Both the failure mechanism calculations and the test results indicated that the critical cross sections of the beams were at the face of the pier for positive moment and at the cut off point of the discontinuous longitudinal reinforcement for negative moment. The cracking and strain gage data suggested that each of the critical cross sections of the beams were hinging or approaching hinging at the maximum load levels. The failure of the strengthened frame through beam hinging was a ductile failure mechanism. In contrast, the predicted failure of the existing frame through a column shear failure would have been a nonductile failure mechanism, possibly causing collapse of the structure. The pier strengthening resulted in a ductile moment resisting frame such as is required by earthquake regulations.

## 6.3 Behavior of the Piers

The pier behavior was governed by flexural action in the exterior 8 in. of the pier and by a compression strut in the interior 5-1/3 in. of the pier.

6.3.1 Flexural Behavior. Flexural tension in the pier was indicated by the flexural cracking which occurred only in the 8 in. exterior thickness of the pier. The interior thickness had no continuous longitudinal reinforcement to transfer tension at the horizontal joint faces. The data on dowels forces and slip did not indicate a transfer of tension at the joint through shear-friction. Therefore, the flexural tension was transferred entirely within the exterior 8 in. of the pier. The keying effect of the pier between the spandrel beams allowed the interior of the pier to transfer compression through lug action into the top and bottom of the beams. Also, compression was transferred across the beam face through shear-friction. The data from the longitudinal reinforcement indicated reverse curvature (frame action) along the pier clear height. The area around the beam-pier joint, with a two beam - two pier configuration, showed very little flexural cracking and low forces in the longitudinal reinforcement. The pier was very conservatively designed for flexure at the joint.

6.3.2 Shear Behavior. The pattern of shear cracking in the pier indicated that a large portion of the shear was transferred through a compression strut in the interior 5-1/3 in. of the window segment. The orientation and width of the strut was outlined by the shear cracks. The strut initiated at the top of the pier window segment near the original column and terminated at the bottom of the window segment at the outside edge of the pier. Data from the slip transducers at the top and bottom of the window segment indicated a transfer of shear across the beam/pier interface at the top and bottom of the compression strut.

The initiation of the strut near the original column at the top of the pier window segment indicated that the interface between the bottom of the beams and the top of the interior window segment was a weak shear plane. This was attributed to a lack of bearing between the surfaces caused by the lack of compaction during construction. This lack of bearing is indicated through slip data for this interface. The weak shear plane could possibly be eliminated by improving compaction. Dowels epoxy-grouted into the bottom of the spandrel beam would increase the shear strength across the interface but would be difficult to place.

The maximum load on the frame was 305 k but the data indicated that the piers had not been loaded to their full shear strength. The stirrups and dowels which crossed shear cracks in the pier were stressed to a maximum of 50% of their yield. The

shear cracking was not extensive in the pier and the cracks were not wide. The exterior 8 in. of the pier, which had at least as much concrete and transverse steel area as the interior 5-1/3 in., did not contribute its full capacity to shear resistance. The nominal shear capacity of two piers calculated using ACI 318-83 was between 378 and 478 k, depending on the equations used for calculation. Based on the low level of distress in the piers, the data indicated that the two piers had a shear capacity in excess of 478 k.

6.3.3 Interaction. Removing the pier to return the frame to its original dimensions was difficult. The difficulty suggested very good adhesive bond between the new and existing concrete. The data from the slip transducers and the instrumented dowels indicated that the bond was overcome and shear-friction took place in the compression zone near the assumed compression strut. The dowels were not instrumented in the compression zones at the top of the assumed compression strut, but the slips were high. Any beam dowels away from these compression zones did not develop stress and were probably unnecessary.

The column dowels in the window segment of the pier developed high stresses where they crossed shear cracks. Those column dowels in the beam area did not develop significant stress. The column dowels were designed, in part, to provide continuous shear reinforcement across the pier section. Shear was not a critical factor for column dowels in the beam area and the number of dowels could probably have been decreased. However, shear was the major factor in the interior of the window segment and the column dowels in the window segment should be increased to a spacing at least equal to the stirrup spacing.

#### 6.4 Conclusions

1. The reinforced concrete piers acted as strong columns which developed the flexural capacity of the beams and caused the frame to fail in a ductile manner.
2. The pier strengthened frame had an initial lateral stiffness three times the initial lateral stiffness of the existing frame.
3. The reinforced concrete piers increased the lateral strength to at least five times the calculated lateral strength of the existing frame. If this increase were

applied to the prototype building, it would give the exterior frame a lateral strength two times the 1982 UBC design earthquake lateral load.

4. The loads applied on the frame did not develop the shear capacity of the piers and developed a small percentage of the flexural capacity of the piers.
5. The adhesive bond and dowel action provided adequate load transfer between the reinforced concrete piers and the original frame. The number of dowels could be decreased in the beam segment and should be increased in the window segment.

## REFERENCES

1. Ichinose, T., Aoyama, H. and Kai, "Experimental Study on Seismic Behavior of Reinforced Concrete Subassemblages with Splitted Spandrel Walls," 8WCEE, San Francisco, California, 1984, Vol. 6, pp. 469-476.
2. Sugano, S. and Endo, T., "Seismic Strengthening of Reinforced Concrete Buildings in Japan," Strengthening of Building Structures - Diagnosis and Theory, IABSE Symposium, Venice, Italy, 1983, pp. 371-378.
3. Higashi, Y., Endo, T. and Shimizu, Y., "Experimental Studies on Retrofitting of Reinforced Concrete Structural Members," Proceedings of the Second Seminar on Repair and Retrofit of Structures, Ann Arbor, Michigan, 1981, Vol. 2, pp.126-155.
4. Kawamata, S. and Ohnuma, M., "Strengthening Effect of Eccentric Steel Braces to Existing Reinforced Concrete Frames," Proceedings of the Second Seminar on Repair and Retrofit of Structures, Ann Arbor, Michigan, 1981, Vol. 2, pp. 262-269.
5. Sugano, S., "An Overview of the State-of-the-Art in Seismic Strengthening of Existing Reinforced Concrete Buildings in Japan," Takenaka Technical Research Report, No. 25, April 1985.
6. Higashi, Y., Ohkubo, M. and Fujmata, K., "Behavior of Reinforced Concrete Columns and Frames Strengthened by Adding Precast Concrete Walls," 6WCEE, New Delhi, India, 1977, Vol. 7, pp. 85-90.
7. Higashi, Y., Endo, Y. and Shimizu, Y., "Effects on Behavior of Reinforced Concrete Frames by Adding Shear Walls," Proceedings of the Second Seminar on Repair and Retrofit of Structures, Ann Arbor, Michigan, 1981, Vol. 3, pp. 265-290.
8. Hirosawa, M., Kitagawa, Y. and Yamazaki, Y., "Retrofitting on Medium - Rise Reinforced Concrete Housing Structures," Proceedings of the Second Seminar on Repair and Retrofit of Structures, Ann Arbor, Michigan, 1981, Vol. 2, pp. 278-321.
9. Wyllie, L. A., Jr., "Strengthening Existing Concrete and Masonry Buildings for Seismic Resistance," Proceedings of the Second Seminar on Repair and Retrofit of Structures, Ann Arbor, Michigan, 1981, Vol. 2, pp. 322-333.

10. Shibata, T. and Ohno, K., "On Damage to the Hokodate College by the Tokachi-oki Earthquake, 1968," Proceedings of the U.S. - Japan Seminar on Earthquake Engineering with Emphasis on the Safety of School Buildings, Sendai, Japan, September 1970, pp. 129-144.
11. Strand, D., "1974 SEAOC Lateral Force Requirements and History," Proceedings ASCE National Structural Engineering Convention. New Orleans, Louisiana, April 1975.
12. International Conference of Building Officials, Uniform Building Code, 1955 Edition, Whittier, California, 1955.
13. International Conference of Building Officials, Uniform Building Code, 1982 Edition, Whittier, California, 1982.
14. Higashi, Y. and Kokusho, S., "The Strengthening Methods of Existing Reinforced Concrete Buildings," Proceedings of the Review Meeting U.S. - Japan Cooperative Research Program in Earthquake Engineering with Emphasis on the Safety of School Buildings, Honolulu, Hawaii, August 1975, pp. 333-351.
15. Sugano, S., "Aseismic Strengthening of Existing Reinforced Concrete Buildings," Proceedings of the Second Seminar on Repair and Retrofit of Structures, Ann Arbor, Michigan, 1981, Vol. 1, pp. 13-40.
16. American Concrete Institute, Building Code Requirements for Reinforced Concrete (ACI 318-83), Detroit, Michigan, 1983.
17. Luke, P. C. C., Chon, C., and Jirsa, J. O., "Use of Epoxies for Grouting Reinforcing Bar Dowels in Concrete," PMFSEL Report No. 85-3, The University of Texas at Austin, Sept. 1985.
18. Jones, E. A. and Jirsa, J. O., "Seismic Strengthening of a Reinforced Concrete Frame Using Structured Steel Bracing," PMFSEL Report No. 86-5, The University of Texas at Austin, May 1986.